PREDICTION OF PILE DRIVABILITY FROM CPT AND WEAP ANALYSIS

By

Jiawei Wang

B. Sc., Tong Ji University, China

M. Eng., Tong Ji University, China

A THESIS SUBMITTED IN PARTIAL FULFILLMENT OF

THE REQUIREMENTS FOR THE DEGREE OF

MASTER OF APPLIED SCIENCE

in

THE FACULTY OF GRADUATE STUDIES

CIVIL ENGINEERING

We accept this thesis as conforming

to the required standard

THE UNIVERSITY OF BRITISH COLUMBIA

September 1992

In presenting this thesis in partial fulfilment of the requirements for an advanced degree at the University of British Columbia, I agree that the Library shall make it freely available for reference and study. I further agree that permission for extensive copying of this thesis for scholarly purposes may be granted by the head of my department or by his or her representatives. It is understood that copying or publication of this thesis for financial gain shall not be allowed without my written permission.

(Signature)

Department of Civil Engineering

The University of British Columbia
Vancouver, Canada

Date Oct. 15 1992

DE-6 (2/88)

Abstract

Pile drivability is a difficult problem because of the complex dynamic pile-soil behaviour. The current procedure in predicting blow count during pile driving uses the Smith's one-dimensional wave equation model with input appropriate soil resistances during pile driving. There is no general consensus to date on one approach for estimating the driving resistances in all types of soils.

The cone penetration test (CPT) is a useful tool for detailed profiling of soil conditions at a site and has been found by many researchers to provide a reliable estimate of long term pile capacity as determined from a static loading test. An attempt has been made in this thesis to use the CPT directly to estimate pile driving resistance for use in pile drivability analysis.

Several approaches were undertaken to estimate the driving resistances from the CPT, and the predicted blow counts from the wave equation analysis were compared to the field measured blow counts. Pile and soil data from three sites: UBC Pile Research Site, Tilbury Island Site and Evanston Campus of Northwestern University (ENCU) Site were analyzed. The piles included steel pipe piles of both closed and open ended as well as H pile.

An empirical correlation approach is proposed which uses CPT cone bearing (q_c) directly to estimate the driving toe resistances. The shaft resistances during driving, however, was estimated in a conventional way from static long term resistance calculated from correlations with CPT q_c data but was then multiplied by a set of empirical determined reduction factors. The application of the proposed method to a steel pipe pile at another site location (not included in the above data base) is illustrated. Reasonable

agreement is obtained between calculated and measured blow counts.

Although the data base in this study is limited, the proposed method appears promising. More research is needed to check the applicability of this method to different soil condition and other pile types.

Table of Contents

List of Tables

List of Figures

Acknowledgement

The author wishes to express his gratitude to his research advisor , Professor R. G. Campanella, for his support, encouragement, patient and valuable suggestions throughout this research and thesis preparation. The author is very thankful to Alex Sy for suggesting the research topic and providing data. His advice and suggestions during our discussions proved invaluable. The author also expresses his sincere gratitude to Professors Liam Finn and Y. P. Vaid for reading this thesis and suggesting improvements.

The financial support in the form of a Research Assistantship from the Natural Science and Engineering Research Council of Canada, which made this study possible, is gratefully acknowledged.

The author is deeply indebted to Mr. Matt Kokan for reviewing and making improvements to the thesis. His suggestions and friendly helps was invaluable. Thank you Matt.

Appreciation is extended to my colleagues, G. X. Wu and Y. C. Shi, for their valuable discussions.

A big thank you also to my parents and my sister, S. N. Wang, for their continued encouragement, understanding and support throughout my studies in UBC. I wish to thank my dear wife Z. Q. Yang, whose love, friendship and understanding I treasure. This thesis is dedicated to them.

Chapter 1

Introduction

In design of driven pile foundations for axial loadings, two types of analyses are usually conducted. Given the design load and soil conditions, the pile type, pile size and length are determined from a static analysis. Then a dynamic analysis is carried out to select an optimum pile driving hammer system and to determine whether the pile can be installed to the design depth. If the pile has to penetrate a dense or hard layer, it may be necessary to predict how long the driving will continue be through the layer and to evaluate whether the driving stresses will exceed the structural strength of the pile. Where the pile tip is driving into in a very dense stratum, a practical refusal criterion or final set (displacement per blow) is determined for the given hammer system to be used during construction. The dynamic pile analysis is conducted in practice using a one-dimensional wave equation program such as GRLWEAP (Goble, 1987).

The problems outlined above require an estimation of net pile displacement or set, given a hammer-pile-soil model. Set is the inverse of blow count, i.e. number of blows for a given displacement increment, typically *onefoot*. The prediction of set or blow count is commonly referred to as a pile drivability problem. Blow counts are often predicted throughout the penetrated soil profile, i.e. as a function of depth. Given the hammer blow rate (blows per minute), the time required to drive a pile can be estimated from the predicted total number of blows.

Pile drivability consideration is important in offshore and onland piling for construction planning, scheduling and cost estimating purposes. The prediction of blow count,

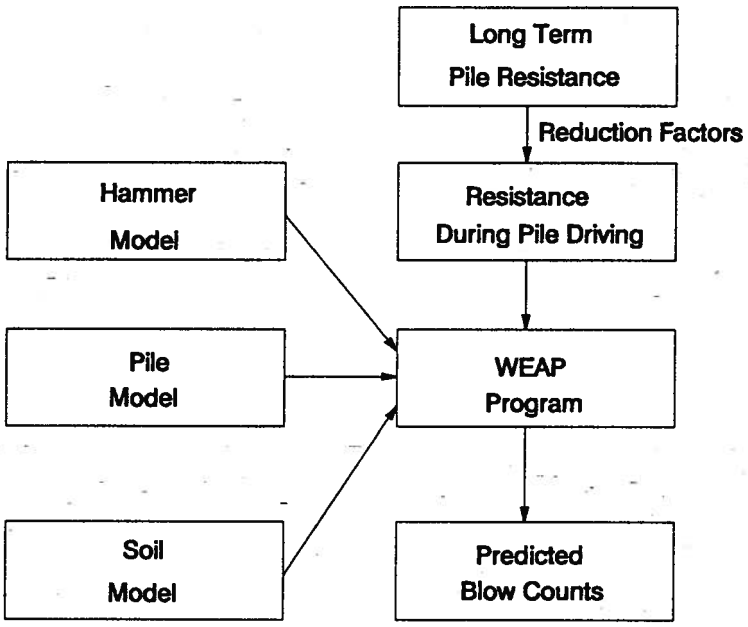

Figure 1.1: The Basic Procedure of Blow Count Prediction of Driven Pile

however, is a difficult task because it requires a knowledge of the resistances acting on the pile during driving. The driving resistances depend on the complex dynamic pile-soil interaction characteristics. Studies (Soderberg, 1962 and Hereema, 1980) have show that the driving resistance, particularly along the pile shaft, is less than the resistances acting on the pile from a static loading test conducted on the pile after construction pore pressure have dissipated. In this study, the pile resistance from a static loading test are referred to as static long term resistance.

The current practice in pile drivability prediction involves two basic steps. First, the long term pile shaft and toe resistances are evaluated from in-situ tests and these are multiplied by some reduction factors based on soil type and/or pile length to arrive at the estimated driving resistances. In the second step, the estimated driving resistance is used in a wave equation analysis of the hammer-pile-soil system to predict the blow counts as a function of pile penetration. This basic procedure is illustrated in Figure 1.1.

There is no general consensus on the reduction factors applied to the static long term pile resistance. Some results of studies (Aurora, 1980; Tang et al, 1988) have shown that the static resistance during driving changed with the undrained shear strength of the clay. In their approach (Tang et al, 1988) a factor of 0.5 was used to multiply undrained shear strength to estimate shaft resistance during driving in clay. The toe resistance in clay and both shaft and toe resistances in sand use the static resistances determined from pile load testing. Chow et al (1988) determined both shaft and toe resistances using remoulded undrained shear strength. They used a reduction factor of 0.33 to determine shaft resistance during driving, but a factor of 9 times the remoulded undrained shear strength was used to determine toe resistance during driving. Heerema (1980) presented a "friction fatigue" theory for describing pile driving behaviour in clay. In his study, the gradual decrease in skin friction during pile driving was considered to be caused not only by clay remoulding but also by the decrease in horizontal stress in the soil around the pile. In their research, using the WEAP86 program, Alm et al (1989) considered the blow count as a non-linear function of input energy and static resistance during driving at a given depth. They used statistical analyses to estimate static resistance during driving from input energy and pile capacity. However, comparison of similar hammers demonstrates that all hammers, unfortunately, do not provide a consistent amount of energy into the pile (Rausche et al, 1985). It is therefore difficult to predict drivability accurately if the effects of input energy and static pile resistance during driving are not considered separately.

The cone penetration test (CPT) provides a repeatable and reliable means of characterizing soil conditions (Campanella and Robertson, 1986). Because the CPT is a model of a displacement pile, it has been correlated to results from static pile loading tests (Bustamante and Gianesalli, 1982 and Burland, 1983, etc.). In fact, the LCPC method has been found to provide pile capacities in good agreement with static loading tests at

several sites in North America (Davies, 1987, Campanella et al, 1989 and Finno, 1989).

The purpose of this study is to explore the possibility of using the CPT in a more direct approach to pile drivability analysis. Data from three sites: UBC Pile Research Site, Tilbury Island Site and Evanston Campus of Northwestern University (ENCU) Site were used. The pile types include steel pipe piles, both closed and open ended, and H piles.

A method is finally proposed which uses the CPT cone bearing (q_c) values directly to estimate the static toe resistance during driving and uses a reduced shaft resistance calculated from the LCPC CPT pile capacity prediction method. It is shown that the detailed profiling of the CPT provides a promising method of evaluating the driving resistance for use in a wave equation analysis to predict blow counts.

Chapter 2

In Situ Test and Research Sites

2.1 Outline

The study in this thesis was based on the data obtained from three pile research sites. The research sites include:

UBC Pile Research Site

Tilbury Island Site

ECNU (Evanston Campus of Northwestern University, USA) site

For each site, the blow count data were analyzed in conjunction with cone penetration test (CPT) data to establish a method which can predict blow counts of different types of driven piles accurately. The CPT tests were done near or at the location of pile test sections. Data from different sites with different soil types were used in the analysis to consider the effects of soil type on the analysis.

2.2 The Cone Penetration Test

The cone penetration test (CPT) is a quasi-static penetration test. The CPT allows for near continuous delineation of stratigraphy. The small end area and low pushing rate, make the CPT a very good tool for modelling pile performance. The CPT has the following advantages:

a) continuous logging

b) rapid procedure

c) good repeatability

d) easy standardization

The CPT can be used to rapidly assess soil variability at a site. The major disadvantage of the CPT is that it can not be used in some soil conditions such as gravels or heavily cemented soils. Hence, the forthcoming analysis will be restricted to soils that are well suited to penetration testing

The electric cone is illustrated in Figure 2.1. It has a tip having base area of 10 cm^2 and an apex angle of 60°. The friction sleeve located immediately behind the cone tip has a standard area of 150 cm^2. The cone is pushed into the soil at a constant rate of 2 cm/sec and has the ability to sample on five different channels at 2.5 cm intervals, measuring the cone bearing (q_c), sleeve friction (f_s), pore pressure (U), temperature (T) and inclination (I). Robertson and Campanella (1986) provide a comprehensive review of equipment, testing procedure and data interpretation. Soil classification from CPT data is based on cone bearing and friction ratio as shown in Figure 2.2 (Robertson and Campanella, 1986).

2.3 Research Sites

2.3.1 UBC Pile Research Site

UBC Pile Research Site is located on the eastern end of Lulu Island, within the post-glacial Fraser River delta, as shown in Figure 2.3. The surficial geology of this part of Lulu Island is typical of a former marine environment no longer dominated by tidal action (Blunden, 1975).

The CPT results in Figure 2.4 show deposits of organic silty clays that has been laid down in a swamp or marsh environment extend to a depth of about 50 $feet$. Below this upper layer, a medium dense sand deposit, locally silty, prevails to roughly 90 $feet$ in

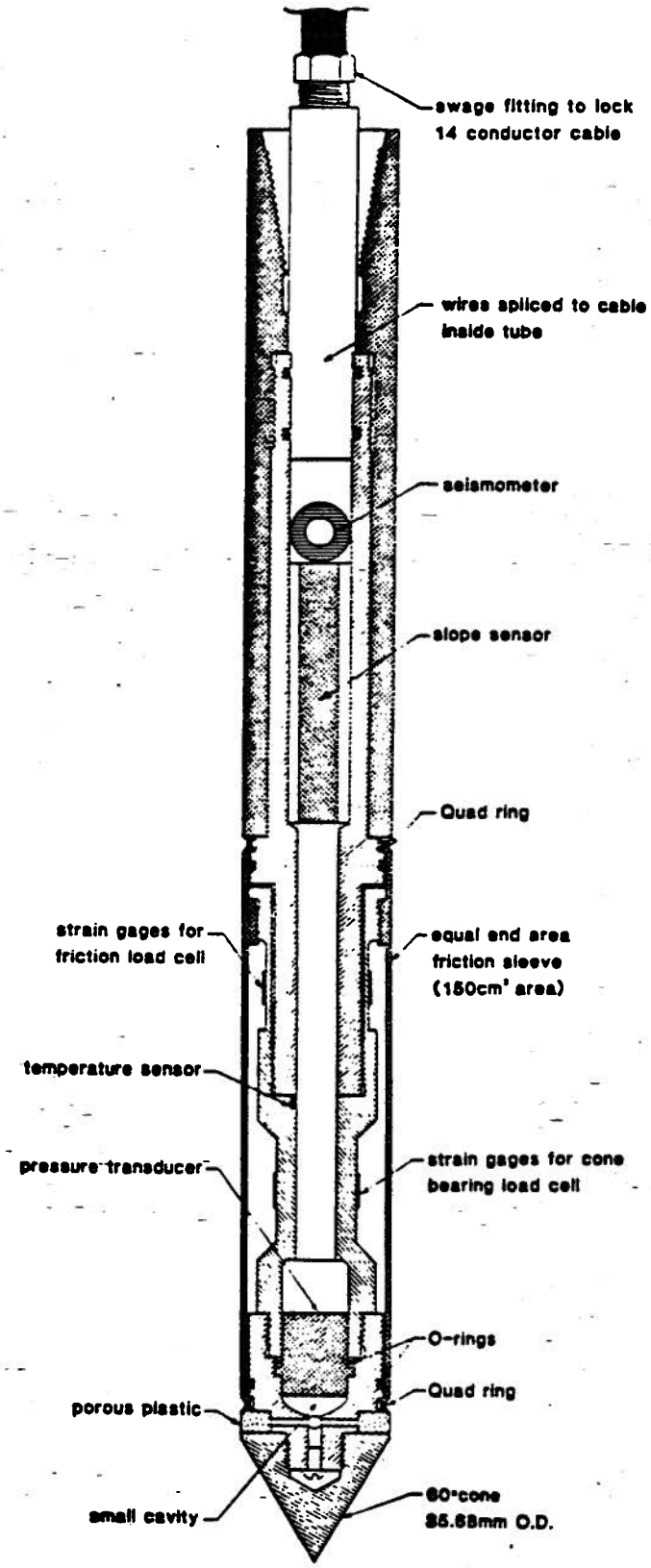

Figure 2.1: Cone Penetrometer Used at UBC

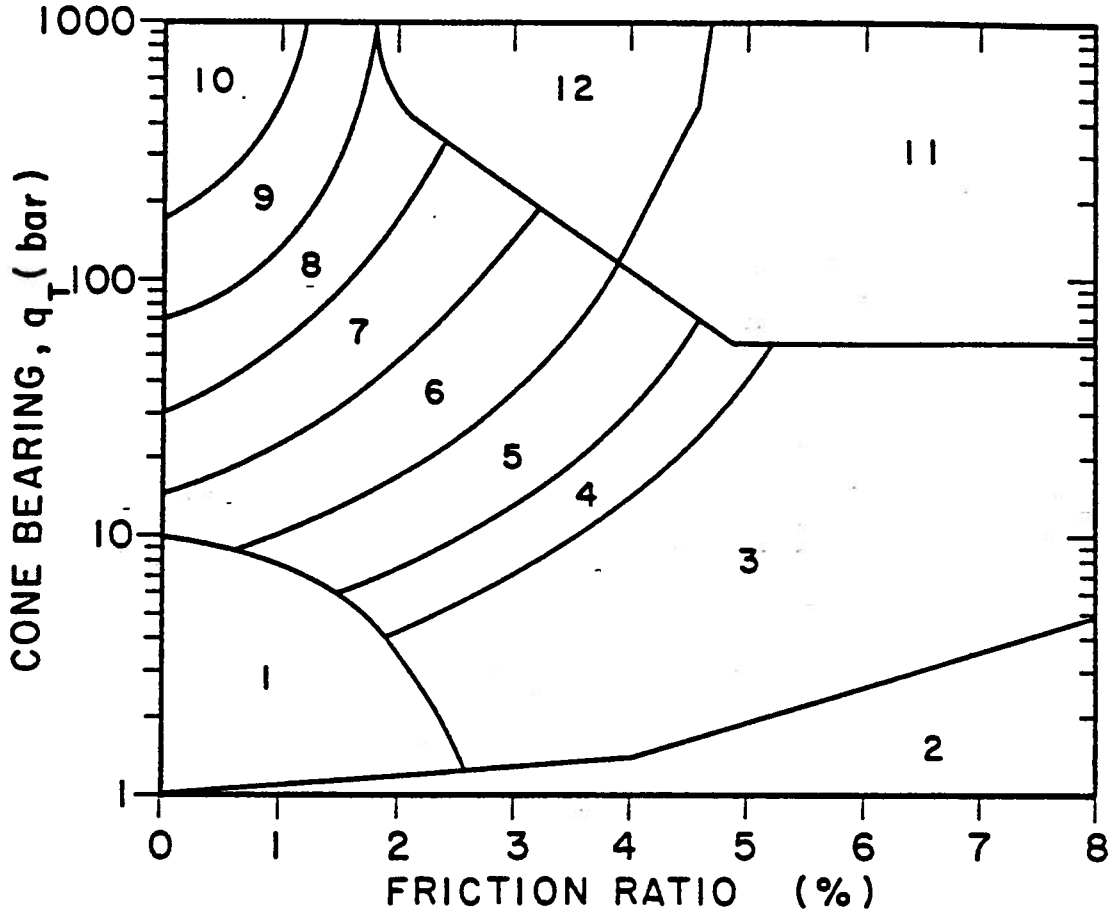

Zone	Qc/N	Soil Behaviour Type
1)	2	sensitive fine grained
2)	1	organic material
3)	1	clay
4)	1.5	silty clay to clay
5)	2	clayey silt to silty clay
6)	2.5	sandy silt to clayey silt
7)	3	silty sand to sandy silt
8)	4	sand to silty sand
9)	5	sand
10)	6	gravelly sand to sand
11)	1	very stiff fine grained (*)
12)	2	sand to clayey sand (*)

(*) overconsolidated or cemented

Figure 2.2: Simplified Soil Classification Chart for the CPT (after Robertson and Campanella, 1986)

depth. A normally consolidated clayey silt containing sand layers underlies the above sequence to a depth of 700 - 800 *feet* depth (Davies, 1987).

2.3.2 Tilbury Island Site

Tilbury Island Site is located in the middle of the Fraser River delta, as shown in Figure 2.3. The CPT results are shown in Figure 2.5. There is a filled sand layer which is medium dense to dense up to 6.5 *feet* in depth. Below this layer is a silt deposit containing thin clay layers to 14 *feet* in depth. Next, a fine to medium grained sand layer with interbedded silt layers exists up to 25 *feet* depth. Below 25 *feet* are sands which appear to increase in density with depth. Above 41 *feet* depth, the sand is fine grained and loose to medium dense. Below 41 *feet* depth, this sand layer changes to fine to medium grained sand with some coarse grained sand, the density of this sand layer changes from medium dense to dense.

2.3.3 ECNU (Evanston Campus of Northwestern University) Site

The data of this test site is from the ASCE Foundation Engineering Congress (Finno, 1989), to evaluate capacity and load transfer characteristics of piles. The test site is located on the lakefill on the Evanston Campus of Northwest University, Evanston, IL, USA. The CPT results are shown in Figure 2.6. With increasing depth from the ground surface, the soils consist of 23 *feet* of fine grained sand, 45 *feet* of soft to medium clay, 12 *feet* of stiff clay and 10 *feet* of hard silt. Beneath the silt Niagaran dolomite bedrock is encountered. The water levels are static within the clay deposits (Finno, 1989).

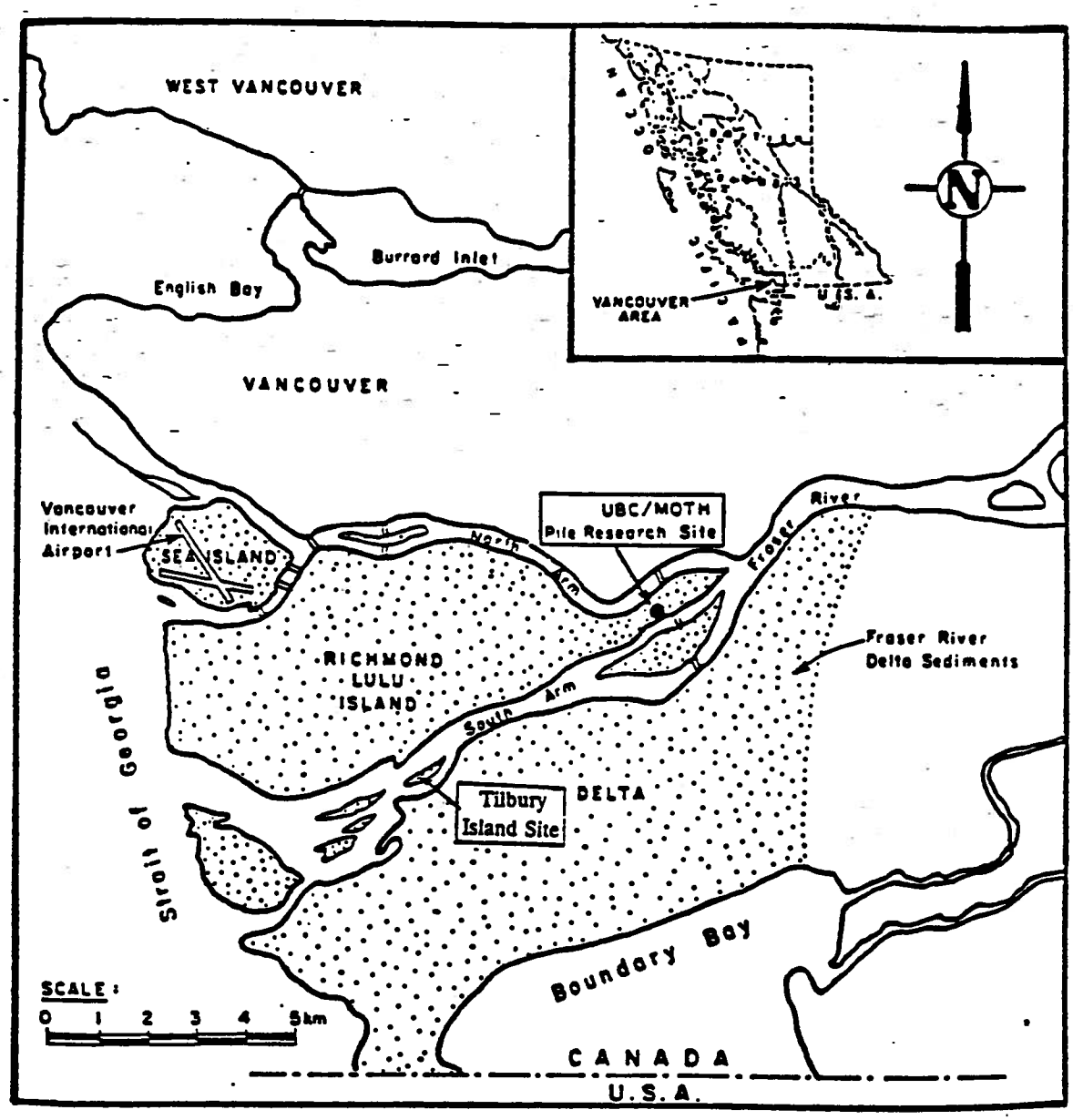

Figure 2.3: Location of UBC Pile Research Site and Tilbury Island Site

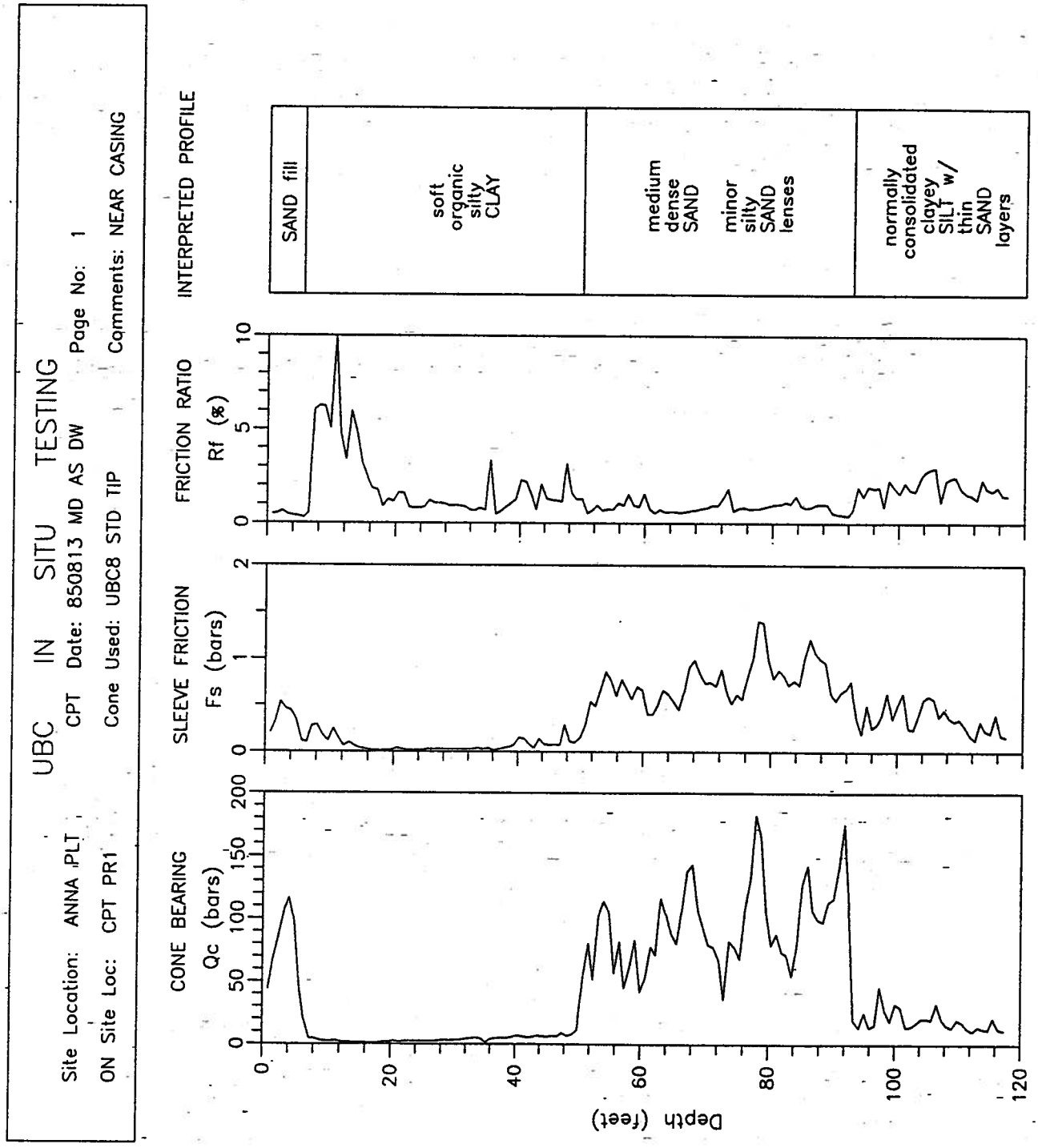

Figure 2.4: CPT results of UBC Pile Research Site

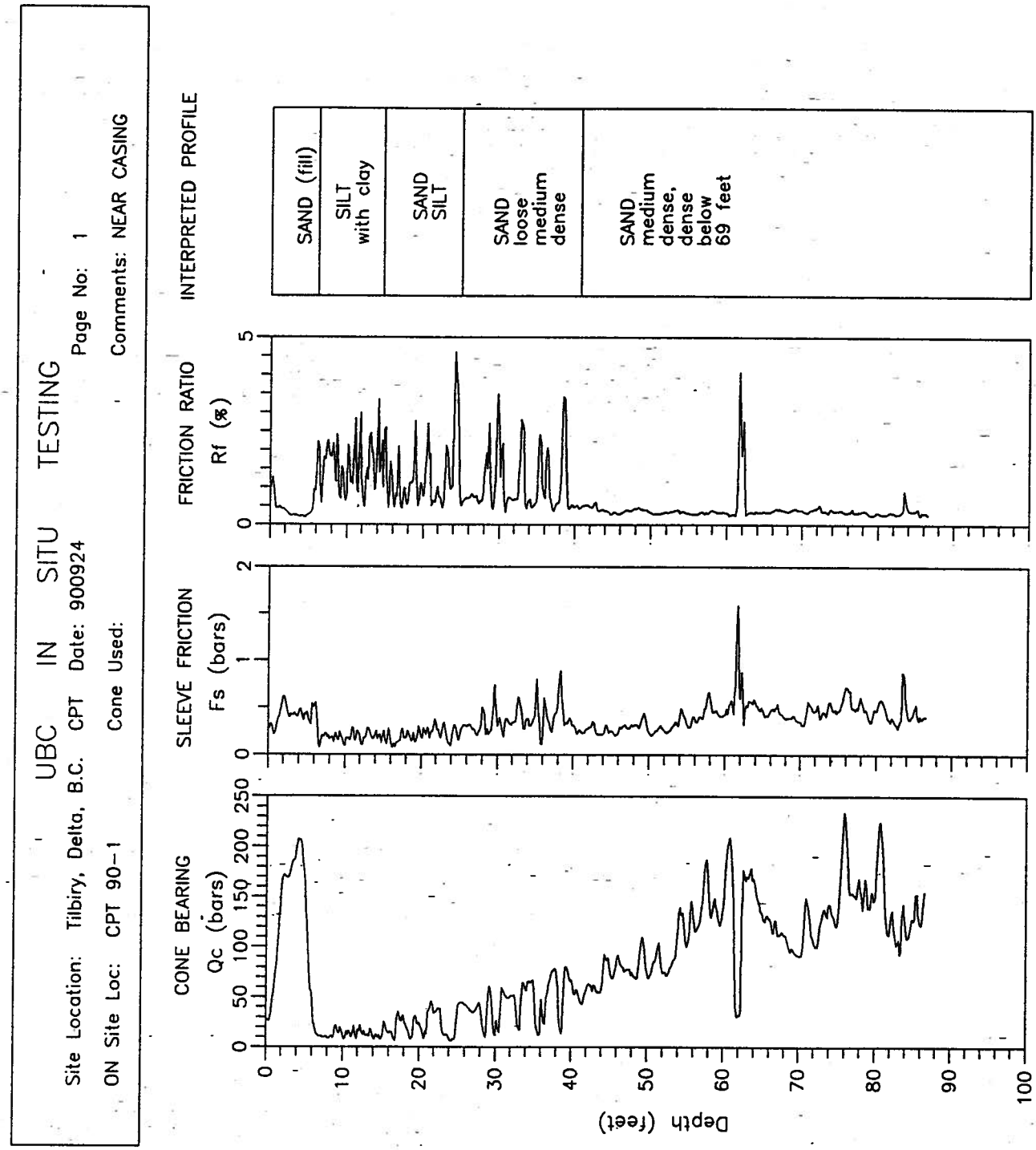

Figure 2.5: CPT Results of Tilbury Island Site

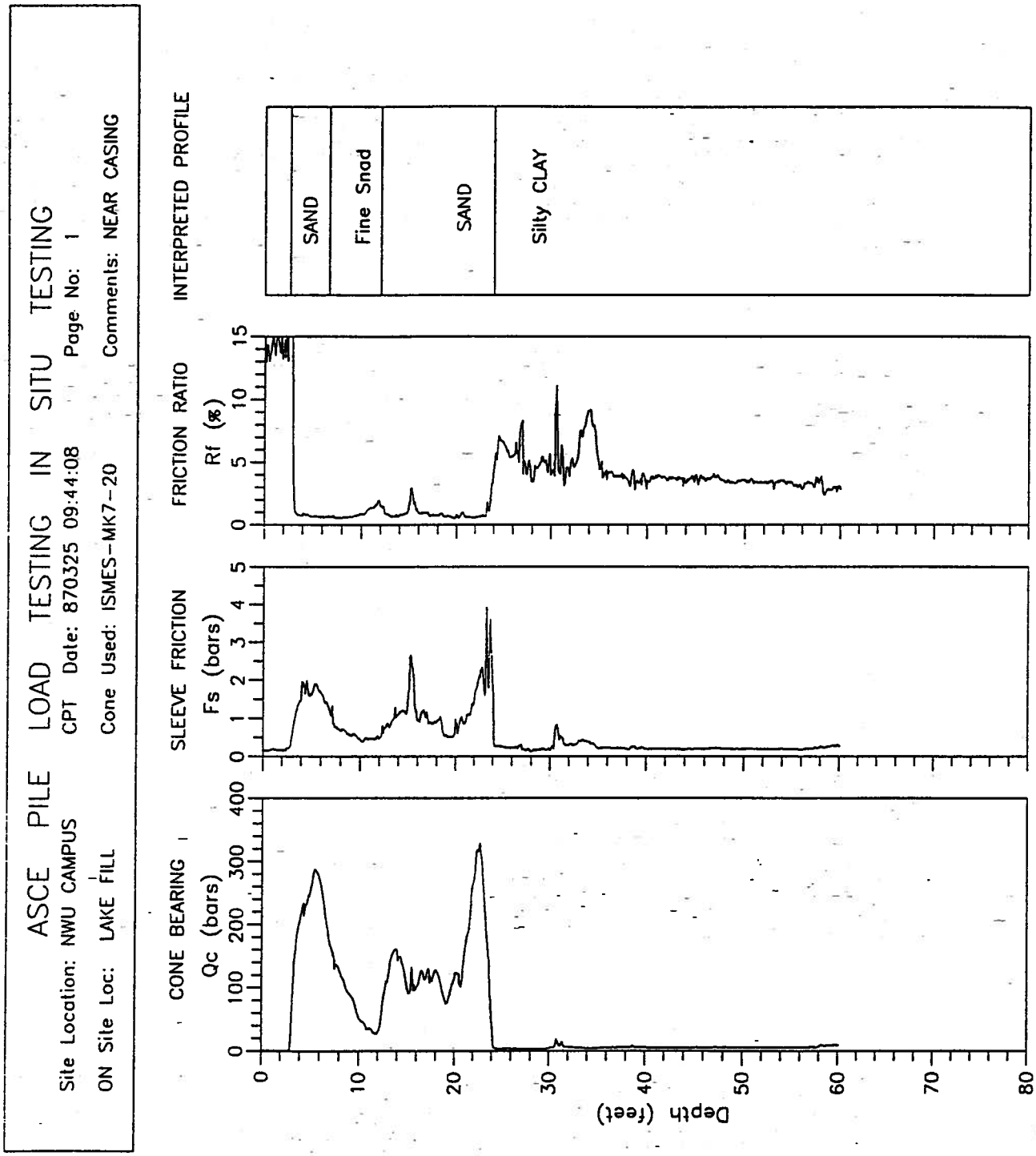

Figure 2.6: CPT Results of ECNU Site

Chapter 3

Pile Installation

3.1 Outline

The test piles installed at the three research sites included H pile and steel pipe piles with closed and opened ends. The hammer types used in installation included drop hammer, diesel hammer and steam hammer. During pile installation, blows per foot were recorded.

Load tests were carried out on UBC piles and ECNU piles. The results of the load testing are presented in tables in order to make comparison between predicted and measured pile capacity. The details of both the piles used and the load testing programs are from Davies (1987) for UBC piles and Finno (1989) for ECNU piles.

3.2 UBC Piles

Six piles were driven at UBC Pile Research Site during Aug. 15 to 19 1985. All of these piles were steel pipe piles. The details of these piles are given in Table 3.1. A summary of the driving and load testing is shown in Table 3.2. The complete driving record can be found in Appendix A (Davies, 1987).

All piles were driven with a steel drop hammer using a metal helmet and plywood cushion. Pile 1 was driven with a 4400 *lb* hammer and the others were driven with a 6200 *lb* hammer. Pile 1,2,3,5, and 6 were driven closed-ended with the base-plate flush with the diameter of the piles. Pile 4 was driven open-ended. Soil plug monitoring was

Table 3.1: Summary of UBC Piles (after Davies, 1987)

Pile *No.*	Outside Diameter (in)	Wall Thickness (in)	Cross Section area (in^2)	Pile Length $(feet)$	Open/Closed Ended
1	12.75	0.375	18.56	50.0	C
2	12.75	0.375	18.56	50.0	C
3	12.75	0.375	18.56	60.0	C
4	12.75	0.375	18.56	90.2	O
5	12.75	0.500	19.24	106.0	C
6	24.00	0.500	36.91	118.3	C

Table 3.2: Summary of Driving and Testing Details of UBC Piles (after Davies, 1987)

Pile *No.*	Embedded Length (in)	Hammer Weight (lb)	Drop Height $(feet)$	Driving Date(s)	Testing Date(s)	Capacity $(kips)$
1	47.0	4400	- 4	19 Aug. 85	9 Nov. 85	38.0
2	45.0	6200	- 3	16 Aug. 85	1 Mar. 86	50.0
3	55.0	6200	- 4	16 Aug. 85	9 Nov. 85	137.0
4	76.0	6200	- 5	16 Aug. 85	1 Mar. 86	270.0
5	102.0	6200	- 6 to 7	15 Aug. 85	22 Sep. 85	241.0
6	103.0	6200	- 10 max	14 Aug. 85	NOT TESTED	
				15 Aug. 85		

performed on pile 4 during driving. After final driving, the top of the soil plug was 26.47 $feet$ below ground surface, thus the total length of soil plug was 49.53 $feet$.

The load testing summary of the UBC piles is given in Table 3.2. The Quick Load Test Method of axial loading (similar to ASTM 43-81 Section 5.6) was used. Davisson's method (1973) of interpreting axial pile load test data was used in determining pile capacities of each pile. Experience has shown that piles driven in the Fraser delta reach their ultimate capacity after 4 to 5 weeks. Thus all capacities given in Table 3.2 are judged to be at their ultimate. Figure 3.1 presents a summary of the load-displacement test results. Based on this data, pile 1, 2, and 5 are interpreted as predominantly shaft

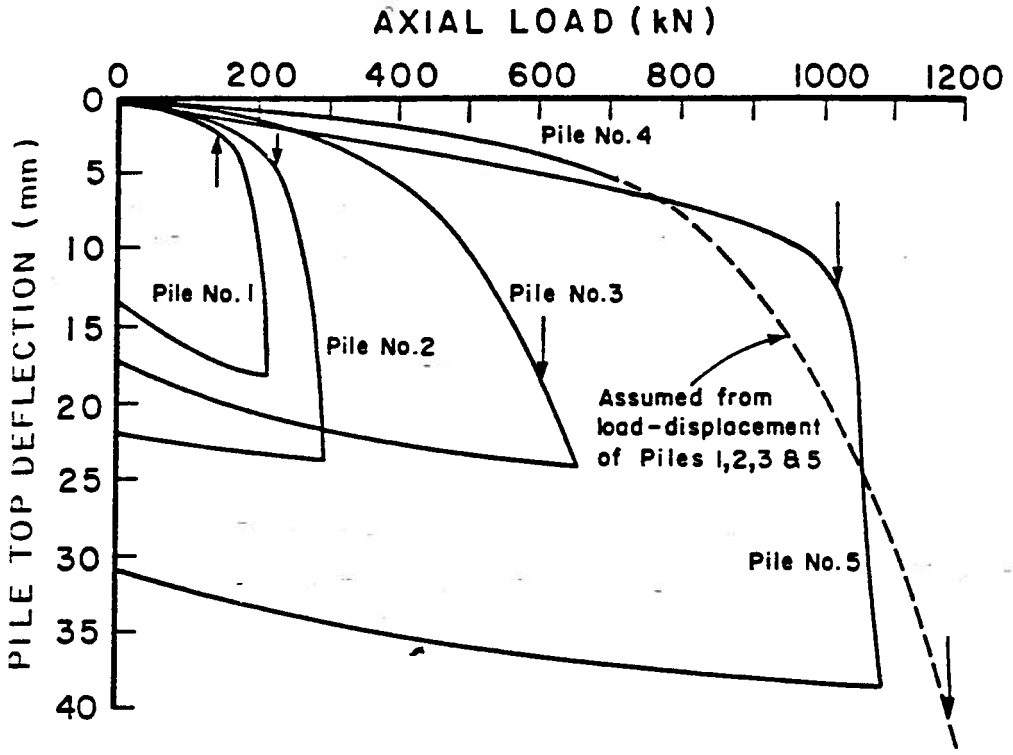

Figure 3.1: Load-Displacement Results of Load Testing for UBC Piles (after Robertson et al. 1987)

resistance piles, whereas pile 3 and 4 had significantly larger contribution to their total capacity from end bearing (Robertson et al, 1987).

3.3 Tilbury Piles

Four piles were driven in Tilbury Island Site during March 4th to 10th 1991. Among these piles, test pile 1, 2 and 3 were steel pipe pile, while pile HP was a steel H pile. For each pipe pile, the end was closed with a flush base plate. The base plate diameter was slightly larger than the diameter of the pile. The details of these piles are given in Table 3.3. A summary of driving data is given in Table 3.4. A complete driving record can be found in Appendix A.

For the first 15 and 24 *feet*, respectively, piles 1 and 2 were driven by a drop hammer with a ram weight of 12000 *lb*. For the first 20 *feet*, pile 3 was driven by a drop hammer

Table 3.3: Summary of Tilbury Piles

Pile No.	Outside Diameter (in)	Wall Thickness (in)	End-Plate Diameter (in)	End-Plate Thickness (in)	Cross Section Area (in^2)	Pile Length ($feet$)	Embedded Length ($feet$)
1	20.00	0.500	20.75	1.375	30.63	82.0	80.0
2	20.00	0.375	20.75	1.375	23.12	62.0	60.0
3	12.75	0.375	12.00	1.500	18.56	82.0	80.0
HP	12×53				15.50	100.0	97.0

Table 3.4: Summary of Driving Details of Tilbury Piles

Pile No.	Embedded Depth ($feet$)	Drop Hammer			Driving Date(s)
		Weight (lb)	Drop Height ($feet$)	Depth ($feet$)	
1	80.0	12000	4	15.0	9/10 Mar. 91
2	60.0	12000	4	24.0	9/10 Mar. 91
3	80.0	8000	4	24.0	9/10 Mar. 91
HP	97.0	8000	4	97.0	10 Mar. 91
D30-13 hammer was used after driving depth of drop hammer					

with a ram weight of 8000 lb. After this, they were driven by a D30-13 diesel hammer, with aluminum plus conbest cushion. The area of the hammer cushion was 238.5 in^2 and 415.5 in^2 for up to 16 in. and to 24 in. diameter piles respectively. The HP pile was driven by a drop hammer with a ram weight of 8000 lb. The blow rates of the diesel hammer were recorded and presented with pile driving records in Appendix I.

3.4 ECNU Piles (Finno et al.,1989)

The piles included one pipe pile, one 14×73 H pile and nine 10×42 H piles. The pipe pile was closed-ended, having a slightly oversized base plate. All test piles were embedded 50 $feet$. The details are given in Table 3.5 (Finno, 1989).

Table 3.5: Summary of ECNU Piles (after Finno, 1989

Pile Types	Outside Diameter (in)	Wall Thickness (in)	End-Plate Diameter (in)	End-Plate Thickness (in)	Cross Section Area (in^2)	Pile Length ($feet$)	Embedded Length ($feet$)
Pipe	18.00	0.375	19.00	0.750	20.76	53.0	50.0
HP1	14×73				21.40	52.0	50.0
HP2	10×42				12.40	60.0	50.0

Table 3.6: Summary of Measured Capacities of ECNU Piles (after Finno et al. 1989)

Pile Type	Measured Capacity ($kips$)		
	2 weeks	5 weeks	43 weeks
HP	180	194	220
Pipe	140	160	233

All piles were driven with a Vulcan 06 hammer. The driving system consisted of the Vulcan 06 hammer, a 5 $in.$ cushion of alternating plates of 1/2 $in.$ thick aluminum (4 plates) and 1 $in.$ thick micarta (3 plates) and a 1000 lb steel helmet. The cushion plates were 11-1/4 $in.$ outside diameter with a 3 $in.$ diameter hole in their centres. A 2-1/2 $in.$ thick striker plate topped off the aluminum-micarta cushion. The driving records of the piles are given in Appendix A. Note that a 12 $in.$ diameter hole was preaugered to a depth of 23 $feet$ at the location of the closed-ended pipe pile to assist in penetration.

The load testing was performed according to Standard Loading Procedures method described in ASTM D-1143-81. Loads were applied until pile failure. Table 3.6 presents the summary of measured capacity for each test with different elapsed time after pile driving (Finno et al., 1989). The ultimate (long term) capacity was not reached in 5 weeks, which was typical of the Fraser delta piles in sand, but took much longer as shown by the increase in capacity from 5 to 43 weeks. Thus longer time to ultimate

strength is likely due to the firm local sands which took longer time for pore pressure dissipation.

Chapter 4

Application of CPT in Pile Capacity Prediction

4.1 Introduction

The CPT is gaining acceptability as a tool for geotechnical investigation and design. It is particularly relevant for predicting the capacity of pile foundation. A summary of different methods of pile capacity prediction is represented by Davies (1987). In this study the pile capacity estimated from the CPT is adopted as a basic parameter to determine the ultimate resistance of a pile. Current methods of predicting pile capacity from CPT are based on measured CPT parameters as well as empirical factors. These method include: direct methods that use the CPT data without evaluating any intermediate values; and indirect methods that required intermediate correlations, such as coefficients of earth pressure, friction angle, etc..

4.2 Methods of Predicting Pile Capacity from CPT

In his earlier research, de Beer demonstrated that a scaling factor must be used to obtain the pile capacity using q_c from CPT. As shown in Figure 4.1, when a probe of zero diameter penetrate into soil layer, the penetration resistance will follow the idealized curve $ABCD$. That means the device would feel the entire effect of a lower soil layer immediately upon penetration. If a large diameter pile is pushed into the layer, the point resistance would not equal that of zero diameter probe until the pile reached a greater depth, at point E. This depth is often termed the critical depth (D_c). De Beer showed

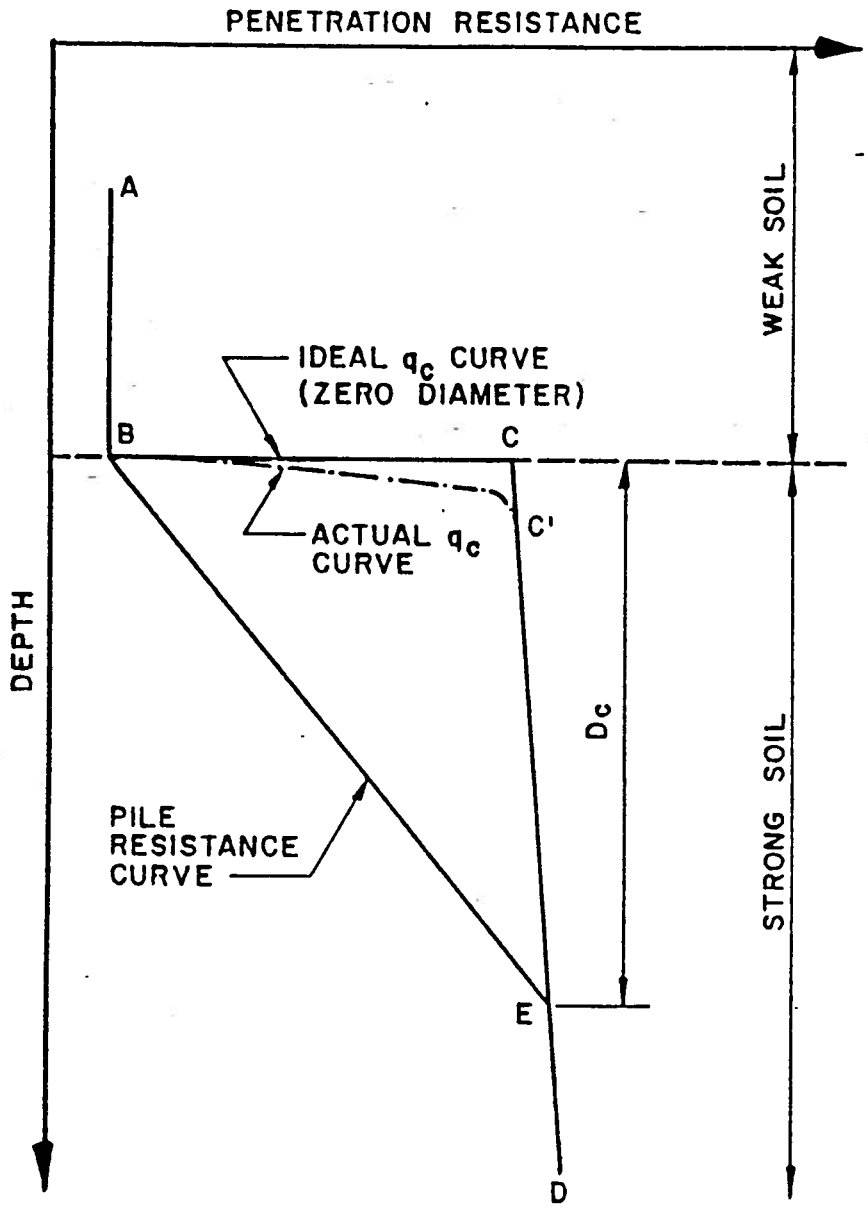

Figure 4.1: de Beer Scale Effect Diagram for CPT Pile Predictions (Adapted from Nottingham, 1975

that it is reasonable to assume that the pile resistance curve between point B and E varies linearly; thus, the pile resistance at any intermediate depth could be determined if the idealized penetration resistance curve and D_c were known. Although there is no probe of zero diameter, the diameter of the cone is sufficiently small that it can be assumed to approximate this condition, following curve $ABC'D$. Meyerhof, de Beer, and others have shown that D_c is a function of foundation size and soil stiffness. Therefore, it is more logical to express critical depth as a ratio $(D/B)_c$ in which B is the foundation diameter. When the thickness of high stiffness soil layers is less than D_c for a large diameter pile, the full penetration resistance may be mobilized on the cone but may not be realized for the pile before the influence of another layer is felt.

There are twelve prediction methods based on CPT data. A summary of these methods was made by Robertson (1986) and is shown in Table 4.1. Based on the study of Davies (1987), the direct and indirect methods both provide reasonable predictions of the measured pile capacity for smaller piles. For large piles however it was shown that while direct methods predict the pile capacities quite satisfactorily, indirect methods predicted pile capacities that were significantly in error and non-conservative when compared to the measured results for the large pile. Since indirect methods rely on correlations between the CPT data and intermediate parameters, they can give erroneous results in complicated soil conditions. Based on his research, Davies suggested that the method of LCPC CPT provided the best prediction for pile capacity. The LCPC CPT method does not require the CPT sleeve friction value other than to define soil type. This is a desirable feature since cone bearing is generally obtained with more accuracy and confidence than the sleeve friction, (Bustamante et al, 1982). In the following analysis, the LCPC CPT method was selected to predict pile capacity.

Table 4.1: Pile Capacity Prediction Methods Evaluated (after Robertson et al., 1987)

Direct Methods	References	Notes
1. Schmertmann and Nottingham CPT	Schmertmann (1978)	Proven CPT Method
2. de Ruiter and Beringe CPT	de Ruiter and Beringen (1979)	European (Fugro)
3. Zhou et al CPT	Zhou et al (1982)	Chinese Railway Experience
4. Van Mierlo and Koppejan CPT	Van Mierlo and Koppejan (1952)	Original Dutch
5. Laboratorie Central des Ponts et Chaussees CPT (LCPC)	LCPC - Bustamante and Gianesalli (1982)	French Method
Indirect Methods		
6. API RP2A	American Pet. Inst. (1980)	Offshore
7. Dennis and Olson	Dennis and Olson (1983 a and b)	Modified API
8. Vijayvergiya and Focht	Vijayvergia and Focht (1972)	"λ" Method
9. Burland	Burland (1983)	"β" Method
10. Janbu	Janbu (1976)	NIT
11. Myerhof Conventional	Myerhof (1976)	Original Bearing Theory
12. Flaate and Selnes	Flaate and Selnes (1977)	NGI

4.3 LCPC CPT method (Bustamante and Gianeselli, 1982)

This method is based upon the interpretation of a series of 198 full-scale static loading (or extraction) tests. The test data analyzed included 96 deep foundations on 48 sites, containing soils made up of such materials as clay, silt, sand, gravel or weathered rock, mud, peat, weathered chalk, and marl (Bustamante and Gianeselli, 1982). There were 31 driven piles with diameter ranging from 30 to 64 cm and lengths from 6 to 45 m. Driven piles included H piles, closed ended pipe piles and concrete piles. All the piles tested were loaded axially. Efforts were made to defined the real geometry of the shaft and the properties of soil around the shaft of pile.

The LCPC CPT method is based upon the work of Begemann (1963) and Van der Ween (1957) for point resistance calculation and Dinesh Mohan (1963) for skin friction calculation. The calculated limit load Q_L of a deep foundation is the sum of two terms, as shown in Equation 4.1.

$$Q_L = Q_L^P + Q_L^F \tag{4.1}$$

In equation 4.1 Q_L^P is the limit resistance under the pile tip. Q_L^F is the limit skin friction on the shaft of embedded length of the pile. They are calculated as follows:

$$\begin{cases} Q_L^P = q_{ca} \cdot k_c \cdot A_t \\ Q_L^F = \int_{i=1}^{n} Q_{Li}^F = \int_i^n f_{pi} \cdot A_{si} \end{cases} \tag{4.2}$$

where:

q_{ca} is the equivalent cone resistance at the level of the pile tip (in kN/m^2)

k_c is the penetrometer bearing capacity factor

f_{pi} is the limit unit skin friction over the thickness of the layer i

A_t is the area of pile tip

A_{si} is the area of pile shaft over the thickness of the layer i

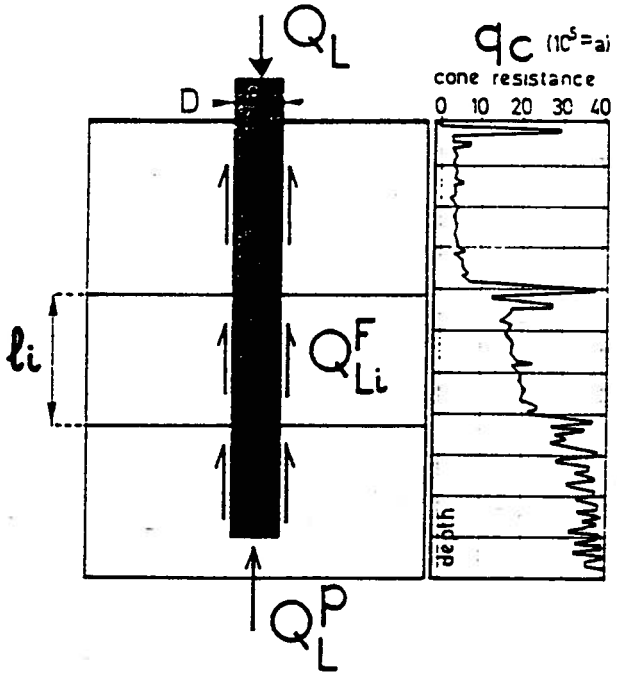

Figure 4.2: Pile Capacity Distribution (after Bustamante and Gianeselli, 1982)

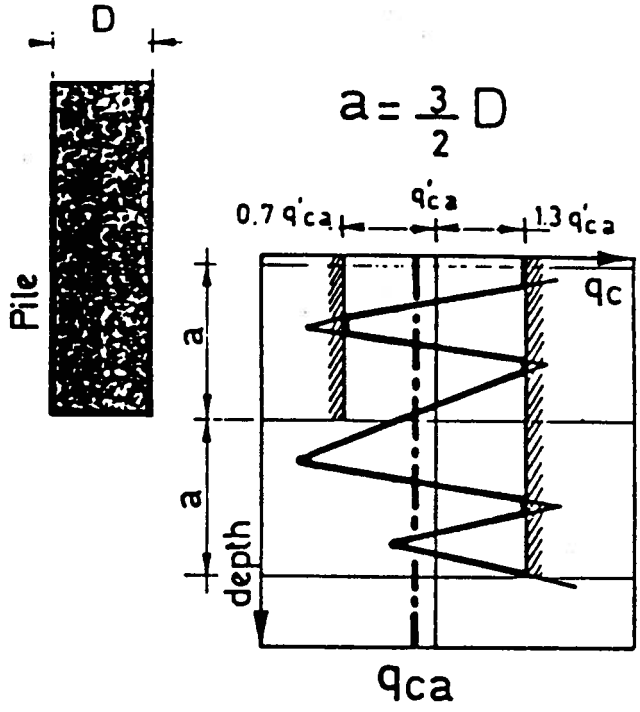

Figure 4.3: LCPC CPT Method to Determine Equivalent Cone Resistance at Pile Tip, (after Bustamante and Gianeselli, 1982)

i is the number of soil layers

The unit end bearing is calculated using an equivalent cone resistance at the pile end, as shown in Figure 4.3. In practice, the equivalent cone resistance q_{ca} is calculated in several steps. Firstly, the curve of the cone resistance q_c is smoothened so as to remove the local irregularities of the data. To be conservative, the smoothened curve is made to pass closer to the valleys than to the peaks. Then using the smoothened curve, q'_{ca} is calculated which is the mean of the smoothened resistance between the values $-a$ to $+a$ where a is 1.5 times the diameter of pile. Finally, the equivalent cone resistance q_{ca} is calculated after clipping the smoothened curve. This peak clipping is carried out so as to eliminate only the values higher than 1.3 $q_{ca'}$ under the pile tip, whereas the values higher than 1.3 $q_{ca'}$ and lower than 0.7 $q_{ca'}$ are eliminated above the pile tip (Bustamante and Gianeselli, 1982).

The value of k_c depends on the nature of the soil, the value of q_c and also, on the pile placement techniques. For driven piles, the value of k_c is without reserve to closed ended pipe piles. For open ended pipe piles and H piles, the value of k_c must be reduced unless it can be demonstrated, either with reference to similar cases or preferably as a result of full-scale loading test, that a soil plug occurs under the pile point, capable of taking up the equivalent forces of a point whose section would be determined by the circumscribed perimeter.

For each layer i, the limit unit skin friction f_p is calculated by dividing the cone resistance q_c corresponding to the given level by a coefficient α as shown in Equation 4.3 which accounts for the nature of the soil, the pile type and the placement method. In selecting the values of α, it is not necessary to account for the diameter of the pile or more precisely for the radius of curvature of the foundation.

$$f_p = \frac{q_c}{\alpha} \tag{4.3}$$

The values of bearing capacity factors k_c and f_p are given in Table 4.2 and Table 4.3 (Bustamante and gianeselli, 1982).

4.4 Pile Capacity Predicted from LCPC CPT Method

The comparison between predicted pile capacities using the LCPC CPT method and the results of load testing are shown in Figure 4.4 on UBC Pile 1, 2, 3, 4, and 5, Figure 4.5 on ECNU pipe pile, and Figure 4.6 on ECNU pile H14×73, respectively. In these figures, the curves of friction and total pile capacities are shown. The difference between the curves for total and frictional capacity is the end bearing capacity. Pile capacity is a function of elapsed time since driving (Soderberg, 1962). Normally, the load testing is performed after sufficient elapsed time. According to the study of Davies (1987) the load testings of UBC piles were performed based on the elapsed time which pore pressure fully dissipated. The elapsed times after driving were 38 days for pile 5, 84 days for pile 1 and 3 and 210 days for pile 2 and 4, respectivelly. The pile capacity determined from load testing was considered to be a long term pile capacity.

In general, predicted pile capacities show very good agreement with measured pile capacities. From the results of the ECNU load testing given in Table 3.6, the predicted pile capacity agree best with the pile capacity measured after a long elapsed time. This demonstrates that the pile capacity determined from LCPC CPT method represents a long term pile capacity. Because of the small end area of the H piles, the determined pile capacities of H piles show a very low end bearing capacity. The frictional component comprises the bulk of total pile capacity. Thus H piles are characteristically friction piles.

Table 4.2: Bearing Capacity Factor k_c (from Bustamante and Gianeselli, 1982)

Nature of Soil	q_c (MPa)	Factors k_c	
		Group I	Group II
Soft clay and mud	< 1	0.40	0.50
Moderately compact clay	1 to 5	0.35	0.45
Silt and loose sand	≤ 5	0.40	0.50
Compact to stiff clay and compact silt	> 5	0.45	0.55
Soft chalk	≤ 5	0.20	0.30
Moderately compact sand and gravel	5 to 12	0.40	0.50
Weathered to fragmented chalk	< 5	0.20	0.40
Compact to very compact sand and gravel	< 12	0.30	0.40
Group I: Plain bored piles Mud bored piles Micro piles (grouted under low pressure) Cased bored piles Piers Barrettes			
Group II: Cast screwed piles driven precast piles Prestressed tubular piles Driven cast piles Jacked mental piles Micropiles (small diameter piles grouted under high pressure with diameter $< 250\ mm$) Driven grouted piles (low pressure grounting) Driving mental piles Driving rammed piles Jacked concrete piles High pressure grouted piles of large diameter			

Table 4.3: Friction Coefficient, α (from Bustamante and Gianeselli, 1982)

Nature of Soil	q_c (MPa)	Coefficients, α				Maximum Limit of f_p (MPa)					
		Category									
		I		II		I		II		III	
		A	B	A	B	A	B	A	B	A	B
Soft clay and mud	< 1	30	30	30	30	0.015	0.015	0.015	0.015	0.035	-
Moderately compact clay	1 to 5	40	80	40	80	0.035 (0.08)	0.035 (0.08)	0.035 (0.08)	0.035	0.08	≥ 0.1
Silt and loose sand	≤ 5	60	150	60	120	0.035	0.035	0.035	0.035	0.08	-
Compact to stiff clay and compact silt	> 5	60	120	60	120	0.035 (0.08)	0.035 (0.08)	0.035 (0.08)	0.035	0.08	≥ 0.2
Soft chalk	≤ 5	100	120	100	120	0.035	0.035	0.035	0.035	0.08	-
Moderately compact sand and gravel	5 to 12	100	200	100	200	0.08 (0.12)	0.035 (0.08)	0.08 (0.12)	0.08	0.125	≤ 0.2
Weathered to fragmented chalk	> 5	60	80	60	80	0.12 (0.15)	0.08 (0.12)	0.12 (0.15)	0.12	0.15	≤ 0.2
Compact to very compact sand and gravel	> 12	150	300	150	200	0.12 (0.15)	0.08 (0.12)	0.12 (0.15)	0.12	0.15	≤ 0.2

IA - Plain bored piles
mud bored piles
Hollow auger bored piles
Micropiles (grouted under low pressure)
Cast screwed piles
Piers
Barettes

IB - Cased bored piles
Driven cast piles

IIA - Driven precast piles
Prestressed tubular piles
Jacked concrete piles

IIIA - Driven grouted piles
Driven rammed piles

IIB - Driven metal piles
Jaked metal piles

IIIB - High pressure grouted piles with diameter $> 250\ mm$
Micro piles grounted under high pressure

Note:
Max. limit unit skin friction, f_p: bracket values apply to careful execution and minimum disturbance of soil due to construction.

Similarly for both open and closed ended pipe piles (UBC Pile 1 to 5), when the pile tip is embedded in a soft soil layer (lower q_c), the end bearing is a small component of the total capacity, and the frictional resistance comprises the bulk of the total pile capacity. From Figure 4.4 (pile 1 and pile 2), Figure 4.5 and Figure 4.6, the predicted pile capacities agree well with measured pile capacities. These results suggest that not only the total pile capacity but also frictional resistance can be predicted well by using LCPC CPT method. Since frictional resistance and end bearing are estimated separately in the LCPC CPT method, both frictional resistance and end bearing can be estimated separately in predicting long term pile capacity

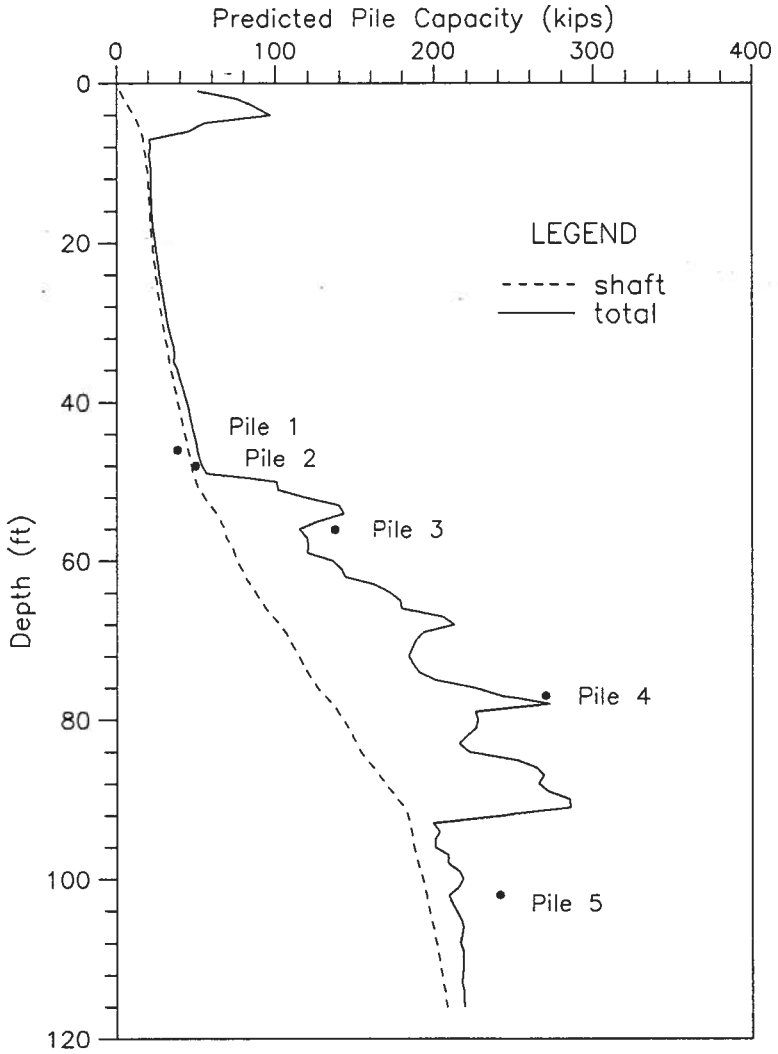

Figure 4.4: Pile Capacity Predicted from LCPC CPT Method on UBC Pile 1, 2, 3, 4 and 5

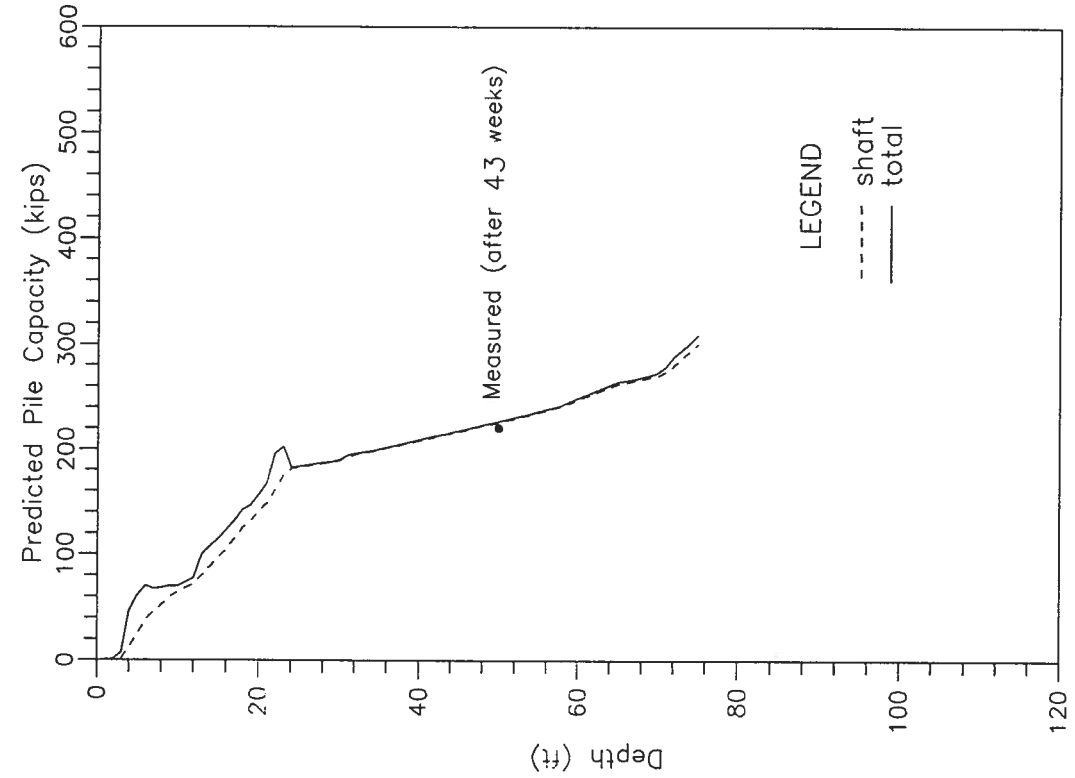

Figure 4.6: Pile Capacity Predicted from LCPC CPT Method on ECNU 14×73 H Piles

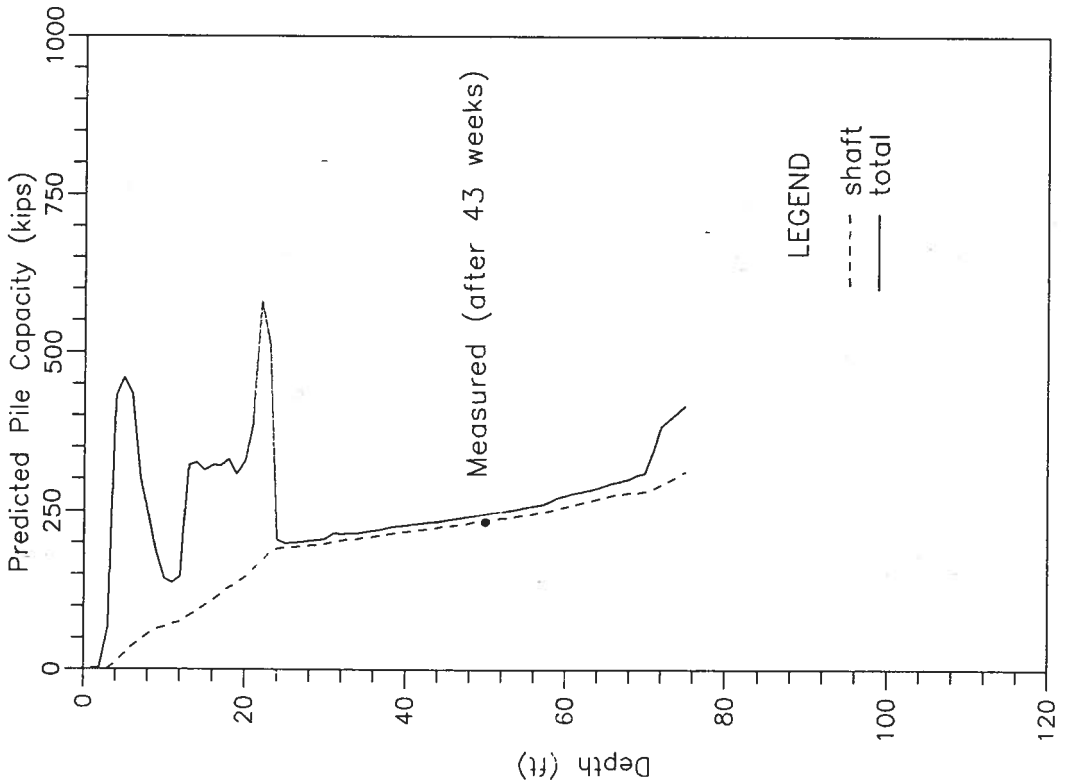

Figure 4.5: Pile Capacity Predicted from LCPC CPT Method on ECNU Pipe Pile

Chapter 5

Wave Equation Analysis of Piles

5.1 Introduction

Since the research of Isascs (1931), it has been recognized that the behaviour of driven piles does not follow the simple Newtonian impact as assumed by many simplified pile-driving formulas. Hence a computational tool for the analysis of pile driving, known as the Wave Equation, was developed based on a one-dimensional wave equation. In 1950, Smith developed a solution to the wave equation that could be used to solve extremely complex pile-driving problems. The solution was based on a discrete element idealization of an actual hammer-pile-soil system using a high-speed digital computer. In a paper published in 1960, he dealt exclusively with the application of wave theory to the investigation of dynamic behaviour of pile during driving. Figure 5.1 shows a schematic representation of the wave equation model. Many Wave Equation programs have been developed. One of the most widely used today is a program called WEAP, developed by Goble and Rausche. Since the original program in 1976, WEAP was updated to WEAP87 and then to GRLWEAP which is the program used in the subsequent analysis.

5.2 GRLWEAP Program

5.2.1 Background of GRLWEAP Program

The pile driving process provides information regarding the soil resistance. The greater the permanent set, S, of a pile under a hammer blow with energy E_k, the less the total

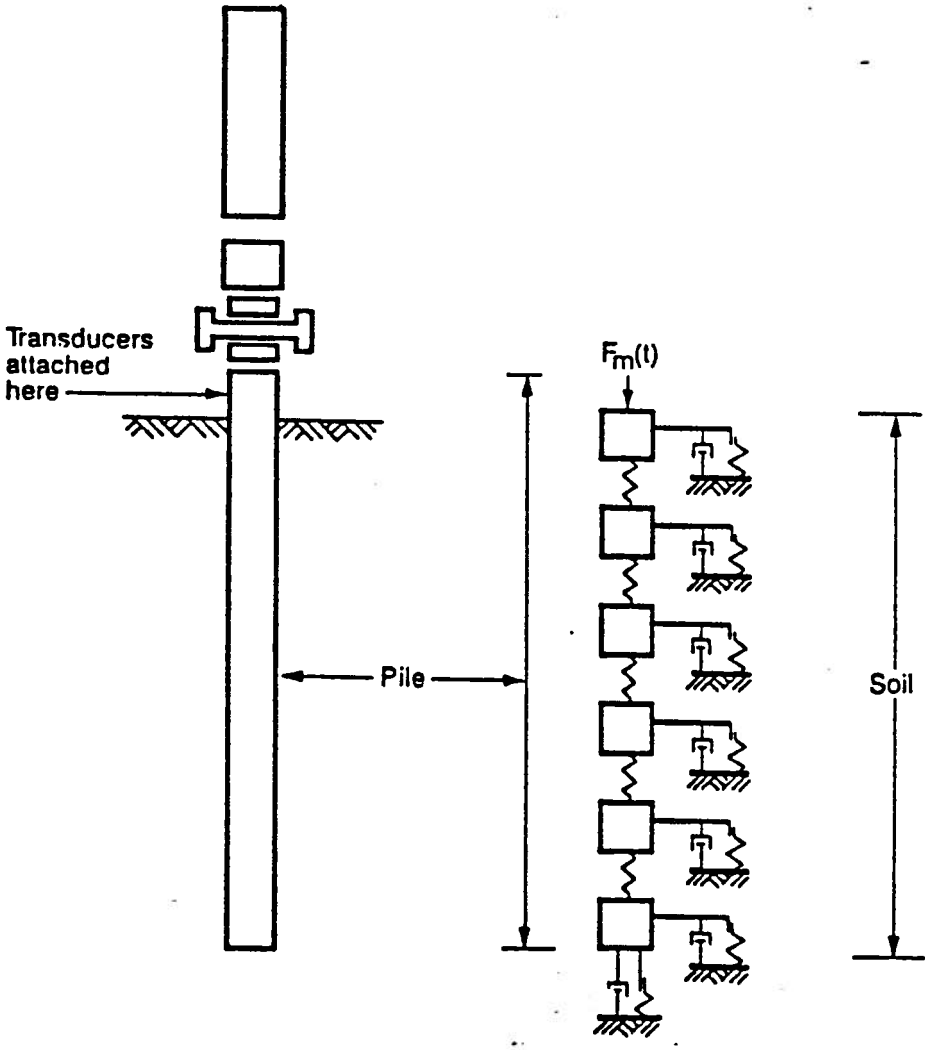

Figure 5.1: Schematic Representation of Driving System for Wave Equation Model

driving resistance R_t, which opposes the pile penetration. The energy formula describing the driving process can be expressed as follows:

$$e_d e_h E_r - E_{pl} - E_{sl} = R_t S \tag{5.1}$$

where:

e_d is coefficient less than 1 to consider energy loss in driving system

e_h is hammer efficiency;

E_r is rated energy given by manufacturer;

E_{pl} is energy lost in pile;

E_{sl} is energy lost in soil;

R_t is total drving resistance, and

S is permanent set of a pile under one blow.

Assuming E_r is known, the values e_d, e_h, E_{pl} and E_{sl} can be estimated, the following can be done:

a) Compute the set s using predicted value of R_t before the pile is driven. The blow count, B_c, is then merely the inverse of s.

b) During pile driving, B_c may be observed and R_t computed. This process is known as a dynamic pile test.

c) A bearing graph can be constructed with the ultimate soil capacity plotted versus blow count for corresponding depth. This is an analysis of drivability.

The wave equation approach differs from the energy formula in that the parameters e_d, E_{pl}, and E_{sl} are computed. They are computed by modelling the driving system, pile, and soil behaviour. Only the hammer efficiency is estimated.

Hammer Model

The following hammer types can be selected in the program:

Diesel hammer with liquid injection.

Diesel hammer with atomized injection.

External combustion hammers (air/steam/hydraulic).

The ram is the most important hammer component. A single mass segment is often used in analysis. For slender rams, often encountered in diesel and modern hydraulic units, more than one ram segment may be necessary for simulation. As a rule, ram segments should not be shorter than 2.5 *feet* or unnecessary computational efforts will result.

Driving System Model

The driving system consists of striker plate, hammer cushion, helmet and, for concrete piles, pile cushion. The spring for the pile cushion is modeled in series with the first pile spring. For external combustion hammers, the hammer cushion spring acts in series with the ram spring, as shown in Figure 5.2. The weight of devices like the striker plate, cushion, pile adaptors etc. should be included in the mass between hammer and pile top.

Pile Model

The pile model consists of springs, masses and dashpots, as shown in Figure 5.3. The pile is divided into N segments whose lengths are given by

$$l_i = a_i L \tag{5.2}$$

L is the total pile length and a_i is a multiplier which describes the length of the segment l_i with respect to the overall length of the pile.

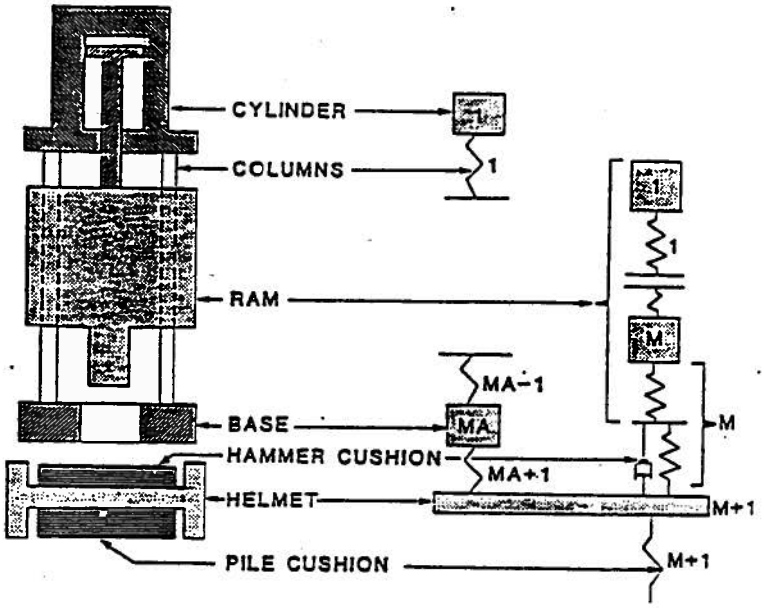

Figure 5.2: Hammer Driving System model for ECH hammer (adapted from GRLWEAP Menu)

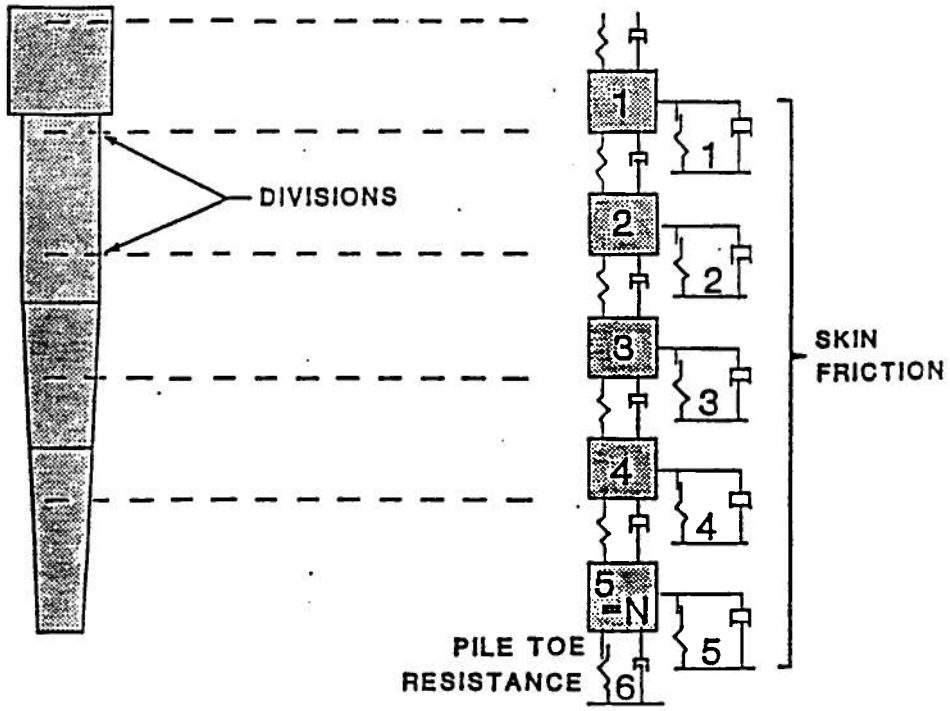

Figure 5.3: Pile and Soil Model used in GRLWEAP Program (adapted from GRLWEAP Menu)

Therefore:

$$\int_{i=1}^{N} a_i = 1.0, \qquad i = 1, 2, \cdots, N. \tag{5.3}$$

The weight of segment i is then:

$$W_i = W_i A_i l_i \tag{5.4}$$

W_i is the average specific weight and A_i is the average cross sectional area of the pile element, both averaged over the distance l_i.

Similarly the segment stiffness are

$$k_{pi} = \frac{E_i A_i}{l_i} \tag{5.5}$$

E_i is the average elastic modulus over the element length.

Viscous damping is assumed with parameters:

$$c_{dp} = \frac{1}{50} c_{dpi} \frac{EA}{c} \tag{5.6}$$

c_{dpi} is a non-dimensionalized input quantity and EA/c is the impedance of the pile top and c_{dp} is assumed equal for all elements.

Soil model

The soil model basically consists of a spring and dashpot, as shown in Figure 5.3. The quake and viscous damping are defined as shown in Figures 5.4 and 5.5. The elastic spring yields at a pile segment displacement equal to q_i (quake). Beyond the quake, there no further increase in static resistance, R_{si}, with increasing displacement, u_i. Thus,

$$\begin{cases} R_{si} = \frac{u_i}{q_i} R_{uti} & \text{for } u_i \leq q_i \\ R_{si} = R_{uti} & \text{for } u_i > q_i \end{cases} \tag{5.7}$$

R_{uti} is the ultimate static resistance during driving at segment i. R_{uti} at each segment is determined from the total ultimate static resistance during driving, R_{ut}, which is

divided into two parts, friction and end bearing. The percentage of friction is determined by the option, $IPERCS$, in the input menu of the program.

For unloading, i.e. when the pile segment has an upward velocity, a spring rate that is equal to that used in the loading path is used.

The damping models used in this study is according to Smith (Goble et al, 1987) which is defined by Equation 5.8.

$$R_{di} = j_{si} R_{si} V_i \tag{5.8}$$

where

R_{di} is a dynamic resistance at segment i;

j_{si} is the Smith damping factor at segment i;

V_i is the velocity of pile segment i , and

R_{si} is the static resistance at segment i.

Smith's damping factor has units of time/length.

Numerical Procedure and Integration

The time increment is chosen as follow:

$$t = \frac{\min(t_{cri})}{p} \tag{5.9}$$

$\min(t_{cri})$ stands for the minimum critical time of all segments, i, and p is a number greater than 1.0. The analysis steps are shown in Figure 5.6.

Analysis Stop Criteria

According to the stop criteria given by GRLWEAP program, the analysis is run until the specified elapsed time, t_{max}, has been covered. The limitation of t_{max} is 499 ms. For a drop hammer, if the user does not specified a time, the analysis will cover an elapsed

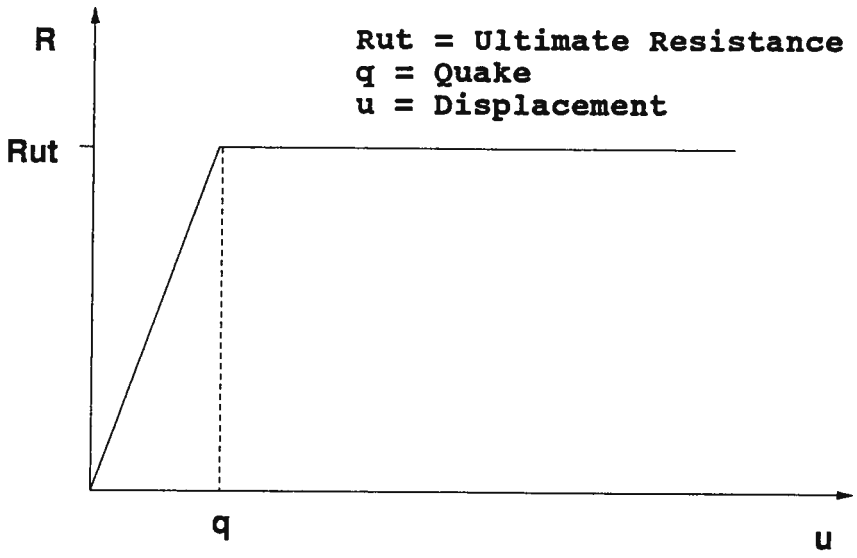

Figure 5.4: Definition of Soil Quake

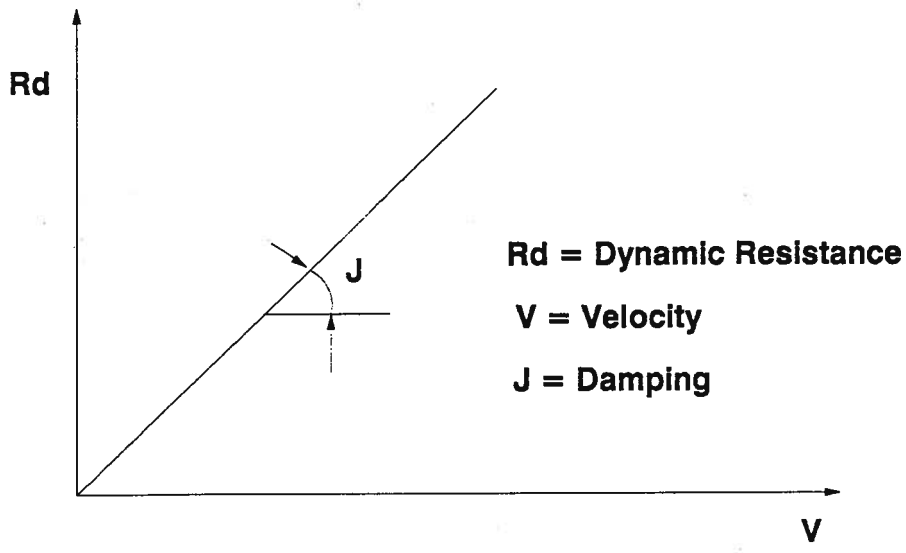

Figure 5.5: Definition of Soil Viscous Damping

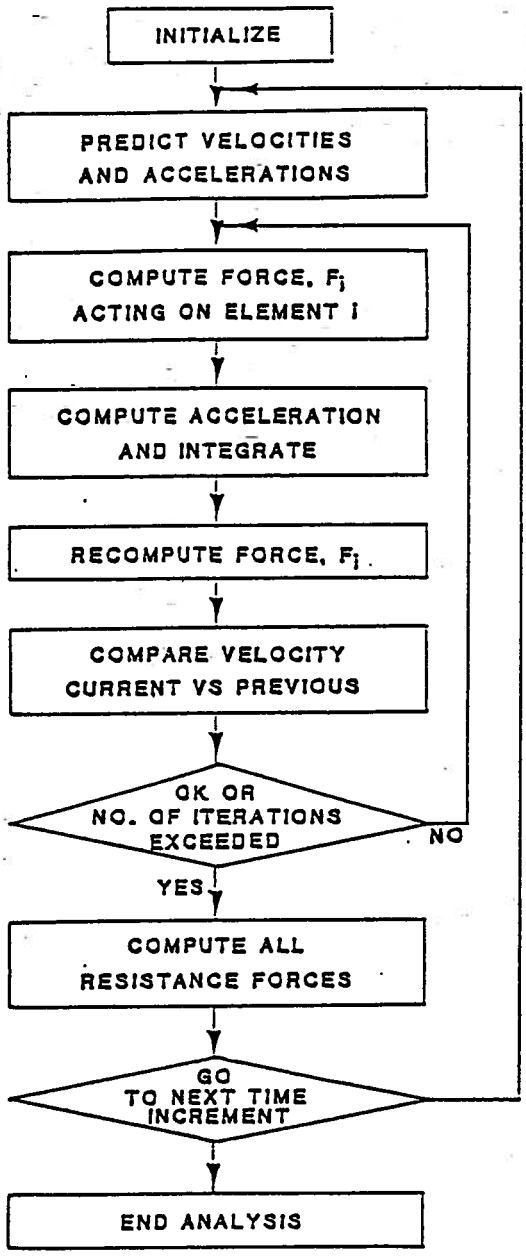

Figure 5.6: Block Diagram of Predictor Corrector Analysis for GRLWEAP Program (adapted from GRLWEAP Menu)

time of at least twice the pile length divided by wave speed or 20 ms. For diesel hammer, if the user does not specified a time, the analysis will cover an elapsed time of $2L/c+5ms$ or 50 ms, whichever is longer.

Non Residual Blow Count Computation

The difference between the maximum toe displacement, u_{mt}, and the toe quake, q_t, is used as a prediction of the final net set of the pile. An average quake used in program is computed as follows:

$$q_{av} = \int_{i=1}^{N+1} \frac{R_{uti} q_i}{R_{ut}} \tag{5.10}$$

R_{uti} and q_i are the individual ultimate static resistance and quake, respectively, and R_{ut} is the total ultimate staic capacity. N is the number of pile segments. The $N+1$ resistance is the end bearing. The predicted permanent pile set is then computed as follows:

$$s = u_{mt} - q_{av} \tag{5.11}$$

and the blow count is calculated as follows:

$$B_{ct} = \frac{1}{s} \tag{5.12}$$

5.3 Preliminary Analysis of the GRLWEAP Program

5.3.1 Outline

When using the GRLWEAP program for pile driving analysis, the hammer, pile and soil parameters are selected according to the driving equipment used, the type of pile and soil type. Some parameters are suggested by the program based on experience and correlations with past field tests. In practice, it is recommended that the influence of the different parameters be examined so that the sensitivity of the parameters can be

Table 5.1: Parameters of UBC Pile 3 and Driving Data

Pile	Length ($feet$)	Outside Diameter (in)	Wall Thickness (in)	Ended	Embedded Depth ($feet$)
	60.00	12.75	0.375	closed	55.00

Driving Data	Hammer		Hammer Cushion		
	weight ($kips$)	drop ($feet$)	area (in^2)	E modulus (ksi)	thickness (in)
	6.20	4.00	144.00	100.0	2.25

determined. This will allow a reasonable range of parameters to be selected for analysis. In order to select the parameters in the analysis, a preliminary analysis was carried out.

5.3.2 Basic Pile and Soil Conditions

UBC pile 3 is a steel pipe pile, the details of this pile are summarized in Table 5.1 with driving data. The ultimate capacity of UBC pile 3 determined from the static axial load test is 133 kips. The soil condition are given in Figure 2.4.

5.3.3 Analyses and Results

The influences of various parameters are examined and the results of the analysis are shown in Figures 5.7 to Figure 5.13. The results are discussed below in terms of the parameters considered.

A. Effect of Friction ($IPERCS$)

From the results shown in Figure 5.7 and Figure 5.8, the effect of $IPERCS$ is small. For the same ultimate total resistance, the blow count generally increased with increasing $IPERCS$, (i.e. with increasing skin friction and decreasing tip resistance). The blow count is only increased 3.3% from 25% $IPERCS$ to 75% $IPERCS$ for an ultimate

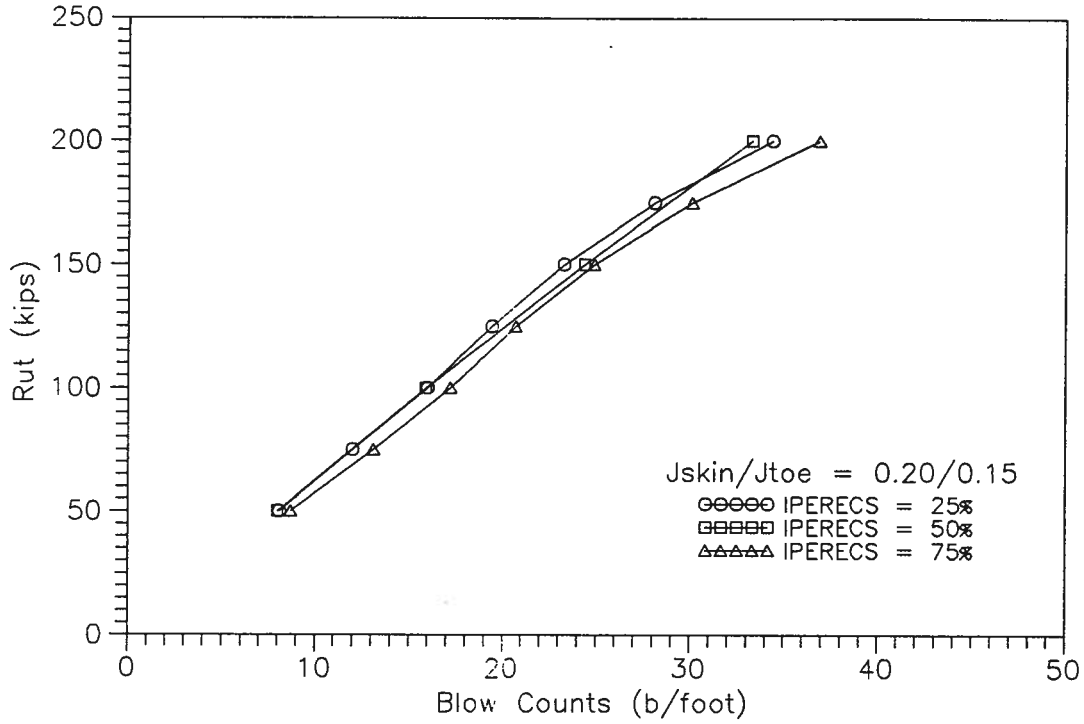

Figure 5.7: Effect of Friction Percentage

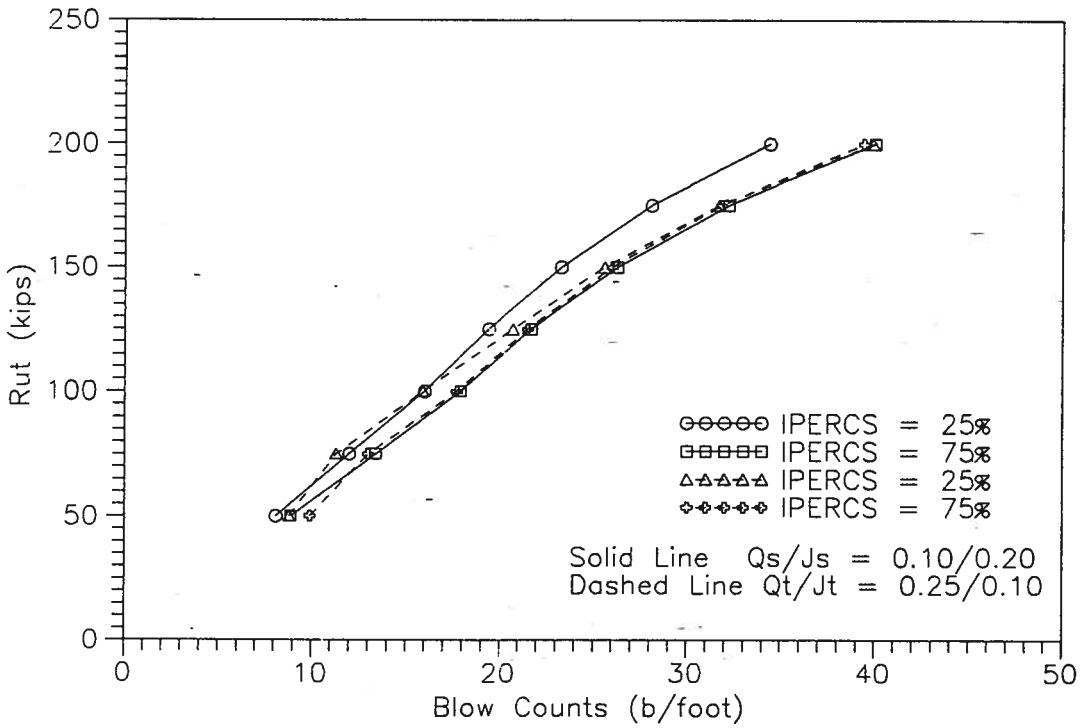

Figure 5.8: Effect of Friction Percentage with Different Values of Quake

capacity equal to 133.0 *kips*. Figure 5.8 also shows that the influence of $IPERCS$ is small for constant $Quake/J$ for both skin and tip.

B. Effect of Hammer Efficiency

The effect of hammer efficiency is very important in the analysis, as shown in the Figures 5.9 and 5.10. Figure 5.9 shows that the blow count increases about 42% when the hammer efficiency decreases from 75% to 50% at an ultimate resistance of 133 *kips*. The change in blow count versus the hammer efficiency is not proportional for different ultimate capacities, as shown in Figure 5.10. When the ultimate resistance is low, lower energy is needed to drive the pile to the desired depth. In this case increasing hammer efficiency does not effect the blow count significantly. When the ultimate resistance is high, the energy needed to drive the pile to the desired depth increases. The higher the ultimate resistance, the more sensitive is the blow count to hammer efficiency.

From the above results, it is clear that hammer efficiency has an important influence on the analysis. In practice, it is a difficult to get accurate hammer efficiency value, unless it is measured in the field during pile driving.

C. Effect of Smith's Damping

Smith's damping values have some influence on the results. The effect depends on the combination of J_{skin} and J_{toe} as shown in Figure 5.11. For the same ultimate capacity, the blow count increased with increasing damping values. The largest difference occurs if both J_{skin} and J_{toe} are increased at the same time. According to the definition of the damping model shown in Equation 5.8, the dynamic soil resistance is proportional to the damping factor. The dynamic resistance will increase with increased soil damping factor. Similarly the total soil resistance during pile driving increases with damping. The blow count will increase with increasing soil resistance for a given hammer energy. On the

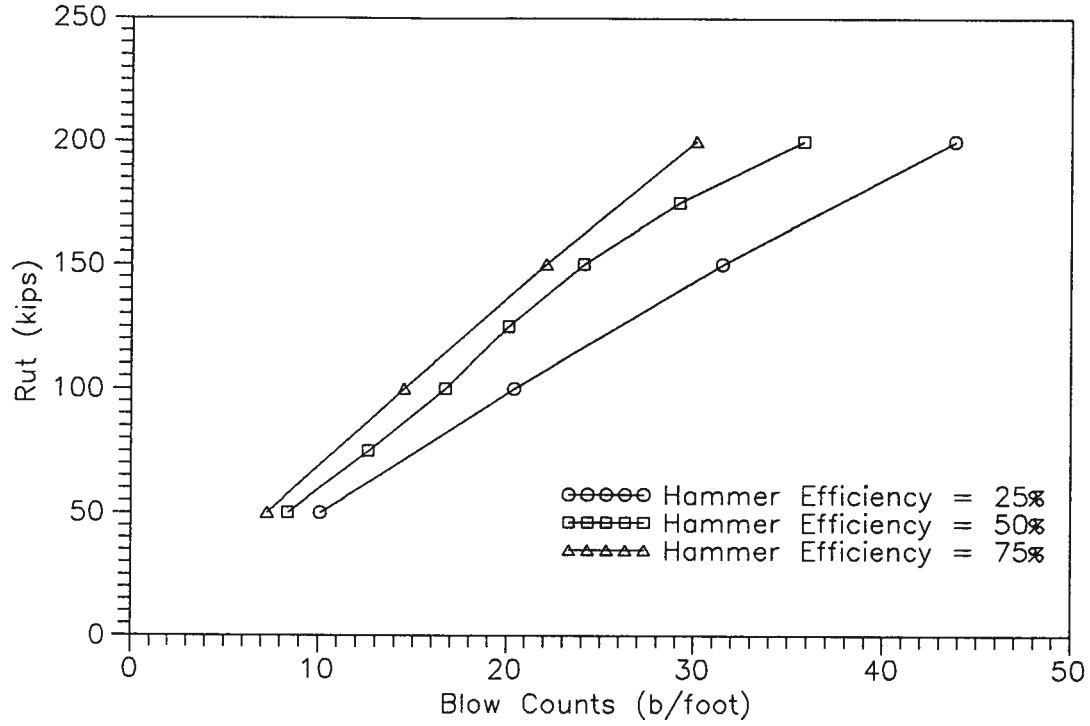

Figure 5.9: Effect of Hammer Efficiency

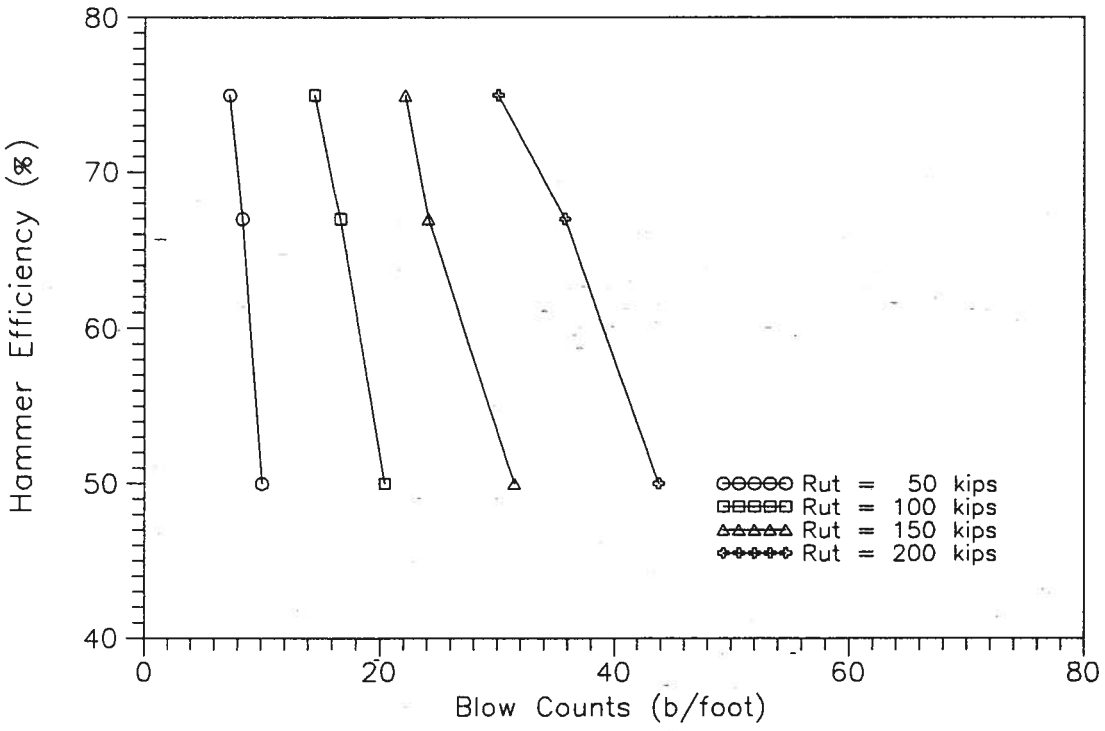

Figure 5.10: Effect of Hammer Efficiency with R_{ut}

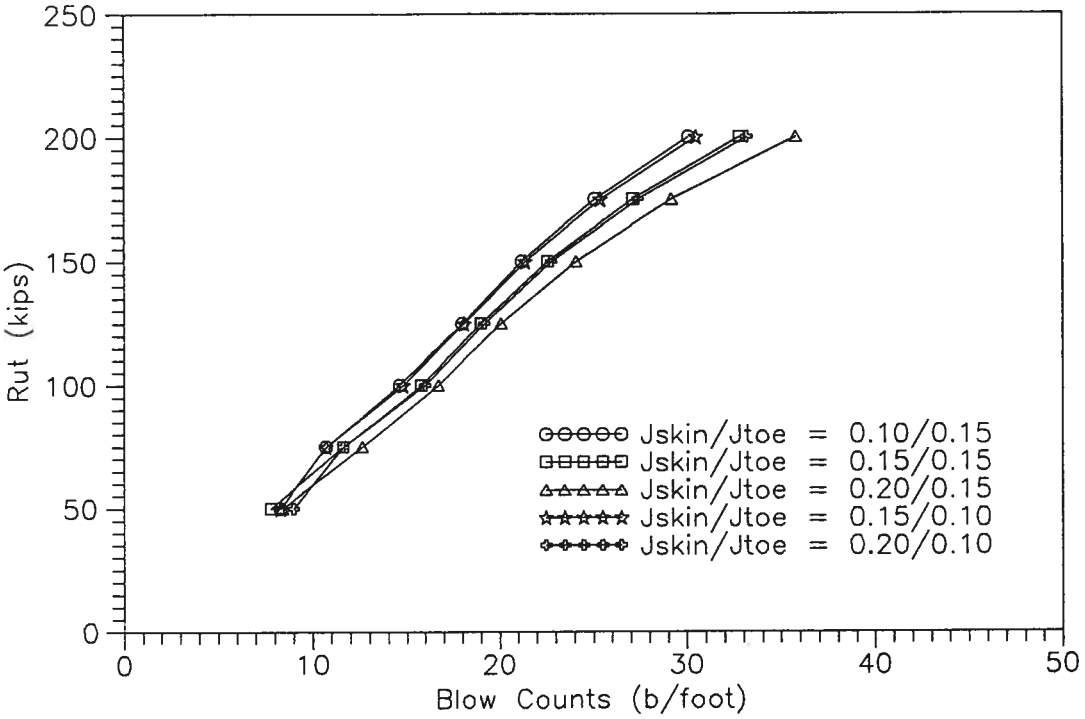

Figure 5.11: Effect of Smith's Damping

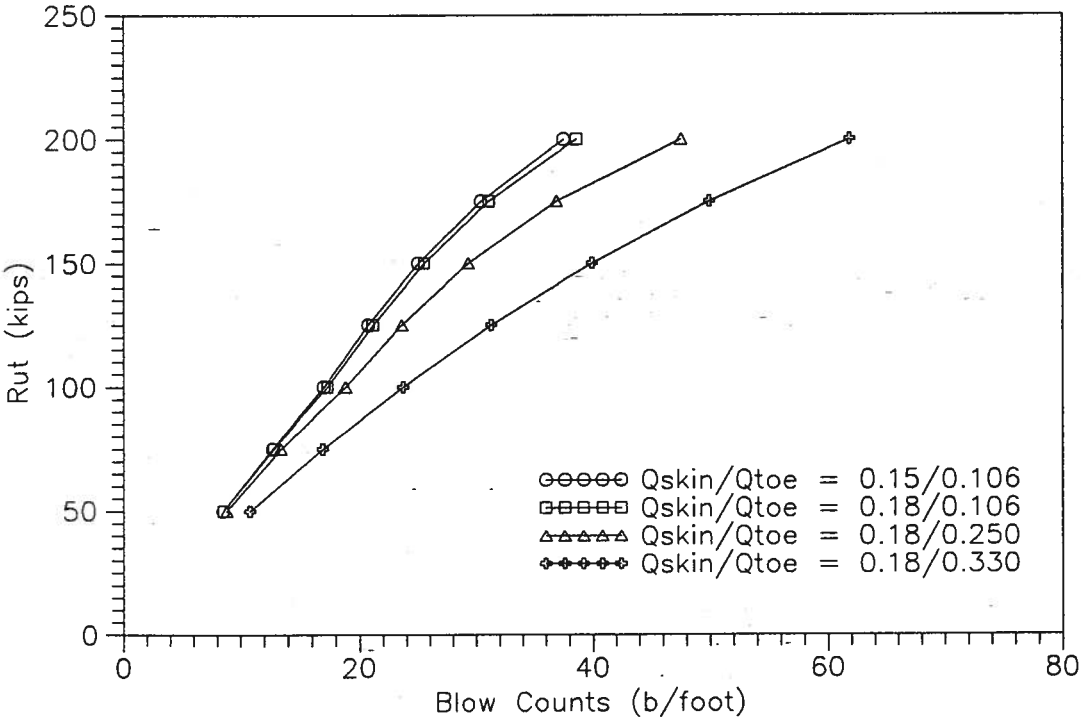

Figure 5.12: Effect of Skin Quake

other hand, the results are nearly the same when one parameter is increased and the other decreased by the same amount, ie. curve 0.15/0.10 is about the same as 0.10/0.15, and the curve 0.20/0.10 is about the same as 0.15/0.15, where the ratio is J_{skin}/J_{toe}. Based on these results the ratio of J_{skin}/J_{toe} is not as important as the overall value of the damping $J_{skin} + J_{toe}$. Damping is generally selected based on experience, however this points out the need for good in situ damping values to confirm the assumption that are being made

D. Effect of Quake

The effect of the quake parameters is similar to Smith's damping parameters, although quake may have a greater influence. When soil quake increases, the soil stiffness decreases, and consequently the maximum amount that the hammer can drive the pile is reduced (Authier and Fellenius, 1980). Figure 5.12 shows that the blow count increases about 30% for values of q_{skin}/q_{toe} increasing from 0.10/0.106 to 0.18/0.33. Keeping the q_{skin} constant, the blow count increased about 10% with the q_{toe} increased from 0.106 to 0.25 at ultimate capacity equal 133 kips, as shown in Figure 5.13. The results show that the quake values have an important influence on the final result of analysis using GRLWEAP program.

5.3.4 Conclusion

Based on the preliminary analysis for UBC Pile 3, it can be concluded that hammer efficiency is the most important factor in the analysis, followed by quake, and Smith's damping values. The influence of *IPERCS* is very small, and the result of the analysis will not change very much for different proportions of skin friction to end bearing.

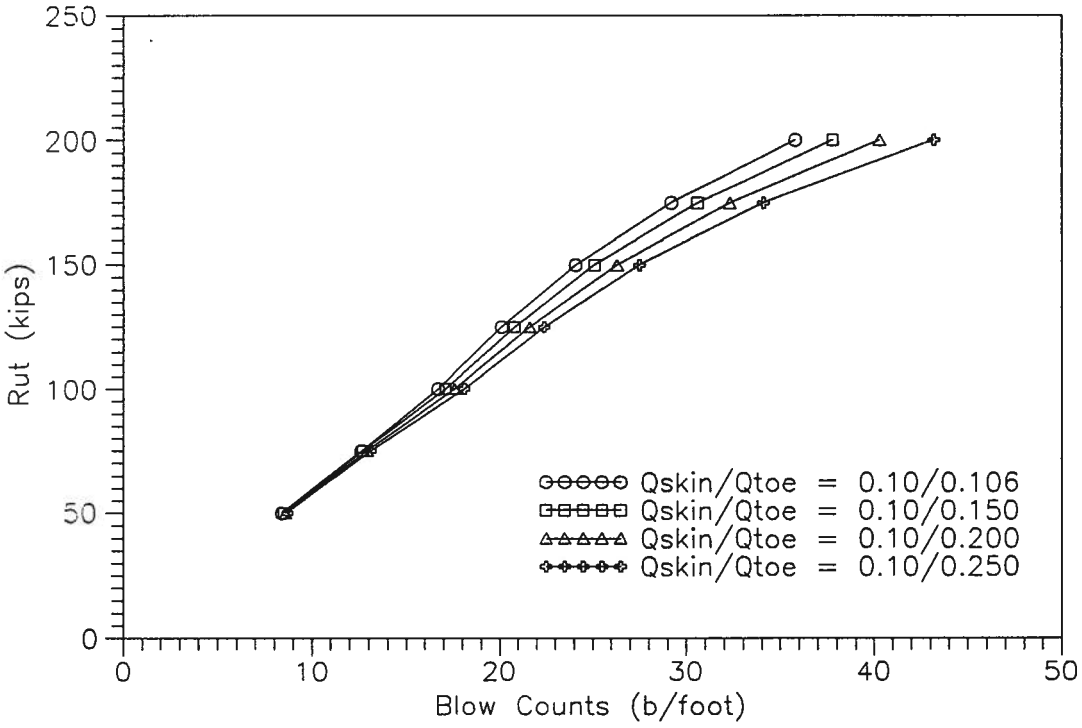

Figure 5.13: Effect of Toe Quake

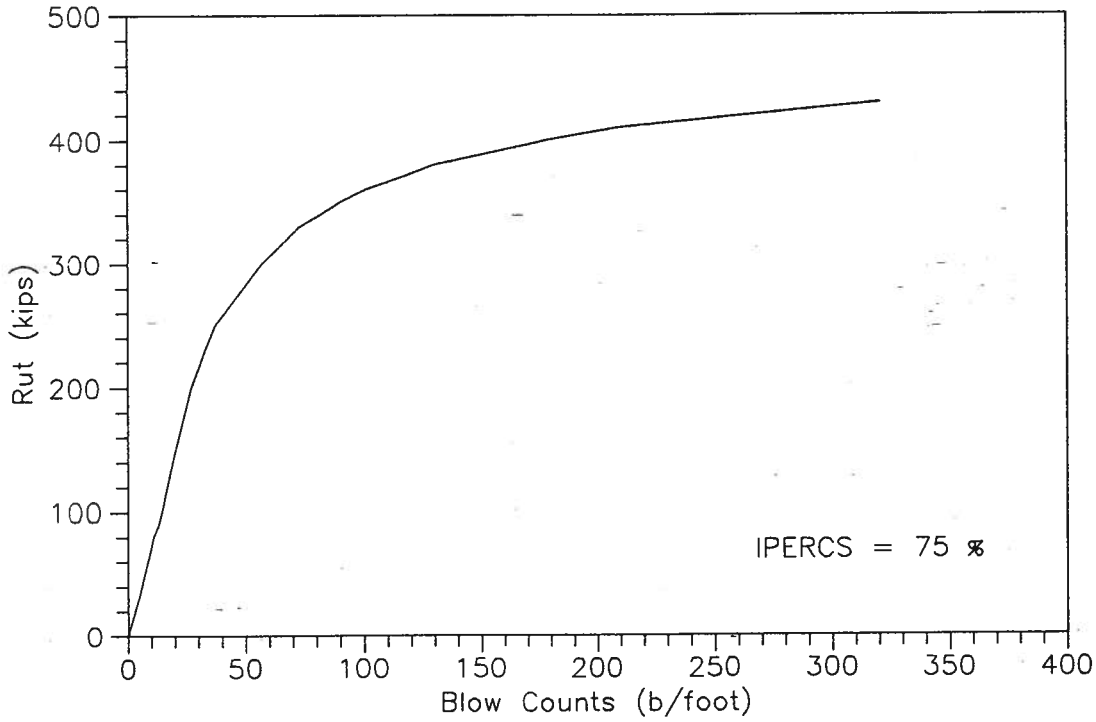

Figure 5.14: Bearing Graph of Pile 3 at Depth of 55 *feet*

Chapter 6

Drivability Analysis - Blow Count Prediction

6.1 Introduction

The purpose of the drivability analysis presented herein is to attempt to predict the blow counts of a driven pile. This will be done using the program GRLWEAP and the pile capacity evaluated from CPT data.

For a given hammer-pile-soil system, the blow count varied with penetration resistance during pile driving. The total driving resistance consists of both static and dynamic soil resistance. According to the definitions in the GRLWEAP program, the static and dynamic soil resistance are determined from the theory of one-dimensional wave equation propagation in the pile and depends on soil parameters such as quake, damping, and ultimate static resistance during driving, R_{ut}. The penetration resistance can be calculated from Equation 6.1.

$$R_t = R_s + R_d \tag{6.1}$$

where:

R_t is the total driving resistance

R_s is a static resistance component of total driving resistance acting on pile shaft and tip

R_d is a dynamic resistance component of total driving resistance acting on pile shaft and tip

The R_s increases linearly with pile penetration displacement before the pile penetration displacement reaches the value of quake. When the pile penetration displacement reaches and exceeds the quake, the R_s keeps a constant value of R_{ut}. R_{ut} is ultimate static resistance during driving as defined in Equation 5.7, which has to be estimated in drivability analysis. The R_d is defined in Equation 5.8, in which the R_d is a composite function of static resistance, pile velocity and damping factor.

The pile capacity determined from the LCPC CPT method (Bustamante and Gianeselli, 1982) was chosen to evaluate R_{ut}, which is used as an input parameter in the GRLWEAP program. As discussed in Chapter 4, the ultimate pile capacity determined from LCPC CPT method represents the long term pile capacity. For many soils, particularly cohesive soil, the ultimate pile capacity several days after pile installation can be significantly greater than the ultimate static resistance during driving and immediately after driving (Fenske and Hirsch, 1986). Figure 6.1 shows how the pile capacity increases with time for piles in cohesive soils (Soderberg, 1962). The maximum load capacity of a pile was the ultimate (or long term) capacity when the pore pressure fully dissipared. Data presented by Soderberg (1962) showed that the increase in ultimate load capacity of a pile depended on the excess pore pressure developed around the pile, and the rate of dissipation of these pore pressure. In prediction long term pile capacity, both shaft resistance and end bearing components increase with time because of soil set up processes, such as pore pressure dissipation and aging, around the pile shaft and under the pile tip. Furthermore, shear failure takes place at the surface between soil and pile shaft during large displacement encountered in continuous pile diving. The elapsed time between blows is very short compared to the soil set up processes described above. Therefore, the soil strength during pile driving will be less than the in-situ soil strength before pile driving. Typical in-situ and remoulded soil shear strength profiles for normally consolidated clays are shown in Figure 6.2 after Fenske and Hirsch, (1986).

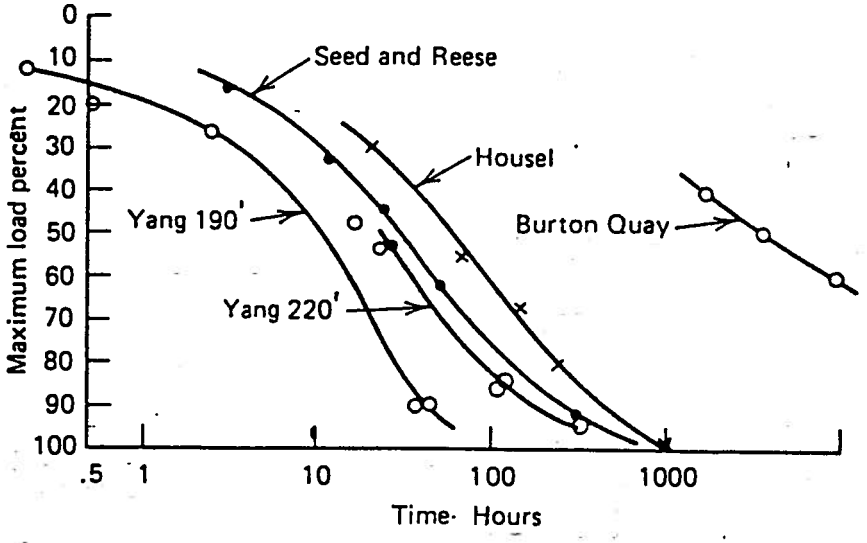

Figure 6.1: Increase of Load Capacity with Time (after Soderberg, 1962)

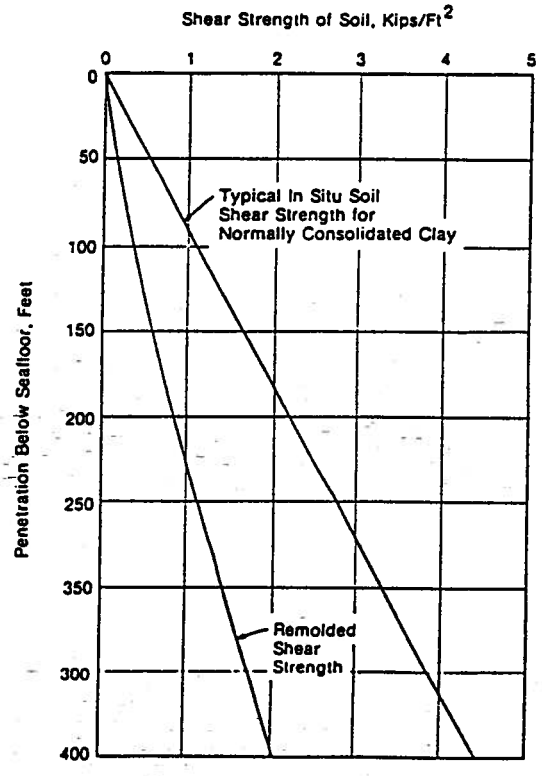

Figure 6.2: Strength Loss by Remoulding for Normally Consolidated clays. (after Fenske and Hirsch, 1986)

We can estimate R_{ut} during pile driving from long term pile capacity by introducing reduction factors, less than 1.0, into the components of pile capacity. Estimating the reduction factors for different soils requires some assumptions to be made that reflect the effects of driving.

The distribution of soil resistance between pile shaft and pile tip is determined by the type of soil in which the pile is embedded. For example, the pile shaft resistance can be much larger than the end bearing if the pile tip is embedded in a soft soil layer as in the case of a friction pile. The pile is considered as an end bearing pile when the pile tip is embedded in hard soil layer. In this study, piles are divided into friction and end bearing piles according to pile resistance distribution. In both cases, the values of CPT q_c are used to evaluate the soil conditions.

Three methods were used to predict blow count of driven piles. These methods are based on total pile capacity, end bearing component, and shaft resistance component, respectively. By using different analysis methods, the writer expects to find the best empirical correlation between R_{ut} and CPT q_c. Based on a preliminary study, the method based on shaft resistance component appears to give most reasonable results. The latter method is done in three steps. The first step is to determine reduction factors for calculating shaft resistance during driving, R_{sr}, from long term shaft resistance. This is done based on experience and in-situ test results. The second step is to determine R_{ut} through simulated modelling calculation using the GRLWEAP program. The simulated modelling calculated blow counts to match the measured blow counts using different values of R_{ut}. The third step establishes empirical correlations for different types of piles by using R_{sr} determined in the first step, R_{ut} determined in second step and q_{ea} which determined from CPT q_c. q_{ea} is known as the equivalent cone bearing. It estimates the soil influence range corresponding to the depth of the blow counts recorded during pile driving. From the empirical correlations developed, R_{ut} can be evaluated from long term

pile capacity and CPT q_c. The details of the result and their limitations as well as factors that affected the results are given in following sections.

6.2 Analysis Parameters Selection

The LCPC CPT method is used as the basic method to evaluate pile capacity from CPT. An equivalent cone bearing, q_{ea}, for a given depth is proposed as shown in Figure 6.3. The UBC Cone Interpretation program CPTINT is used to give an average value of q_c for each *foot* in depth using data files that have q_c measured every *inch* or 2 *inches*. Then, q_{ea} is calculated by taking the average values of q_c over the selected depth range. The range includes 1.5 D above the pile tip and one *foot* plus 1.5 D below the pile tip, where D is the diameter of pile. The additional one foot below the pile tip, that is different from the LCPC CPT method, is used since we need to know the penetration resistance in one *foot* penetration intervals. In this way, the penetration resistance at the pile tip can be considered by taking average values of q_c corresponding to the depth of blow counts recorded during pile driving. The equivalent cone bearing will be used as an in situ measured parameter in the empirical method proposed. The remaining parameters used to determine pile capacity from CPT are the same as those proposed in the LCPC CPT method.

In the GRLWEAP analysis, program parameters, such as quake, damping, and hammer efficiency, etc., were selected from the GRLWEAP menu. Based on the study on the sensitive of wave equation by Ramey (1977) the skin damping is third of the toe damping. For stratified sand and clay with pile tip in sand a reasonable skin damping is 0.067 to 0.10. Therefore, the damping for clay and sand use the values recommended by GRLWEAP, however a skin damping value of 0.10 s/ft for silt was used in this study. Table 6.1 shows the values of quake and damping for different types of soils as recommended

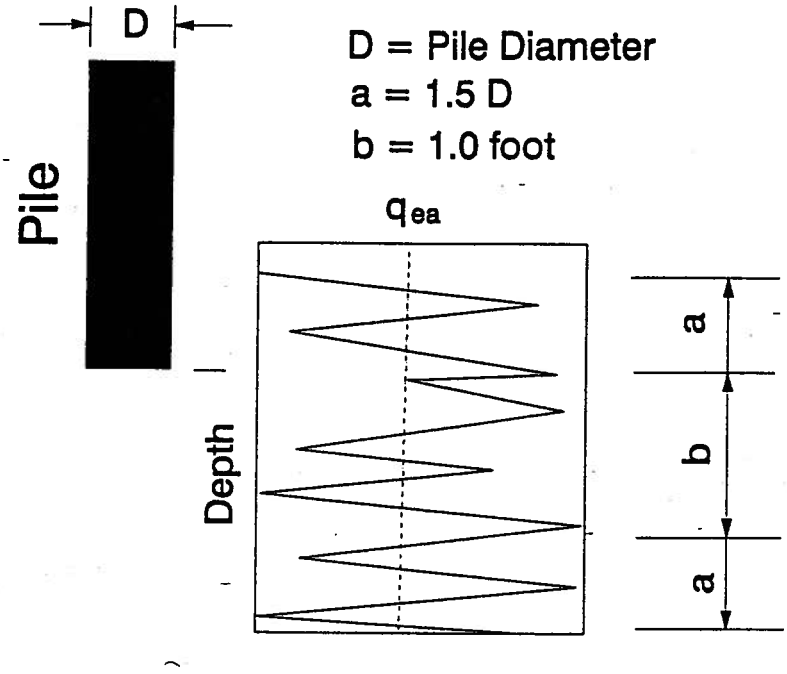

Figure 6.3: Proposed Model for q_{ea}

in GRLWEAP (1987). In Table 6.1, d is the effective toe diameter for a displacement pile. For open cross sections, the full pile width or diameter is only applicable if the soil forms a plug in the pile. There were three types of hammer in the study: drop hammer, diesel hammer and stream hammer. The hammer efficiency was selected according to the values suggested by the GRLWEAP menu, 0.67 for drop hammer and 0.72 for diesel hammer. The energy of a diesel hammer changes with different combustion chamber pressure (GRLWEAP, 1987). The blow rate of a diesel hammer effects the energy transmitted to the pile. The lower the hammer blow rate, the higher the energy delivered into the pile. An adjustment method is proposed when using diesel hammers to normalize the predicted blow count in terms of blow rate. This is necessary so that predicted and measured blow count can be compared at a similar hammer efficiency.

Each pile was divided into 5 *foot* segments for the analysis. An adjustment was made

Table 6.1: Proposed Quake and Damping Values Used in Study

Soil Type	Quake (in)		Damping (s/ft)	
	Skin	Toe	Skin	Toe
Clay	0.10	$d/120$	0.20	0.15
Silt	0.10	$d/120$	0.10	0.15
Sand	0.10	$d/120$	0.05	0.15

for each segment so that it could be located in only one type of soil.

A relative dimensionless magnitude distribution of skin friction was selected, which is defined by option $ITYS = -1$ in GRLWEAP. With this option, the shaft resistance is accumulated with increasing penetrating depth. Figure 6.4 shows a an example of the skin friction distribution on UBC pile 5 which was installed to a depth of 102 $feet$.

6.3 Selection of Prediction Methods Based on Pile Capacity

In order to establish a method to predict blow counts of driven piles based on the CPT, correlations between R_{ut} and CPT q_c were evaluated in this study. Three methods were carried out based on total pile capacity, end bearing component, and shaft resistance component.

The analysis based on total pile capacity multiplies a reduction factor, less than 1.0, to the pile capacity determined from LCPC CPT method to get R_{ut}. R_{ut} is then input into the GRLWEAP program, which computes blow counts. The ratio of shaft resistance to total pile capacity before reduction was taken as $IPERCS$. It is assumed that $IPERCS$ is constant at a given depth. The reduction factor, defined as the ratio of R_{ut} to total pile capacity, was determined by making the blow counts calculated equal to the blow counts measured during driving. The calculated blow counts were determined by GRLWEAP simulated modelling calculations. A reduction factor of 0.70 was determined for all soil types based on the results of total pile capacity analysis on UBC pile 5. Figure 6.5

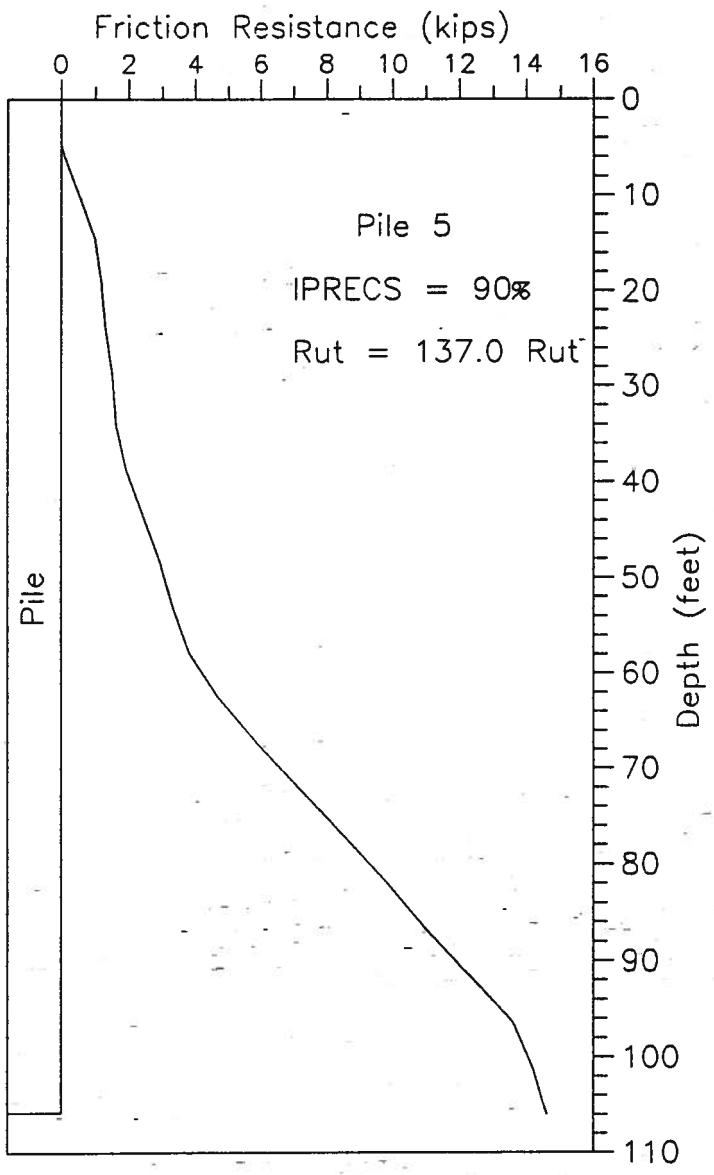

Figure 6.4: Shaft Resistance Distribution of UBC Pile 5 at a Depth of 102 Feet

shows comparison of predicted blow counts to measured blow counts of UBC pile 5. Two hammer drop heights, 6 *feet* and 7 *feet*, were used in the modelling according to the field tests. The same reduction factor was used in the analysis of UBC pile 6. Table 6.2 shows results from UBC pile 5 and 6. The results in Table 6.2 show that predicted and measured blow counts are close for UBC pile 5 and for UBC pile 6 at depths of 48 and 102 *feet*. However the predicted blow counts were larger than measured at the depths of 60, 80 and 90 *feet* for pile 6. Large differences are made in end bearing pile condition for UBC pile 6 because of overestimation of R_{ut}. In order to fit the predicted and the measured blow counts better, a smaller reduction factor, less than 0.7, is required to estimate R_{ut} for UBC pile 6 where end bearing pile conditions are present. The predicted blow counts are very close to the measured ones in friction pile condition for both pile 5 and 6. Also, the results of Table 6.2 suggest that the reduction factor changes with different sizes of piles for end bearing conditions. Hence pile size must be considered in total pile capacity analysis. When the pile size increases, the pile capacity increases for both shaft resistance and end bearing. The shaft resistance changes because the pile shaft area increase. A study by Meyerhof (1982) showed that the ultimate unit skin friction of driven piles in sand of a given density is practically independent of the pile diameter. The results of this study also show that a good blow count prediction was made by using the R_{ut} determined from one reduction factor for friction piles of different sizes. However it was not clear how pile size affects the end bearing during pile driving.

The results from UBC piles 5 and 6 suggest that it is difficult to determine R_{ut} from long term total pile capacity using only one reduction factor for different size piles. However, it is possible that one reduction factor can be used for shaft resistance and another reduction factor for end bearing. The results also show that the end bearing and shaft resistance during pile driving are smaller than that of long term capacity. The

Table 6.2: Predicted Blow Counts Based on Total Pile Capacity Method

Soil	Depth	Pile 5		Pile 6	
Type	(*feet*)	Predicted	Measured	Predicted	Measured
Clay	48	3.5	3.0	8.8	5.0
Sand	60	8.6	6.0	33.8	21.0
Sand	80	13.1	15.0	45.0	29.0
Sand	90	16.0	19.0	61.1	37.0
Clay	102	11.5	11.0	27.7	25.0

general agreement observed for UBC pile 5 suggests that using reduced pile capacity in the GRLWEAP program to predict blow counts produces reasonable results.

The method based on end bearing uses the end bearing component of long term pile capacity to determine end resistance during driving. Again, a reduction factor, less than 1.0, is multiplied to the end bearing component of pile capacity to get the end resistance during driving for a given depth. Then, in the modelling calculation, end resistance is kept constant while R_{ut} is changed until the calculated blow counts fit the measured blow counts. In the calculation, the end resistance was kept constant and the $IPERCS$ was allowed to vary with R_{ut}. The final R_{ut} and $IPERCS$ was then used to determine shaft resistance, R_{sr}. Figure 6.6 shows the results of R_{ut} and R_{sr} determined from end bearing analysis on UBC pile 5. A reduction factor of 0.7 was used to calculate end resistance during driving from long term end bearing. It is observed from Figure 6.6 that the R_{sr} reaches its maximum value of 180 *kips* at a depth of 84 *feet*, then, decreases as low as 50 *kips* at a depth of 91 *feet*. In practice, accumulated friction resistance has to increase as pile penetrating depth increases. The results from Figure 6.6 suggest that the accumulated friction resistance decreases considerably with increasing depth. This apparent contradiction occurs because the end resistance is difficult to model using only one reduction factor as mentioned in total pile capacity method. The higher the end bearing, the lower the shaft resistance for a given R_{ut}. If a higher shaft resistance

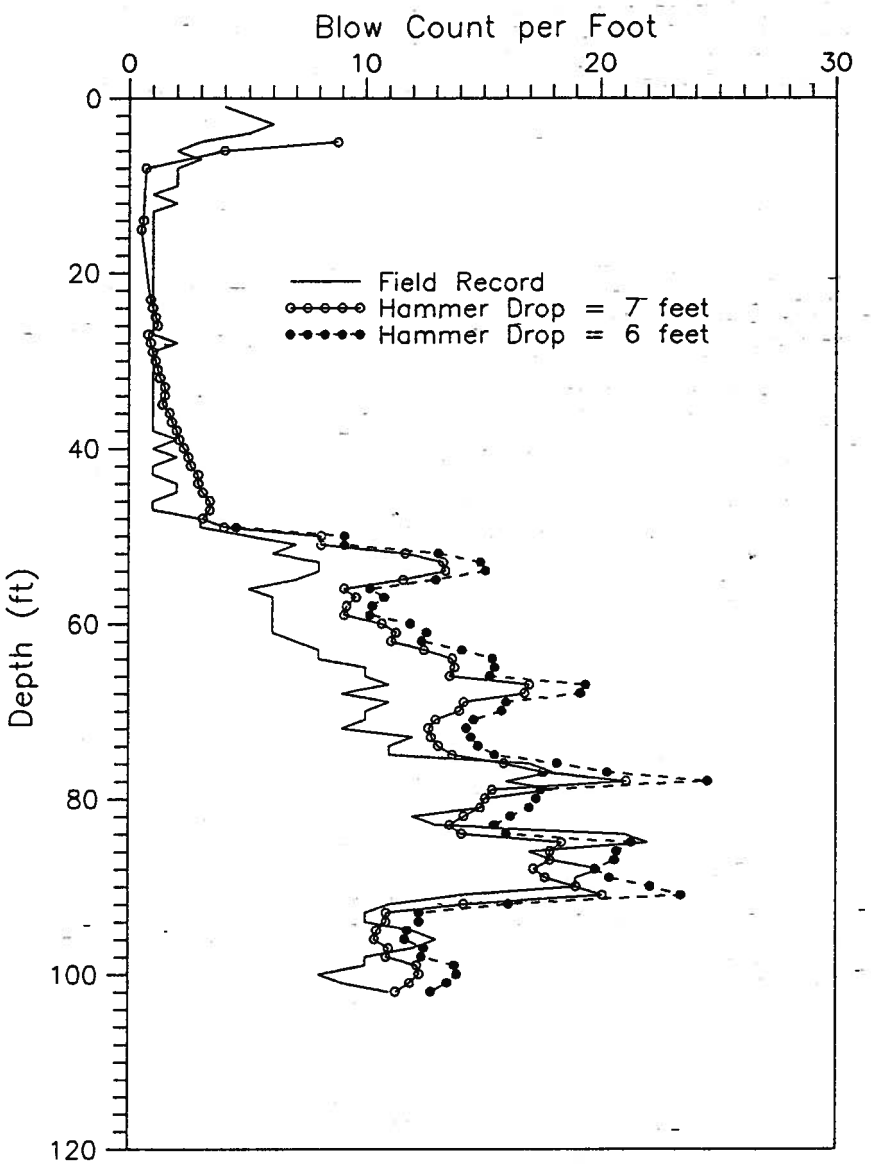

Figure 6.5: Predicted Blow Counts for UBC Pile 5 Based on Total Pile Capacity Method

is desired, a smaller end bearing is required. Therefore a smaller reduction factor (less than 0.7) must be used. Figure 6.6 demonstrates that when one reduction factor is used for all soil depths to obtain end resistance, it is not possible to keep the shaft resistance increasing with increasing depth.

The analysis based on shaft resistance component of pile capacity is very similar to that of the end bearing, the only difference is that the long term shaft resistance is multiplied by a reduction factor to obtain the shaft resistance during driving. Based on the following result, this method is considered to be useful. The details of this method are given in following sections.

6.4 Blow Count Prediction Based on Pile Shaft Resistance

6.4.1 Introduction

The blow count prediction based on shaft resistance component of pile capacity was carried out by establishing an empirical correlation between R_{sr}/R_{ut}, and CPT q_c. R_{sr} is the shaft resistance during pile driving and is determined by introducing a reduction factor, less than 1.0, into the long term shaft resistance determined from LCPC CPT method. Since R_{ut} is summation of static shaft and toe resistance during driving the determination of R_{ut} reflects the static toe resistance during driving if R_{sr} known.

As discussed previously, in the total pile capacity method, it is possible to use a single reduction factor to estimate R_{ut} for friction pile because the predicted blow counts matched well with the measured blow counts. When predicting pile capacity from the LCPC CPT method, the shaft resistance increases steadily with increasing depth. The ratio of shaft to total pile capacity at a given depth can be used to indicate static resistant condition of the pile. This ratio is larger for friction piles and smaller for end bearing piles as demonstrated in Figure 6.7. Figure 6.7 also shows that the change in the ratio

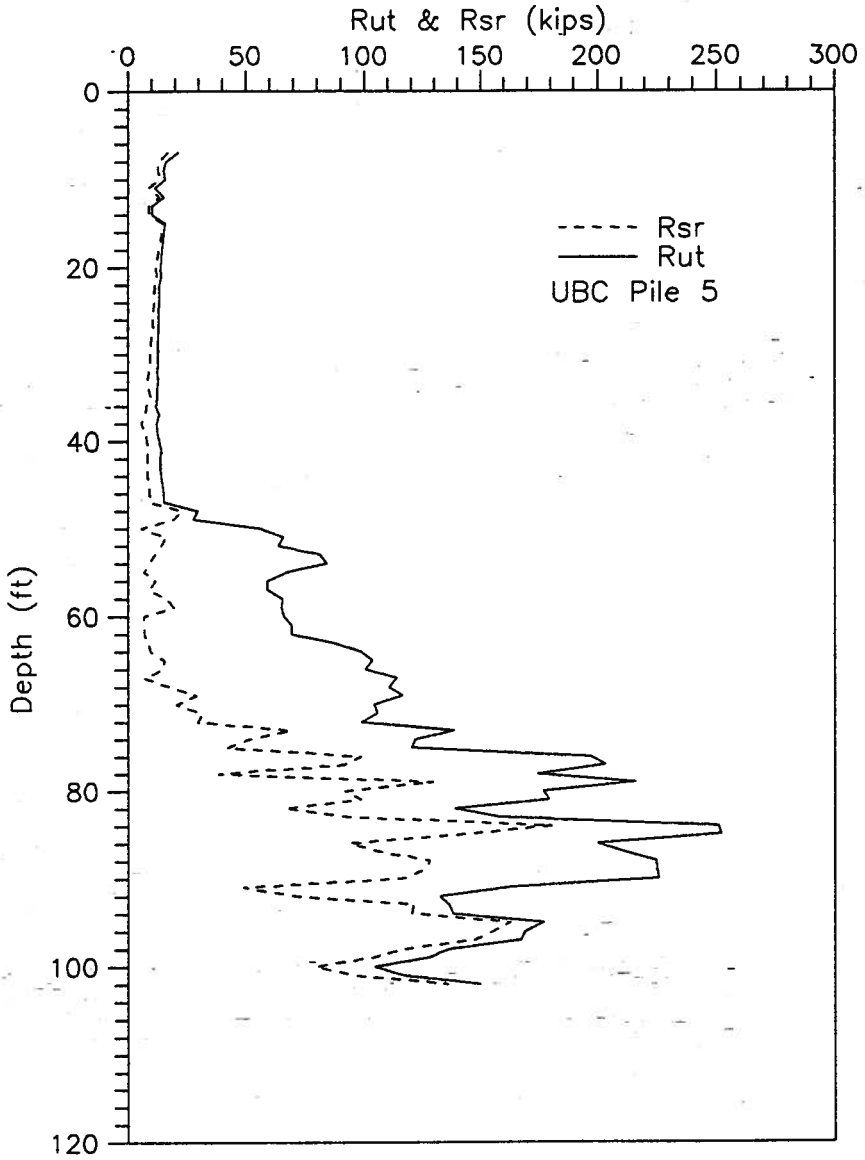

Figure 6.6: R_{ut} and R_{sr} Determined from Analysis of Blow Counts Prediction Based on End Bearing Method

of shaft to total pile capacity is inversely proportional to the values of q_c. If the same inverse relationship exists between R_{sr}/R_{ut} and q_c during pile driving, it is possible that a correlation between R_{sr}/R_{ut} and CPT q_c can be found to determine R_{ut}, assuming the following criteria are met:

(1) for a particular soil a single reduction factor can be used to determine R_{sr} from long term shaft resistance;

(2) R_{sr} remains constant for a given depth during pile driving;

(3) R_{sr} increases with increasing depth.

An empirical correlation between R_{sr}/R_{ut} and q_c was established using GRLWEAP program stimulated modelling calculations. In the following discussion, data from different sites and pile types are used to find empirical correlation between R_{sr}/R_{ut} and q_c. The analysis was initiated by estimating the reduced shaft resistance during pile driving, R_{sr}, from long term pile capacity. Then, different values of R_{ut} were input into GRLWEAP program to calculate blow counts until the calculated blow counts equal those measured during pile installation for a specific depth. A final R_{ut} and ratio of R_{sr}/R_{ut} was determined for every *onefoot* depth increment. Finally an empirical correlation between R_{sr}/R_{ut}, $(IPERCS)$, and equivalent cone bearing, q_{ea}, was established to determine R_{ut}.

6.4.2 Determination of Reduction Factor

The shaft resistance during driving, R_{sr}, was determined by introducing a reduction factor to the long term shaft resistance determined from the LCPC CPT method. For cohesive soils, the increase in pile capacity with time is significant, as shown in Figure 6.1 (Soderberg, 1962). The static frictional resistance during pile driving may be significantly less than the long term static shaft resistance after pile driving (Fenske and Hirsch, 1986). The effects of driven pile in clay are classified into four categories by de Mello (1969):

(a) remoulding or partial structure alteration of the soil surrounding the pile;

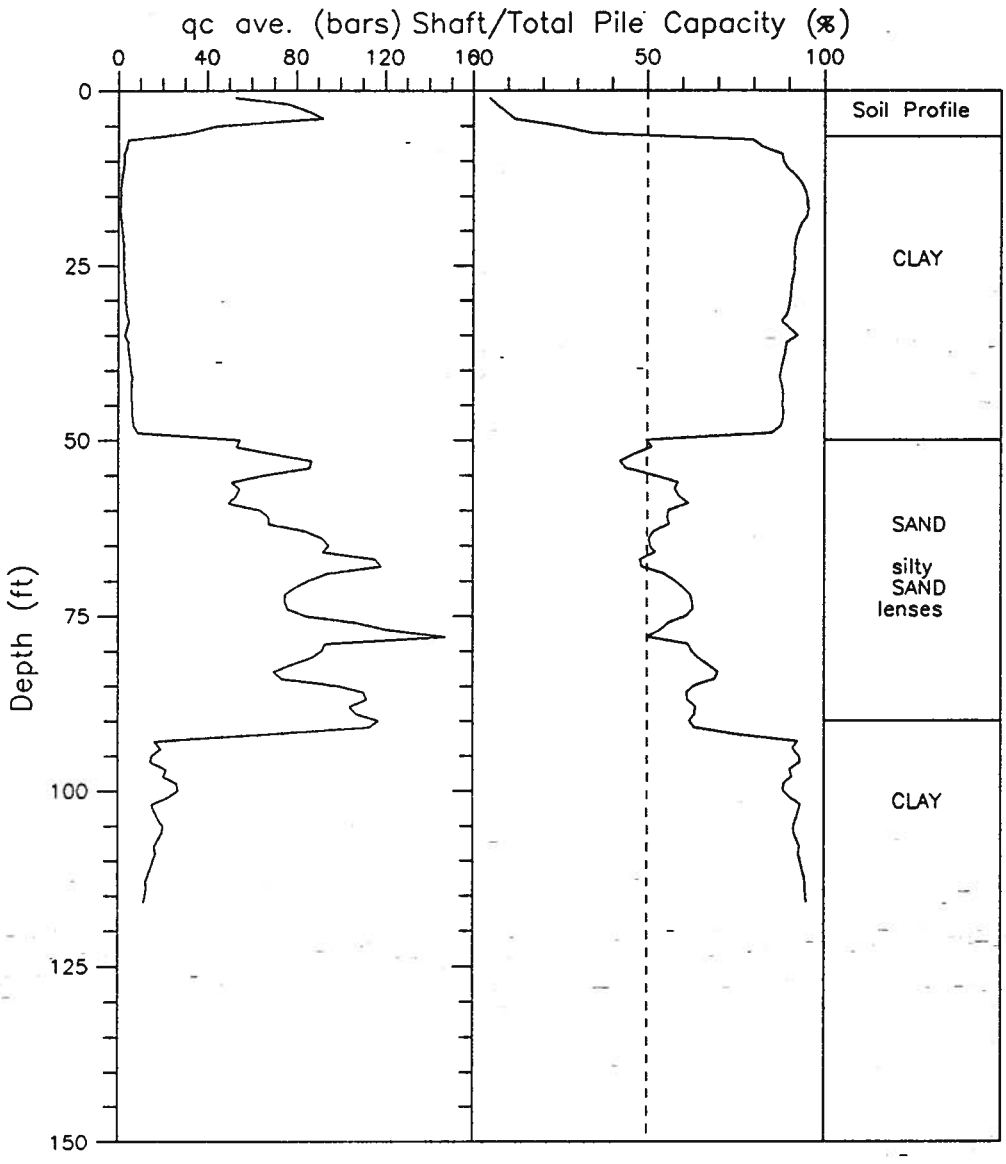

Figure 6.7: Shaft Resistance to Total Pile Capacity vs Depth with CPT q_c, UBC Pile Research Site Pile 1 to 5

(b) alteration of the stress state in the soil in the vicinity of the pile;

(c) dissipation of the excess pore pressures developed around the pile; and

(d) long-term phenomena of strength-regain in the soil.

For cohesionless soils, when a pile is driven, the soil is usually compacted by displacement and vibration, resulting in permanent rearrangement and some crushing of soil particles. The frictional resistance depends on the stress history of soil, the shape and roughness of pile, and other factors (Meyerhof, 1982). It is usually assumed that in sand the static friction resistance during driving is equal to the static resistance after driving. Reduction factors of 0.5 for clay and 1.0 for sand, were used in a pile driveability study by Tang et al (1988). However in research on soil set up, Fellenius et al (1989) showed that the frictional resistance increases significantly up to twice of the frictional resistance during initial driving in restriking after 1 *day* when a pipe pile embedded in stratum of sandy clay and silty sand. In the following analysis, reduction factors, less than 1.0, were used for both clay and sand. The reduction factors were determined using friction pile conditions on UBC pile 5 and 6 assuming the followings:

(1) The pile tip was embedded in soft soil layers where the values of CPT q_c were smaller than 10 bars;

(2) R_{sr}/R_{ut} ($IPERCS$) remains constant at 90 % in the GRLWEAP simulated modelling calculation.

Based on the proceeding assumptions, R_{ut} was determined for each one $foot$ depth increment and R_{sr} was calculated from R_{ut} using R_{sr}/R_{ut} of 90%. The reduction factors were finally determined by comparing R_{sr} to long term shaft resistance. In this manner, reduction factors of 0.5 for clay and 0.7 for sand were determined. Many factors, such as OCR, structural failure of soil, volume displacement of the soil and pile geometry will affect the shaft resistance of the pile (Meyerhof, 1982). The reduction factors chosen reflect the comprehensive influence of these factors.

6.4.3 Results

The analysis procedure is presented in the flow chart shown in Figure 6.8. Each pile type was analyzed separately. For each pile, R_{sr} was first calculated from long term shaft resistance at given depth by using the reduction factors of 0.5 for clay and 0.7 for sand. The R_{ut} was determined by making the calculated blow counts match the measured blow counts. In the calculation procedure, the $IPERCS$ varied with R_{ut}. Final $IPERCS$, i.e. R_{sr}/R_{ut}, and R_{ut}, were determined for each one $foot$ depth interval. The correlation between R_{sr}/R_{ut} and q_{ea} was established and a linear best fit was applied to the data to indicate the proposed correlation.

Results on Closed-Ended Steel Pipe Pile

This analysis is based on UBC pile 1, 2, 3, 5 and 6 as well as Tilbury pile 1 and 2. The details of sites, piles and pile installation procedures were given in Chapter 2 and 3.

For the UBC piles, when the pile was driven above 50 $feet$ or below 92 $feet$, the pile tip was embedded in cohesive soil where values of q_c were lower than 20 $bars$. The calculated ratios of R_{sr}/R_{ut} were 80 to 100 percent, indicating a lower end bearing, and confirming the friction pile behaviour. When the pile was driven from 50 to 90 $feet$, the calculated values of R_{sr}/R_{ut} varied from 70 to 45, indicating higher end bearing and showed end bearing pile behaviour. The R_{sr}/R_{ut} versus q_{ea} is shown in Figure 6.9 for UBC pile 3 and 5 and in Figure 6.10 for UBC pile 6. Since UBC pile 1 and 2 were only driven into depth of 47 $feet$ and 45 $feet$, respectively, all calculated values of R_{sr}/R_{ut} were in the range of 80 to 100. Clearly when the pile tip was embedded in hard soil the R_{sr}/R_{ut} was lower, whereas, when pile tip embedded in soft soil the R_{sr}/R_{ut} was higher.

If q_{ea} is adopted as parameter to give the relative strength of the soil, a correlation between R_{sr}/R_{ut} and q_{ea} can be established to show the tendency of R_{sr}/R_{ut} to change

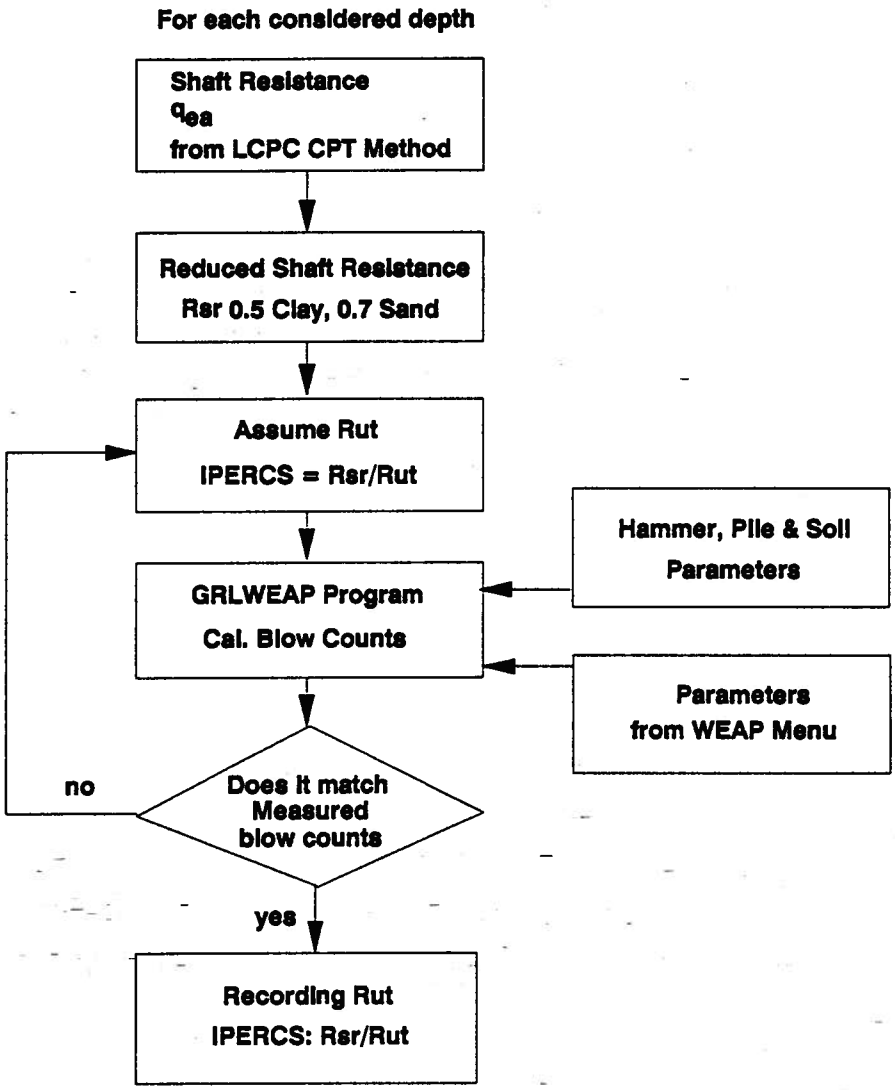

Figure 6.8: Calculation Steps of Establishing Empirical Correlation between $\bar{R}_{sr}/R_{ut}$ and q_{ea} for Specified Depth

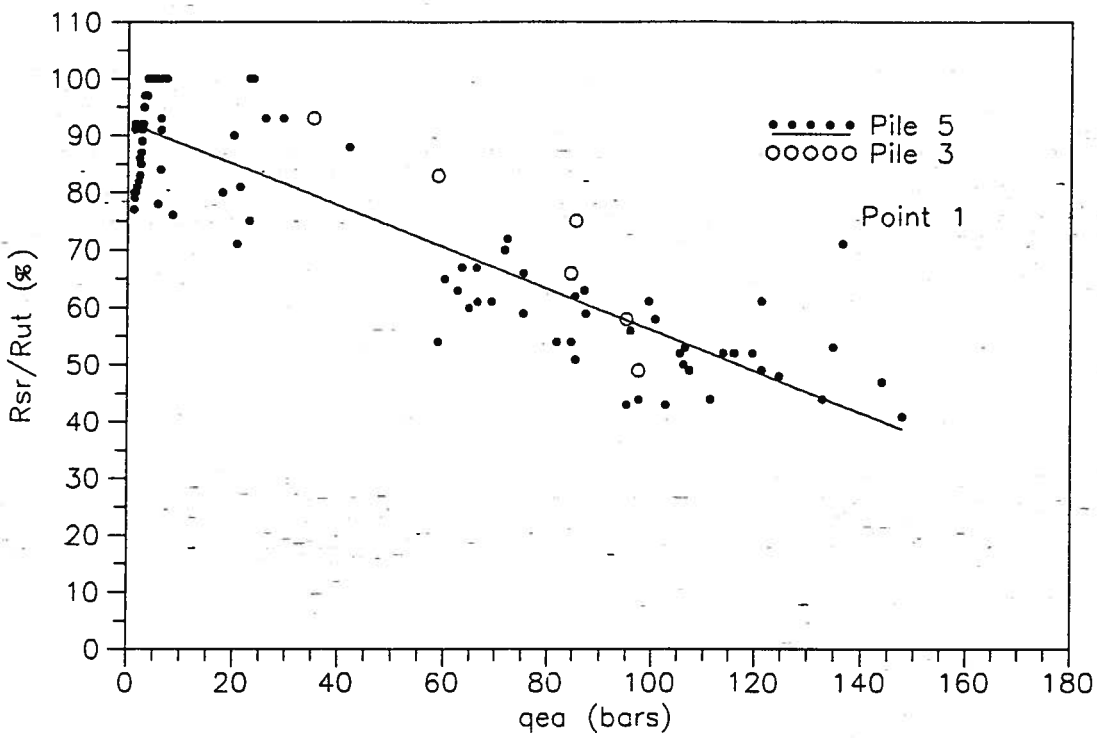

Figure 6.9: R_{sr}/R_{ut} vs q_{ea} for UBC Pile 3 and 5

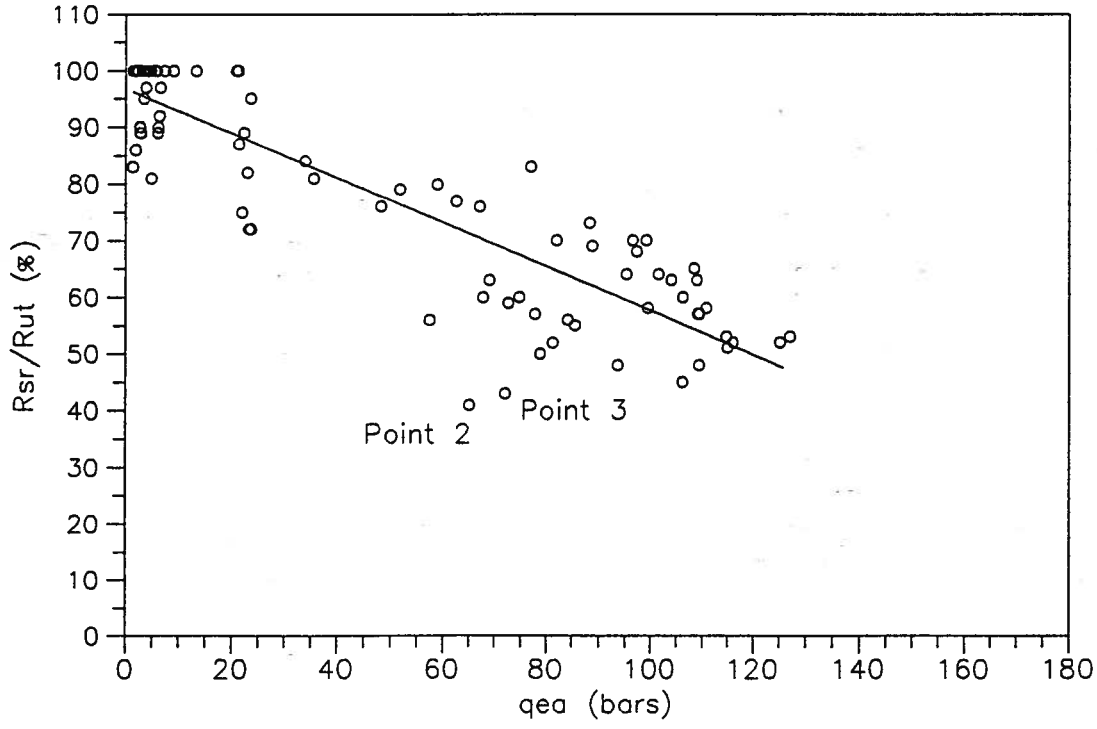

Figure 6.10: R_{sr}/R_{ut} vs q_{ea} for UBC Pile 6

with soil variation. The results show values of R_{sr}/R_{ut} decrease with increasing q_{ea}. When a linear best fit line is plotted through the data, the trend of R_{sr}/R_{ut} versus q_{ea} for UBC piles 5 and 6 agree well, as shown in Figure 6.11. At the range of q_{ea} from 50 to 110 bars, most data points are located below the line for pile 5. For pile 6 the line appears to give an average values. The calculated values of R_{sr}/R_{ut} were unreasonable low above 10 $feet$ for pile 5 and above 5 $feet$ for pile 6 for the values of q_{ea}. A threshold penetration depth must be reached to get reasonable results. This depth is defined as the effective beginning depth. Some values deviate significantly from the best fit lines. This is somewhat controlled by soil type, especially when the soil type changes either from soft to hard or from hard to soft. This point will be discussed in the following section.

For the Tilbury piles, the values of R_{sr}/R_{ut} were calculated for piles 1 and 2. A diesel hammer, D30-13, was used for pile 1 below 24 $feet$ and for pile 2 below 15 $feet$. Figure 6.12 shows the results of calculated values of R_{sr}/R_{ut} corresponding to the values of q_{ea} at different depths. For a given value of q_{ea} and pile end bearing, R_{sr}/R_{ut} increases with increasing depth because shaft resistance increases. Pile 1 was used to examine the depth influence. From the pile 1 data in Figure 6.12, the values of R_{sr}/R_{ut} tend to be a constant value of about 50 percent. A non-linear tendency is clearer for the Tilbury piles than for the UBC piles.

A comparison of UBC and Tilbury piles is given in Figure 6.13. All three linear best fit lines agree well. For UBC pile 5 and both Tilbury piles, most of the points are scattered beneath the best fit lines when the values of q_{ea} are smaller than 110 $bars$. When the values of q_{ea} are larger than 125 $bars$, R_{sr}/R_{ut} tends to be constant. The variation of R_{sr}/R_{ut} with q_{ea} will be discussed later in the statistical analysis.

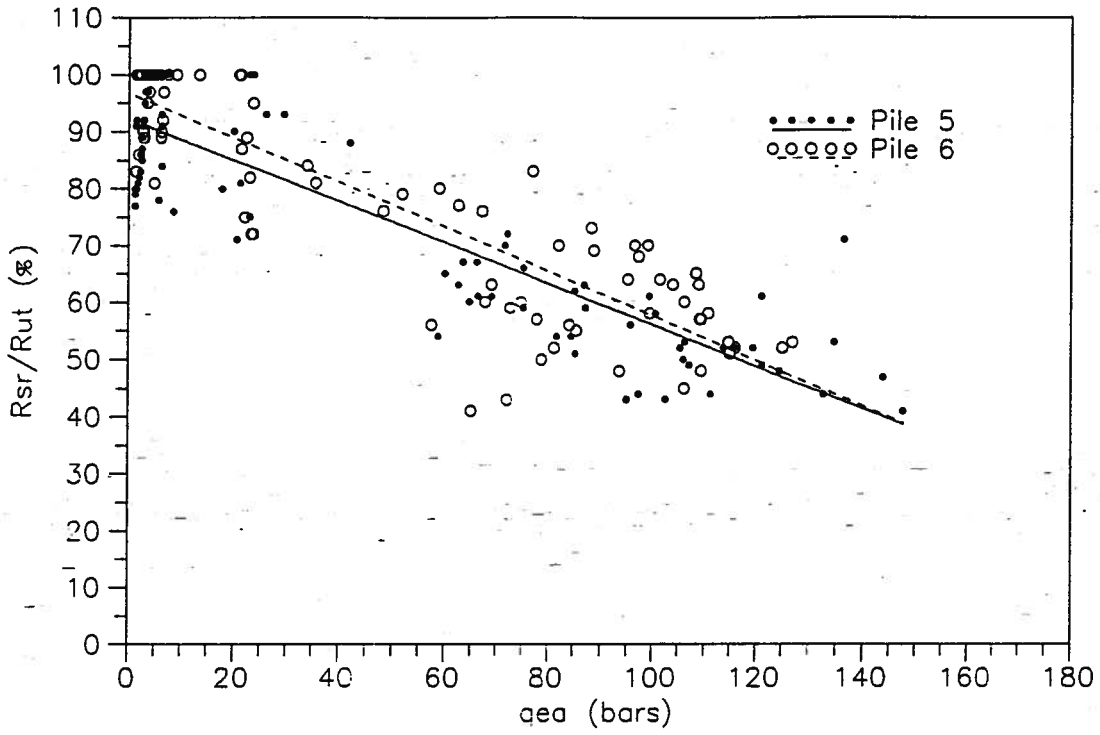

Figure 6.11: R_{sr}/R_{ut} vs q_{ea} for UBC piles

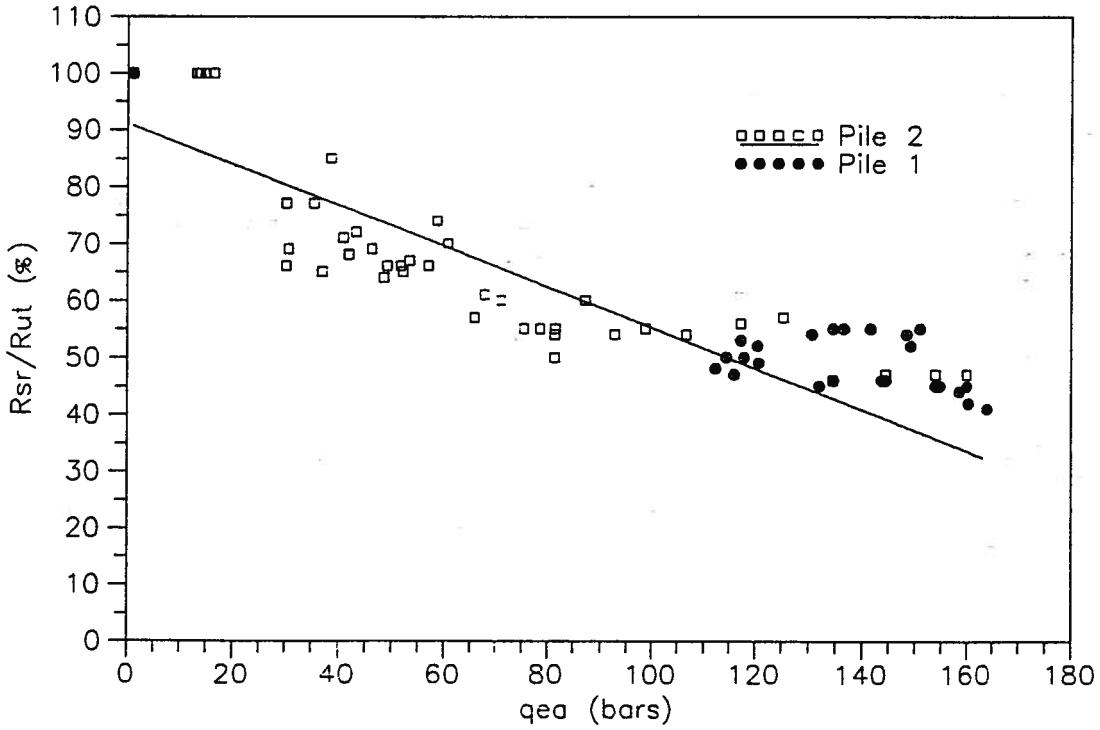

Figure 6.12: R_{sr}/R_{ut} vs q_{ea} for Tilbury piles

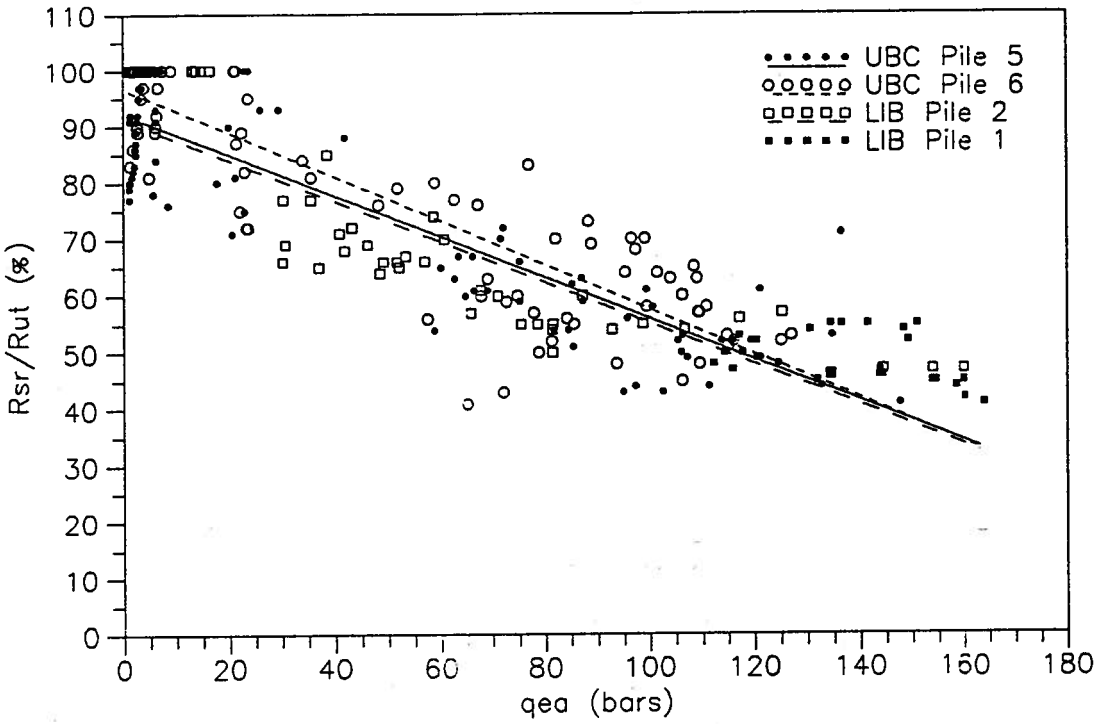

Figure 6.13: R_{sr}/R_{ut} vs q_{ea} for UBC and Tilbury piles

Results on Open-Ended Steel Pipe Pile

The analysis on open ended steel pipe pile was carried out only for UBC pile 4. From the observation (Davies, 1987) soil plug was formed during pile driving. However in the GRLWEAP program, the pipe pile with soil plug is simply modelled as a nonuniform pile. Such that the properties of the pile change in the soil plug reflect the combined pile and soil properties (Goble et al.,1987). According to this model, relative movement and friction between soil plug and pile interface are ignored.

Field records of the soil plug are given in Table 6.4 (Davies, 1987). The results of calculated R_{sr}/R_{ut} for piles 4 and 5 are given in Table 6.3 to show the difference between open-ended and closed-ended piles. The field record shows that relative movement between soil plug and pile did take place during pile driving. This movement causes an increase in shaft resistance. The resistance of open-ended pile tends to increase because

Table 6.3: Record of Soil Plug and Calculated R_{sr}/R_{ut}

Data	Pile 4					Pile 5
	Measured				Calculated	Calculated
Embedded Depth ($feet$)	Length Without Plug ($feet$)	Length of Plug ($feet$)	Interval Embedded Depth ($feet$)	Interval Plug ($feet$)	R_{sr}/R_{ut} (%)	R_{sr}/R_{ut} (%)
48	21.2	29.1			78	76
50	59.6	30.6	2	1.5	65	54
55	56.0	34.2	5	3.6	56	51
60	52.3	37.9	5	3.7	73	67
65	48.8	41.4	5	3.5	85	50
68	46.7	43.5	3	2.1	62	61
71	44.3	45.9	3	2.4	73	61
76	40.8	49.4	5	3.5	70	48

of friction between the soil plug pile interface, however the resistance also tends to decrease because of smaller end bearing of the open-ended piles. The results indicate that the values of R_{sr}/R_{ut} of open-ended pile are larger than for equal diameter closed-ended piles. Looking at depths below 60 $feet$, the open-ended pile 4 behaved like a friction pile, whereas the closed-ended pile 5 behaved like an end bearing pile. It can be concluded that for open-ended piles, when relative movement exists between soil plug and pile, the resistance is mainly composed of shaft resistance, hence an open-ended pile will behave like a friction pile. Also R_{sr}/R_{ut} is larger for an open-ended pile than that for a closed-ended pile.

Results on H Piles

The H piles included Tilbury H12×53 pile, ECNU H10×42 and ECNU H14×73 piles. Since the end bearing is very small due to small end areas, H piles always behave like friction pile as discussed in Chapter 4.

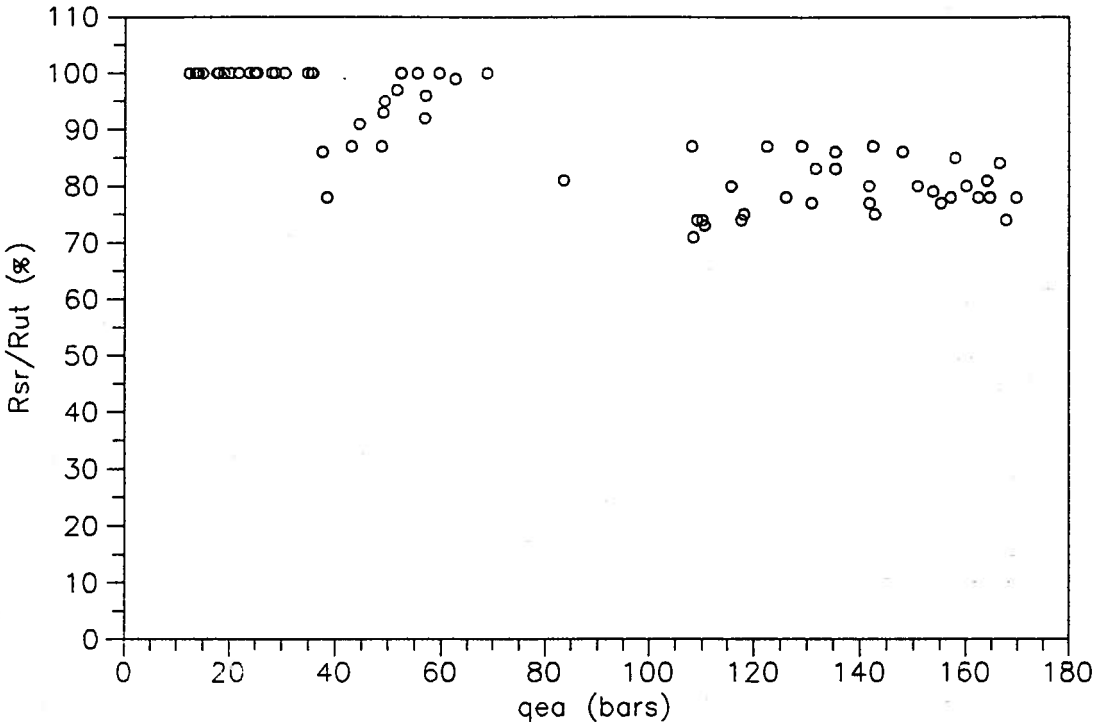

Figure 6.14: R_{sr}/R_{ut} vs q_{ea} for Tilbury H12×53 pile

The calculated values of R_{sr}/R_{ut} were from 75 to 100 percent. Figure 6.14 shows the results of the Tilbury H pile. Figure 6.15 shows the results of the ECNU H piles. In these figures, numerous points are located in a band of 25 percent where the values of q_{ea} change from 45 to 170 *bars*. The linear best fit line appears to give average values of calculated values. The linear best fit lines agree well for these three H piles even though the points scattered in relative wider band, as shown in Figure 6.16.

In this study, unreasonable results were made in determining end bearing for some depths. The end bearing, determined by calculated R_{ut} minus the shaft resistance during driving, was larger than the end bearing predicted from the CPT. In order to explain this problem it is necessary to consider the determination of shaft resistance of the H piles. The shaft resistance of H piles was estimated using the outside rectangular area. During pile driving, a soil plug may be formed in the hollow sides of the H pile. This soil plug will affect the magnitude of the shaft resistance. Estimating the change in shaft

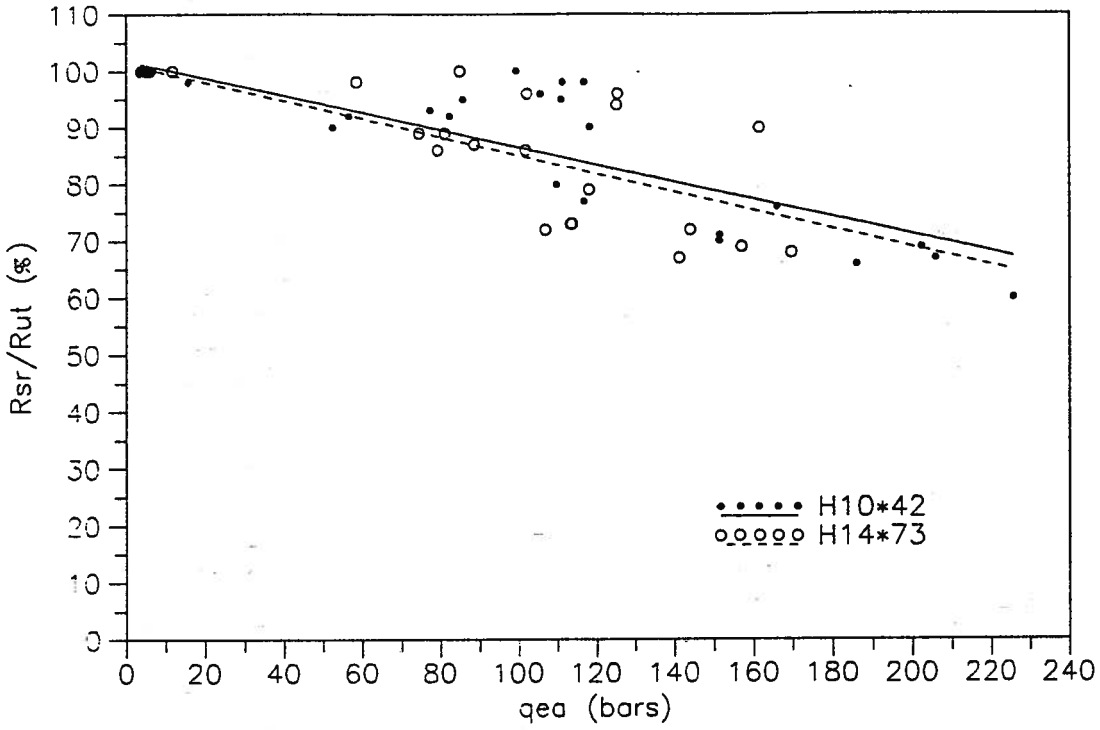

Figure 6.15: R_{sr}/R_{ut} vs q_{ea} for ECNU H piles

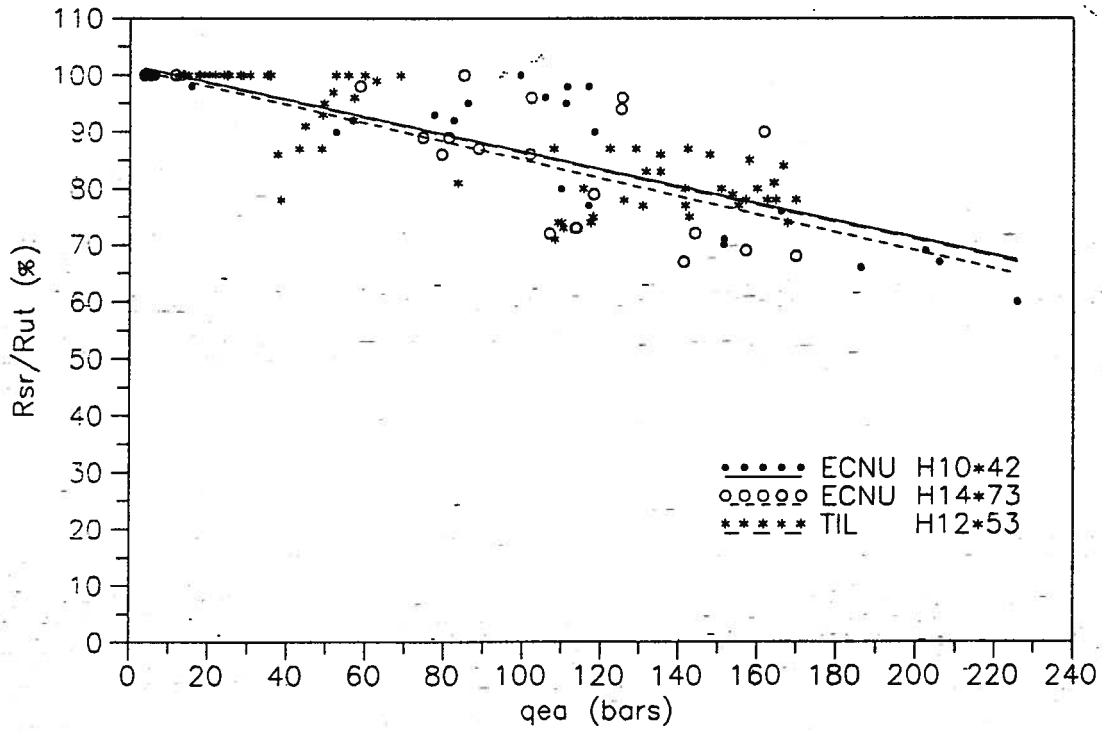

Figure 6.16: R_{sr}/R_{ut} vs q_{ea} for H piles

resistance is more complex since it is difficult to model the types of soil plug formed in H piles. Based on the results, as shown in Figure 6.16, an average value of 90 for R_{sr}/R_{ut} can be used to predict R_{ut} when q_{ea} is smaller than 75 *bars*. The relationship given by the best fit line in Figure 6.16 can be used when q_{ea} is larger than 75 *bars*. This will be discussed further in the statistical analysis.

6.4.4 Influence Factors

The empirical correlation between R_{sr}/R_{ut} and q_{ea} is affected by many factors. The recorded blow count during pile driving is influenced by many variables within the hammer-pile-soil system. Firstly, soil conditions change from site to site. The values of CPT q_c may be very different even for the same kind of soil. In this study, the CPT results are only used to indicate the relative strength of the soil. Secondly, the values of R_{sr}/R_{ut} will change with increasing depth and pile size. Also the soil plug formed within open-ended piles must be considered when more complex soil resistance condition influence the values of R_{sr}/R_{ut}. The final and perhaps most important factor is the hammer efficiency. The energy of diesel hammer changes with different combustion chamber pressure and soil conditions. The recorded blow count is always related to a hammer blow rate. In order to make comparisons between predicted and measured blow count, adjustment of blow counts for hammer blow rate is proposed for diesel hammers.

Soil Profile

q_{ea} is an average of q_c values and therefore describes the soil resistance to end bearing type penetration. The soil profile of each site is described by CPT data. When the values of q_c are small, the soil is considered soft. In soft soils the pile end bearing is low, and the pile behaves like a friction pile. Hence the values of R_{sr}/R_{ut} determined are large. When the values of q_c are large, the soil layer is considered hard. In hard soils the pile end

bearing is high, and the pile behaves like an end bearing pile. The values of R_{sr}/R_{ut} are then small. The values of q_{ea} normally provide reasonable predictions of R_{ut}. However, in some instances values of R_{sr}/R_{ut} deviate significantly from what is expected. This happens especially when soil layers changed from soft to hard or from hard to soft. In these situations the q_{ea} is influenced by the values of q_c for different soils, as shown in Figure 6.17 in which the points 1, 2 and 3 correspond to the points in Figure 6.9 and 6.10. Because of the high values of q_c at a depth of 91 $feet$, a low value of R_{sr}/R_{ut} is expected, however, a very high value of R_{sr}/R_{ut} is calculated, as shown in Figure 6.9 point 1. The reason is that the value of q_{ea} is influenced by hard soil layer, but the pile tip is embedded in a soft soil layer. The contrary phenomena can be seen in Figure 6.10, where points 2 and 3 show low values of R_{sr}/R_{ut} which normally correspond to high values of q_{ea} at depth of 52 and 53 $feet$. In fact the values of q_{ea} are less than 80 bar. In this situation, the soil layers changed from soft to hard. The pile tip had embedded in hard soil layer, but the values of q_{ea} were influenced by the soft soil layer above the tip. In order to make better prediction, a comparison of blow count has to be made when the pile tip locates in both the upper and lower soil layers in the boundary zone where soil types change.

Pile Embedded Depth and Pile Scale

From the results, the ratio of R_{sr}/R_{ut} reflect the pile resistance conditions, i.e. friction pile or end bearing pile. However this ratio only make sense after a certain depth, defined as effective beginning depth. The values of R_{sr}/R_{ut} are not reliable above the effective beginning depth since shaft resistance is not large enough. For example, a very low value of R_{sr}/R_{ut}, 18 percent was determined corresponding to a value of 99 $bars$ q_{ea} at a depth of 3 $feet$ for UBC pile 5. The effective beginning depth is affected by the pile size because the shaft resistance increases with increasing pile size. For example, the effective beginning depth is 5 $feet$ for UBC pile 6, and 10 $feet$ for UBC pile 5.

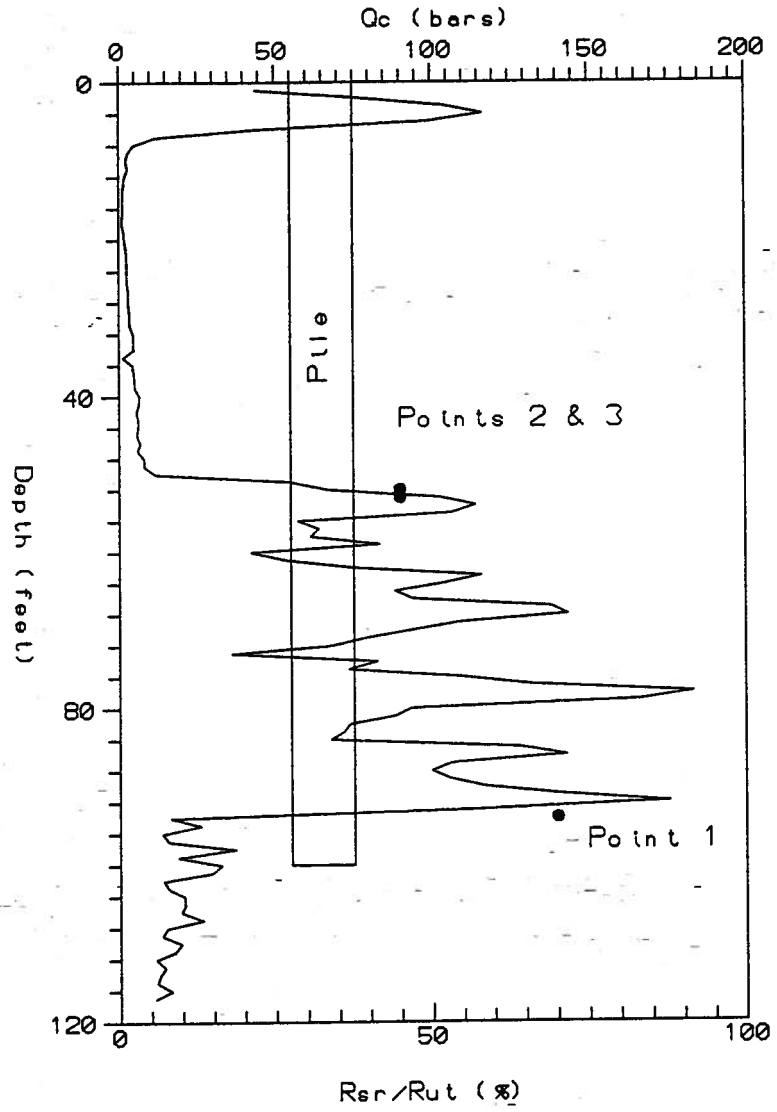

Figure 6.17: Influency of Soil Profile Change to the R_{sr}/R_{ut}

The value of R_{sr}/R_{ut} tends to be constant with increasing depth when q_{ea} is greater than 110 bars, as shown in Figure 6.12 on Tilbury pile 1. From Figure 6.12, R_{sr}/R_{ut} tends towards a constant value of 52 percent below the depth of 70 $feet$ while q_{ea} changes from 110 to 160 $bars$. This means that shaft resistance increases with increasing depth at the same rate as q_{ea} increases. If q_{ea} is the same at different depths, then R_{sr}/R_{ut} will increase with increasing depth. Therefore, higher values of R_{sr}/R_{ut} have to be selected corresponding to the same q_{ea} value when a pile is driven deeper. This tendency is observed at shallower depths for large piles since R_{sr} increases with increasing pile size. Figure 6.18 shows that the average value of R_{sr}/R_{ut} increases from 47 to 52 percent while the depth increases from 55 to 90 $feet$. It is important to understand what depths are likely to show increase in R_{ut} caused solely by further increase in embedded depth. An adjustment is proposed based on statistical analysis in the following chapter.

Soil Plug

From the test records, the measured blow counts of UBC pile 4 are nearly the same as measured blow counts of other UBC piles when the piles were driven in cohesive soils above 50 $feet$. While the open-ended pile has a small end bearing compared to the closed-ended pile, the R_{ut} may be nearly same for both kinds of piles because the low end bearing of the open-ended pile is balanced by the increased friction between soil plug and pile interface. When the tip of UBC pile 4 was driven in sand, relatively low blow counts were measured compared to the measured blow counts of the closed-ended pile of the same size, and the R_{ut} of open-ended pile was smaller than the R_{ut} of the closed-ended pile. The record shows that relative movement between soil plug and pile did take place during pile driving. Table 6.4 gives a comparison of blow counts at normalized hammer energies for UBC pile 4 and pile 5. There were some difference in length and wall thickness between pile 4 and pile 5, but, from preliminary analysis, these difference

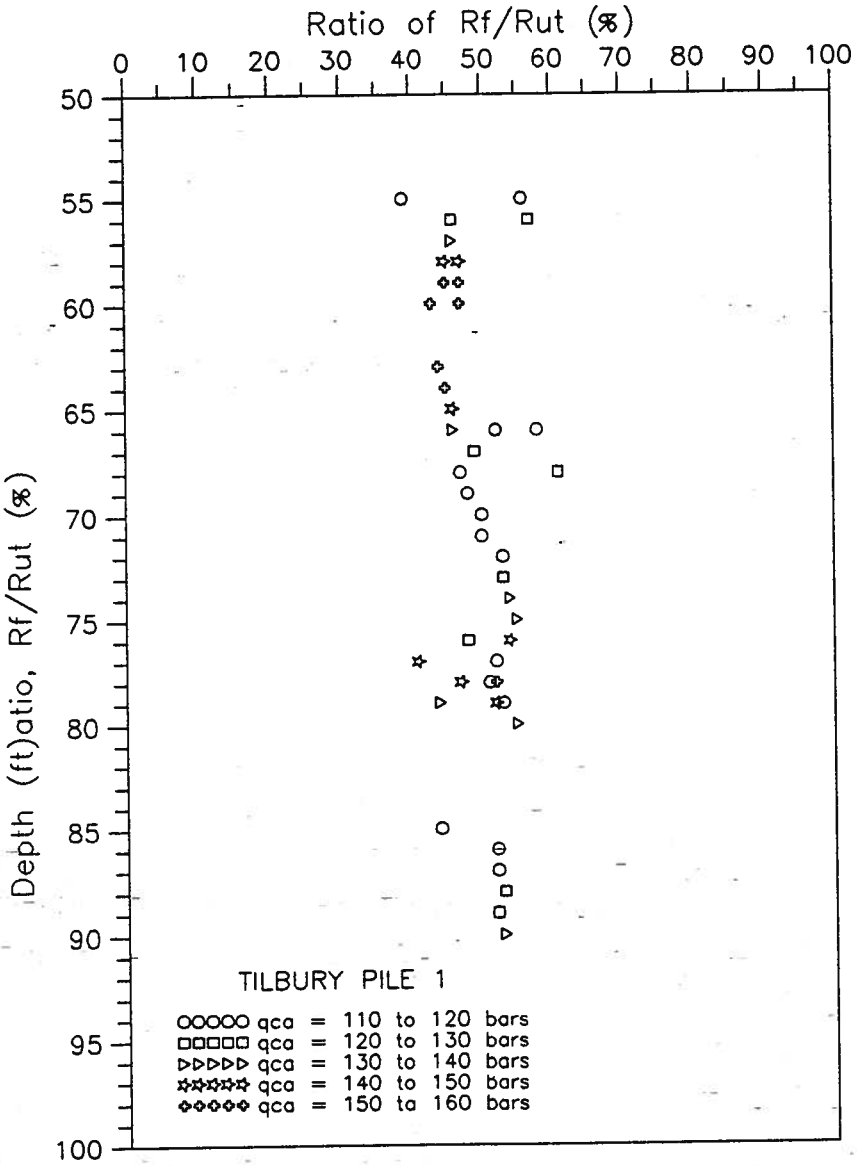

Figure 6.18: Depth Influence to R_{sr}/R_{ut}

Table 6.4: Blow Counts Comparison For UBC pile 4 and 5

Depth	Pile 4		Pile 5
(*feet*)	Energy Used in Pile 5	Measured	Measured
48	2.6	3	3
50	3.4	4	5
55	6.2	7	7
60	5.3	6	6
65	5.2	6	10
68	8.7	10	9
71	7.8	9	10
76	9.4	10	17

should not affect the results significantly. The ratio of R_{sr}/R_{ut} is higher for open-ended pile than that for closed-ended pile at the same pile size. An average value of 5 percent is suggested to be added to R_{sr}/R_{ut} for open-ended pile based on same size closed-ended pile.

When the soil inside the pile is fully compacted, the length of soil plug in the pile will no longer increase. In this case the end bearing for both closed and open ended piles may be similar and an R_{ut} may be determined by using the same value of R_{sr}/R_{ut}. In the GRLWEAP program, when modelling the pile with soil plug, it is assumed that the soil has negligible stiffness compared to the pile. Thus, the pile area and modulus specified described the pile stiffness, and the specific weight of the pile reflects the combined pile and soil properties. A non-uniform pile model was used in the analysis. To do more accurate analysis, a model that considers friction between the soil plug and the pile may be necessary, such as in the model proposed by Heerema and de Jong (1979).

6.4.5 Dynamic Effects during Driving

The CPT is a quasi-static penetration test yet the analysis of pile driving is a dynamic problem. The fact that the LCPC CPT method is very good at predicting pile capacity is a result of the fact that the CPT measures parameters that are more relevant to soil failure during static loading, such as during a pile load test. Since pile driving is a dynamic process it is not too surprising that in some cases measured static parameters do not apply while static and dynamic resistance of soil are related, the relationship can not be expressed simply. An example of this problem is the comparison of SPT N to q_c carried out by Roberson and Campanella (1986). The authors showed clearly that the relationship was a function of grain size and the relationship is non-linear. The dynamic effects caused by driving must be considered in determining R_{ut} from q_{ea}, especially for cohesionless soils. Since the grain size of soil is relatively small compared to the size of the pile the soil is usually compacted by the displacement and vibration during driving. Detailed investigation of extent of compaction of sand and the increase in relative density around the pile have been carried out by Meyerhof (1959) and Robinsky and Morrison (1964). The tests of Robinsky and Morrison showed that the process of sand displacement and compaction below a pile tip is followed by sand movement adjacent to the pile sides. These movements tend to decrease the sand density in the immediate vicinity of the sides and thus nullify some of the benefits gained by the primary compaction. The pattern of displacements around a typical pile is shown in Figure 6.19.

From the results of Tilbury pile 2, the values of R_{sr}/R_{ut} scatter below the linear best fit line as shown in Figure 6.13. It seems that the best fit line under-estimated the values of R_{sr}/R_{ut} for Tilbury pile 2 more than for the UBC piles. The reason for this is that the q_c values increase with increasing density of sand in Tilbury site below 14 $feet$. The values of q_{ea} are lower in loose sand than in dense sand. However the soil resistance

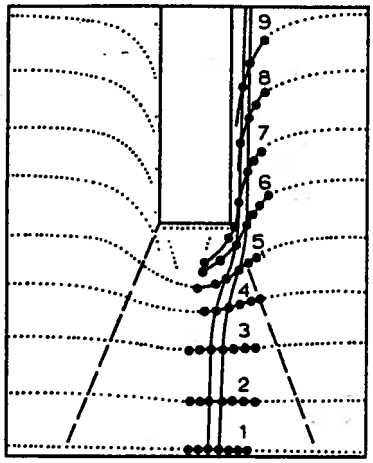

Figure 6.19: Displacements around Driving Pile in Sand (after Robinsky and Morrison, 1964)

increases because of the increase of relative density caused by the driving. Therefore the calculated values of R_{sr}/R_{ut} in loose sand corresponds to slightly lower values of q_{ca}. More research on this problem is required to better understand the limitation of the CPT.

Correction for Diesel Hammer Blow Rate

In the analysis of Tilbury piles, the blow counts as well as hammer blow rate were recorded for the D30-13 diesel hammer. The hammer blow rate is related to the hammer energy and soil resistance during pile driving. The higher the hammer blow rate, the lower is the energy delivered to the pile. Figure 6.20 shows the working principle of a liquid injection open end diesel hammer.

The hammer energy changes with combustion chamber pressure. If the fuel is adjusted

to a lower level, the combustion chamber pressure is lower. Also, the hammer rebound will be lower resulting in higher hammer blow rate. If the R_{ut} is higher, the hammer rebound will be higher which results in the lower hammer blow rate. In order to consider driveability when using a diesel hammer, the hammer blow rate is always recorded along with blow count. The different blow counts can be observed corresponding to different hammer energy delivered to the pile, however the ratio of R_{sr}/R_{ut} is the same for a specified depth. In order to make comparison between predicted and measured blow count, adjustment of blow count according to hammer blow rate is proposed for diesel hammer.

Figure 6.21 shows the blow counts change with hammer blow rate for different values of R_{ut}. When R_{ut} is lower, the change in hammer blow rate does not cause significant change in blow counts. However, when R_{ut} is higher, changes in hammer blow rate result in large change in measured blow counts. This can be explained by Figure 6.23 and also by the bearing graph Figure 6.22. By setting combustion chamber pressure, the input hammer energy is fixed. Then the hammer blow rate only changes with R_{ut} as shown by the family of curves in Figure 6.23. The hammer blow rate decreases with increasing R_{ut}, but tends to a constant value when R_{ut} increases. This is because ram rebound increases with increasing resistance towards an upper limit. When R_{ut} is large enough the gravity energy of ram rebound balances the maximum energy provided by the explosion of combustion chamber pressure. The height of the ram rebound remain constant and the hammer blow rate become constant as well. The combustion chamber pressure provided the hammer energy. The higher the combustion chamber pressure, the higher the hammer energy. The higher the ram rebound, the lower the hammer blow rate. Figure 6.23 shows the hammer blow rate decreases with increasing energy and it also shows that the values of R_{ut} that cause ram rebound to become constant increase with increasing energy. Before a constant hammer blow rate is reached, the blow counts

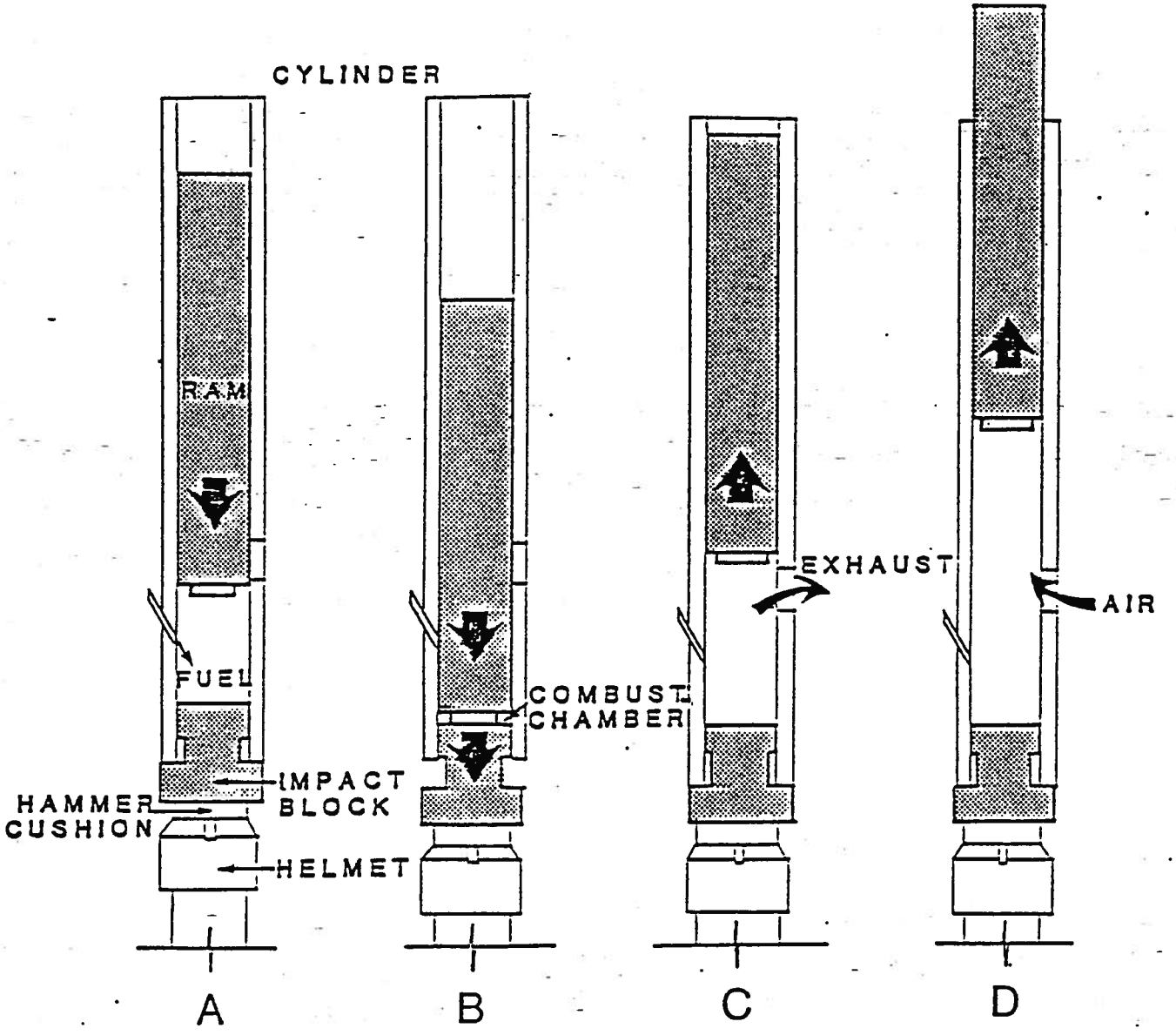

Figure 6.20: Working Principle of a Liquid Injection Open End Diesel Hammer (adapted from GRLWEAP Menu)

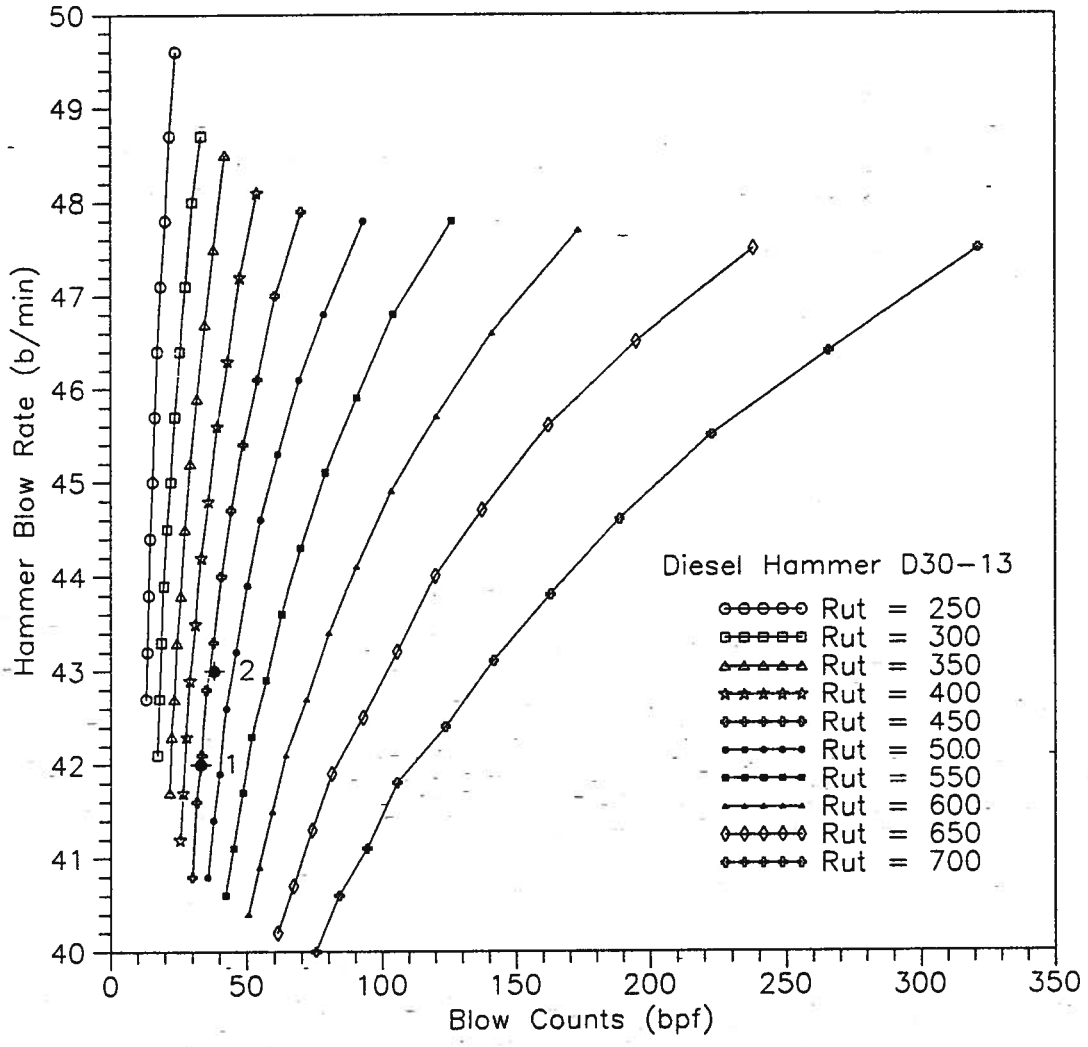

Figure 6.21: Influence of Diesel Hammer Blow Rate to the Pile Blow Counts with Constant R_{ut}

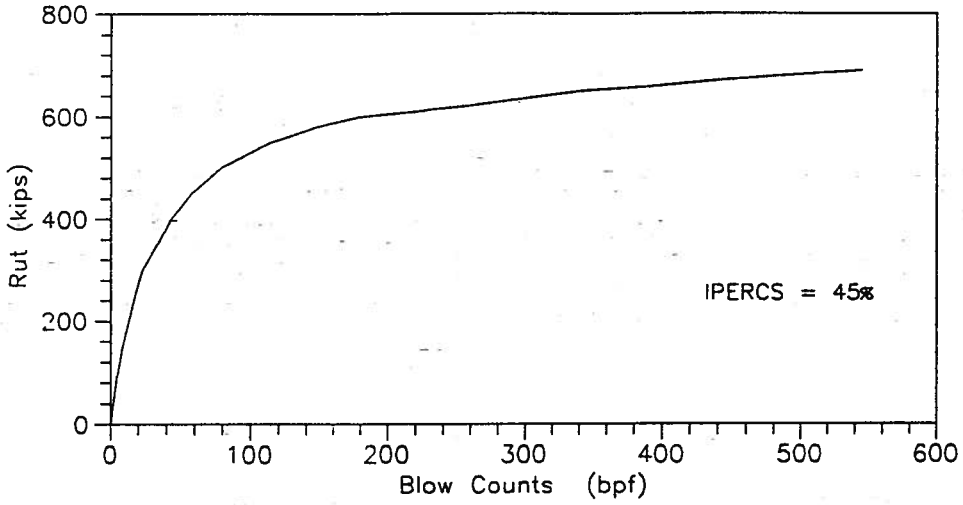

Figure 6.20: Bearing Graph of Tilbury Pile 2 at Depth of 56 feet

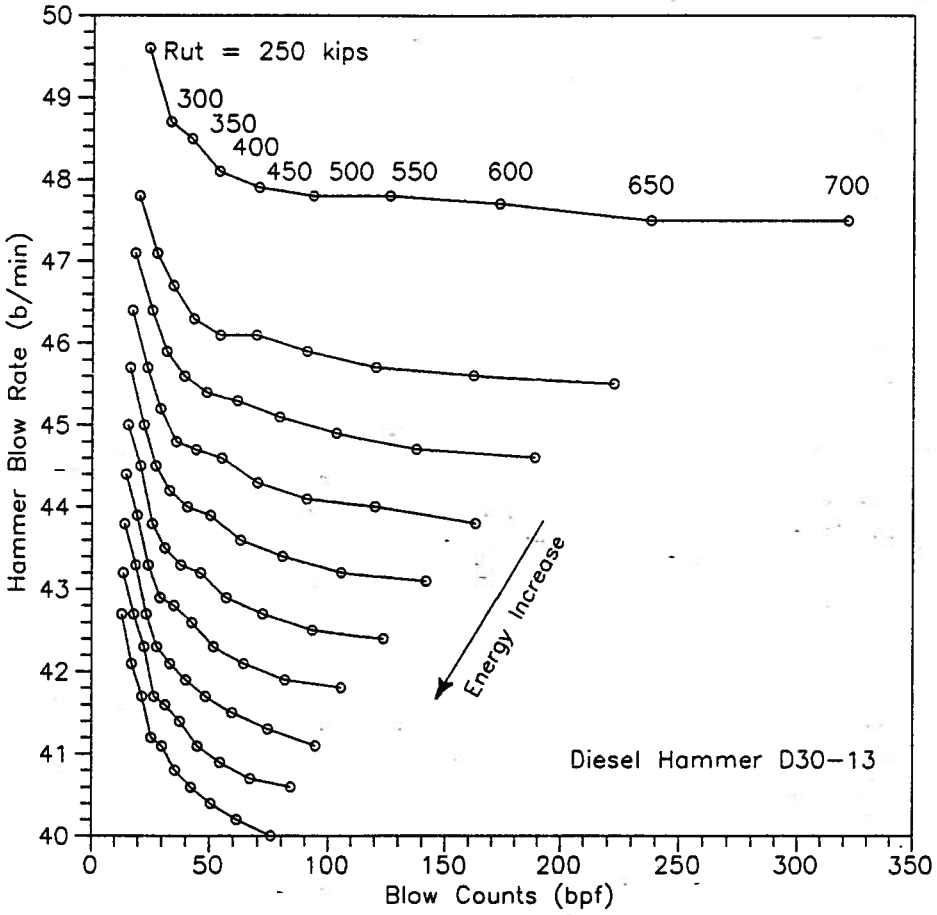

Figure 6.23: Influence of Diesel Hammer Rate with Constant Energy to the Pile Blow Counts

increase slowly with increasing R_{ut}. After a maximum hammer rate is reached, the blow counts increase faster with increasing R_{ut}. This explains the nonlinear characteristic of R_{ut} versus blow counts shown in Figure 6.22. When R_{ut} is lower, the hammer energy does not operate efficiently because the ram rebound is low. When a constant ram rebound is reached, corresponding to a value of R_{ut}, the hammer energy is at its maximum. The value of R_{ut} at this stage is noted as R_{utm}. If R_{ut} is smaller than R_{utm}, the energy transmitted to the pile will increase with increasing R_{ut} due to increasing ram rebound. The energy needed to cause pile penetration is provided by the hammer. As the hammer blow rate increases, the blow count increases slowly. If R_{ut} is larger than R_{utm}, the energy transmitted to the pile can not increase because the energy is at its maximum. In this case the hammer blow rate becomes constant, but blow count increases significantly, as a small increase in R_{ut} causes a notably increase in blow counts.

In Figure 6.21, point 1 shows the blow counts of 33 $blows/foot$ with hammer rate of 42 $blows/min$ for Tilbury pile 2. Point 2 shows the blow counts of 38 $blows/foot$ with hammer rate of 43 $blows/min$ for Tilbury pile 1. Both piles were embedded at a depth of 57 $feet$ where R_{ut} was predicted at 459 $kips$. Thus a great difference in blow count may be caused by a small difference in hammer blow rate. If a diesel hammer is used when predicting blow counts, the predicted blow count must be presented with hammer blow rate. It is suggested that for every types of diesel hammers a figure like Figure 6.21 should be developed.

6.5 Conclusion

Three assumptions based on pile capacity determined from CPT were made to establish the empirical correlation between R_{ut} and q_c in order to predict the blow counts of driven piles. From the results, the assumption based on shaft resistance component was selected,

and empirical correlations between R_{sr}/R_{ut} and q_{ea} were found for steel pipe piles and H piles. The ratio of R_{sr}/R_{ut} is considered to reflect the resistance condition of pile embedded in different soil layers. The values of q_{ea} determined from CPT q_c are affected by the size of pile. The main conclusions are as follows:

(1) The ultimate resistance R_{ut} during pile driving is smaller than pile capacity determined from CPT. A reduction must be properly selected in order to model soil resistance condition during pile driving. The reduction factor is a function of soil type.

(2) The ratio of R_{sr}/R_{ut} reflects pile resistance conditions, i.e. shaft resistance or end bearing pile. R_{ut} can be evaluated through establishing correlation between R_{sr}/R_{ut} and q_{ea}, where q_{ea} reflect soil strength.

(3) For the same kind of piles, the correlations between R_{sr}/R_{ut} and q_{ea} show very similar results. The correlations are independent of driving system and are affected by the soil strength, pile embedded depth and pile size.

(4) For the different types of piles, the correlations between Rsr/R_{ut} and q_{ea} are very different. The difference are related to the pile resistance distribution.

(5) There is potential to use the method proposed in this study to predict blow count of driven concrete and timber piles. But, it is necessary to determine reasonable reduction factor and establish the correlation analogous to those established in this study.

Chapter 7

Statistical Analysis and Criteria for Blow Count Prediction

7.1 Introduction

The main purpose of predicting blow counts of a driven pile is to ensure good performance of the hammer-pile-soil system. Good performance should be defined realistically in terms of error limits with a given confidence level. The predicted blow counts change with the ultimate resistance R_{ut} which can be determined from q_c and R_{sr}. Due to the non-linear nature of the bearing graph, as shown in Figure 6.22, at lower levels of R_{ut}, a change of R_{ut} causes a small change in blow count. But, at higher levels of R_{ut}, even a very small change of R_{ut} will cause a big change in blow count. In Chapter 6, it was observed that points of computed R_{sr}/R_{ut} were scattered in a band. The band width and slope was different for different types of piles and different magnitude of q_{ea}. The values of R_{ut} determined from the R_{sr}/R_{ut} versus q_{ea} figures depend on the slope of the bands. Any error in R_{ut} will result in an error in predicted blow count, especially at high R_{ut} level. Statistical analysis allows a better understanding of limitation of the proposed method and gives an indication of the reliability in applying the proposed method.

Statistical analysis can be used to draw information about a sample, and thus estimate values that help characterize the population from which the sample was chosen. Through statistical analysis, a confidence interval for an expected value can be determined to indicate the reliability of the result. Because of the limited availability of data, we would choose one pile sample to do a single pile statistical analysis. The statistical analysis

performed herein will consider UBC pile 5 and 6, Tilbury pile 2 and Tilbury H12×53 pile.

7.2 Linear Regression Analysis

In order to describe a correlation between two variables, the analysis must combine the distributions of all the measured variables with respect to a particular reference to reach the accuracy with which some variables can be determined from the others. In the drivability analysis, the measured parameter q_{ea} is an independent variable. It is proposed that the computed value R_{sr}/R_{ut} is a dependent variable. The extent to which q_{ea} controls the computed values of R_{sr}/R_ut will determine the correlation coefficient.

A linear correlation is assumed between R_{sr}/R_{ut} and q_{ea} based on the results of Chapter 6. The following assumptions are made in proposing a straight line regression through the data.

1. The q_{ea} values based on q_c are error free.

2. The regression of R_{sr}/R_{ut} and q_{ea} is linear.

3. The deviations $Y_i - E(Y|X_i)$ are mutually independent, where x is q_{ea} and y is R_{sr}/R_{ut}.

4. These deviations have the same variance (σ^2, not usually known exactly).

5. These deviations are normally distributed.

Based on above assumptions the regression straight line can be described by Equation 7.1 [44].

$$y_i = a + bx_i + \varepsilon_i \ ,\varepsilon \sim N(0, \sigma^2) \tag{7.1}$$

If the estimators of a and b is $\hat{a}$ and $\hat{b}$, the estimator of y is $\tilde{y}$. The equation $\tilde{y} = \hat{a} + \hat{b}x$ is called a regression function.

The Least Square Method is used to estimate $\hat{a}$ and $\hat{b}$ [44]. The results of the linear

Table 7.1: Regression Analysis Results

Pile	$\hat{a}$	$\hat{b}$	$\hat{\sigma}$
UBC P5	92.216	-0.3622	8.7457
UBC P6	97.195	-0.3917	8.7178
TIL P2	91.134	-0.3597	9.2687
TIL HP	101.570	-0.1527	5.6972

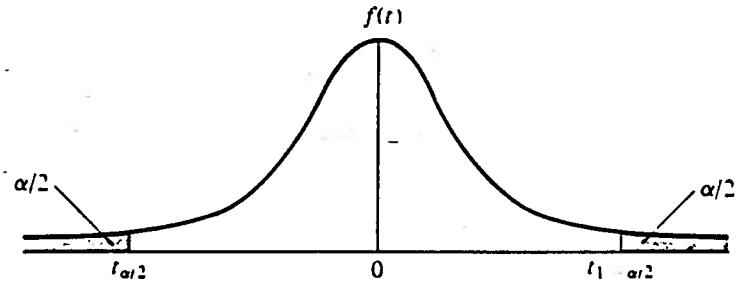

Figure 7.1: Probability of Student Distribution

regression for different piles are given in Table 7.1. The unbiased estimator of $\hat{\sigma}$ of the maximum likelihood estimator, σ are determined [44] and given in Table 7.1 also. The figures of R_{sr}/R_{ut} versus q_{ea} in Chapter 6 show that the linear regression lines agree well for the same type of piles.

7.3 Confidence Interval Analysis

In the regression analysis, y_i was assumed to be normally distributed for each fixed x_i. Supposing, it is necessary to know a 100(1-α) percent confidence interval of y for $x = x_0$. That probability of 100(1-α) percent confidence interval is defined the white area, as shown in Figure 7.1 [44]. The mathematic details of confidence interval are presented in Appendix B [44].

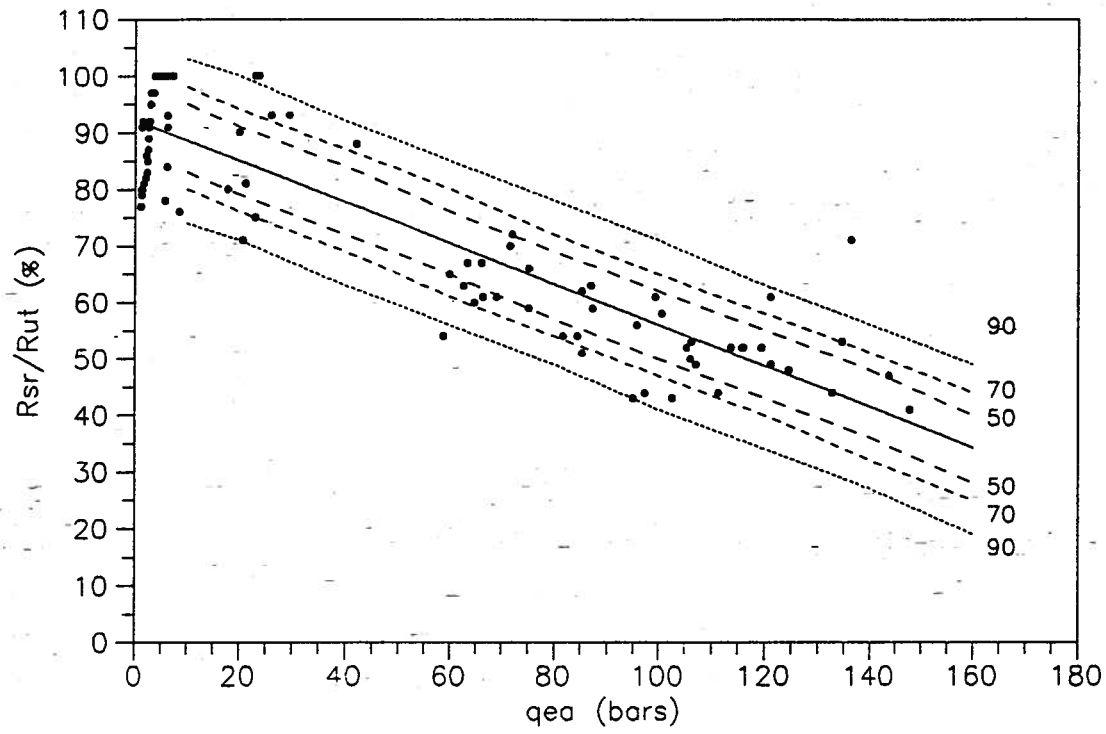

Figure 7.2: Bands of Different Confident Interval for UBC Pile 5

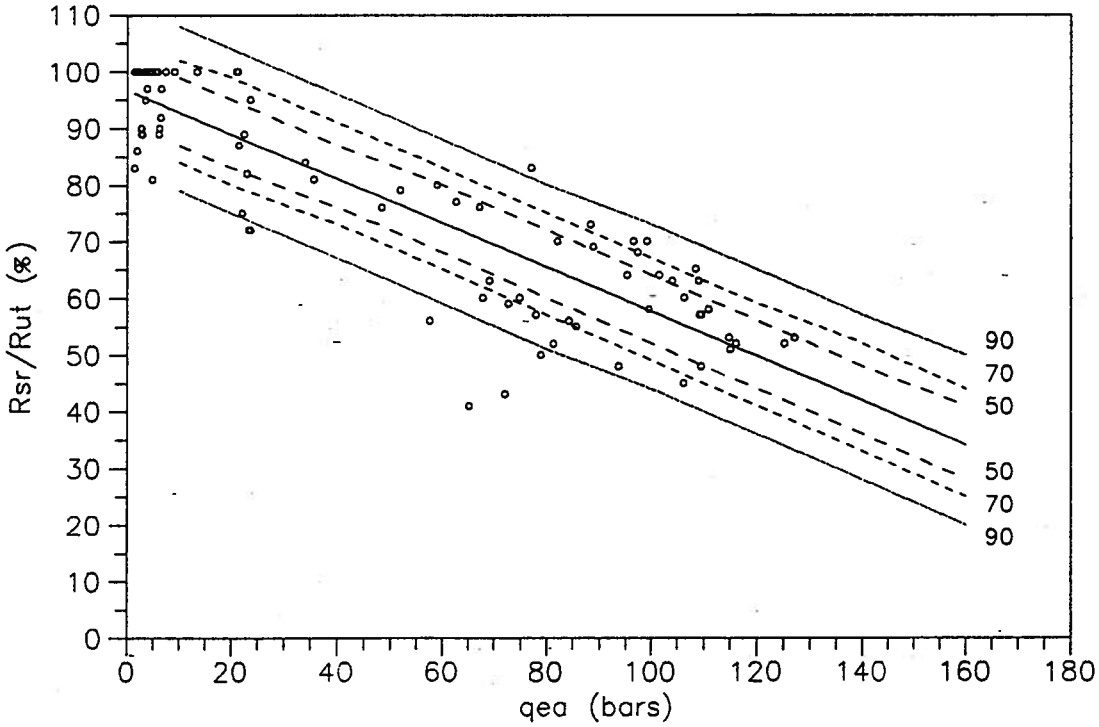

Figure 7.3: Bands of Different Confident Interval for UBC Pile 6

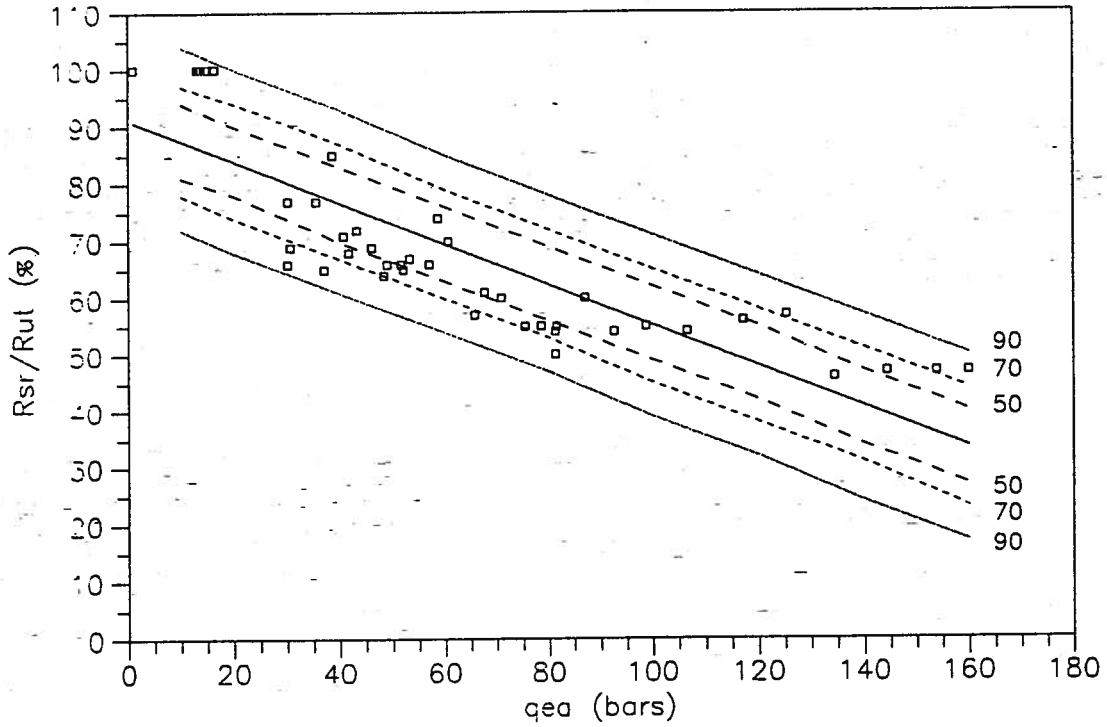

Figure 7.4: Bands of Different Confident Interval for Tilbury Pile 2

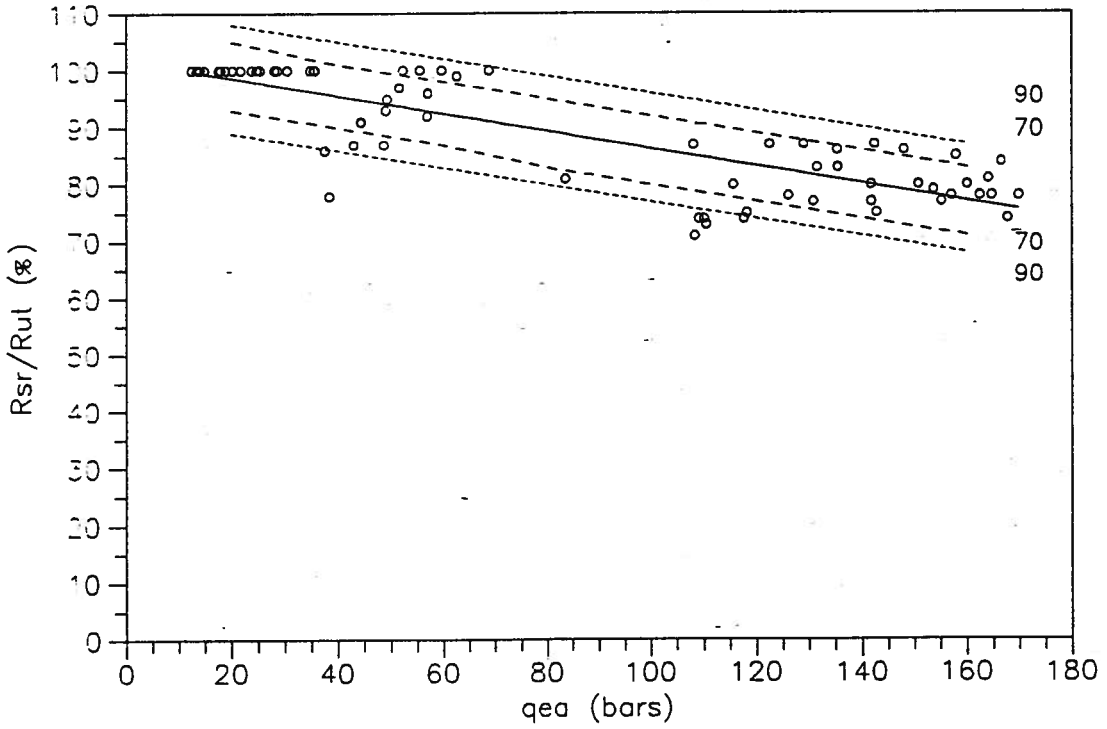

Figure 7.5: Bands of Different Confident Interval for Tilbury H12×53 Pile

The calculated results of y_0 for selected values of x_0, together with the lower and upper bounds for different 100(1-α) percent confidence interval, on UBC pile 5 and 6, Tilbury pile 2 and H12×53 pile are shown in Figures 7.2 to 7.5.

7.4 Criteria Study of Predicted Blow Counts Based on Statistical Analysis

7.4.1 Outline

From the results of statistical analysis, lower and upper bounds are determined according to different confidence levels. For a given value of q_{ea} and R_{sr}, the lower bound relates to a lower value of R_{sr}/R_{ut} which give a larger value of R_{ut}, and the upper bound relates to a higher value of R_{sr}/R_{ut} which give a smaller value of R_{ut}. The predicted blow count increases with increasing R_{ut} if other parameters remain constant. The range of predicted blow counts corresponds to lower and upper bounds of R_{ut} depends on the various confidence levels. In order to keep the error of predicted blow counts as low as possible, different levels of confidence have to be taken into account for different value ranges of q_{ea}. Due to the nonlinear relationship between R_{ut} and blow counts, as shown in Figure 6.22, when the R_{ut} value is high, a small error in estimated R_{ut} can result in a very large difference in the predicted blow counts. An error study of predicted blow counts based on the regression and confidence analysis results was made on UBC piles 5 and 6, and the Tilbury H pile. The purpose of this section is to examine the change of predicted blow counts with a defined confidence and to give a reliable lower and upper bound in determining R_{ut}. The results of this study are given in Appendix C.

7.4.2 Steel Pipe Pile

Figures 7.6 and 7.7 show the results of predicted blow counts using the values at regression line, lower and upper bounds with different confidences for UBC piles 5 and 6.

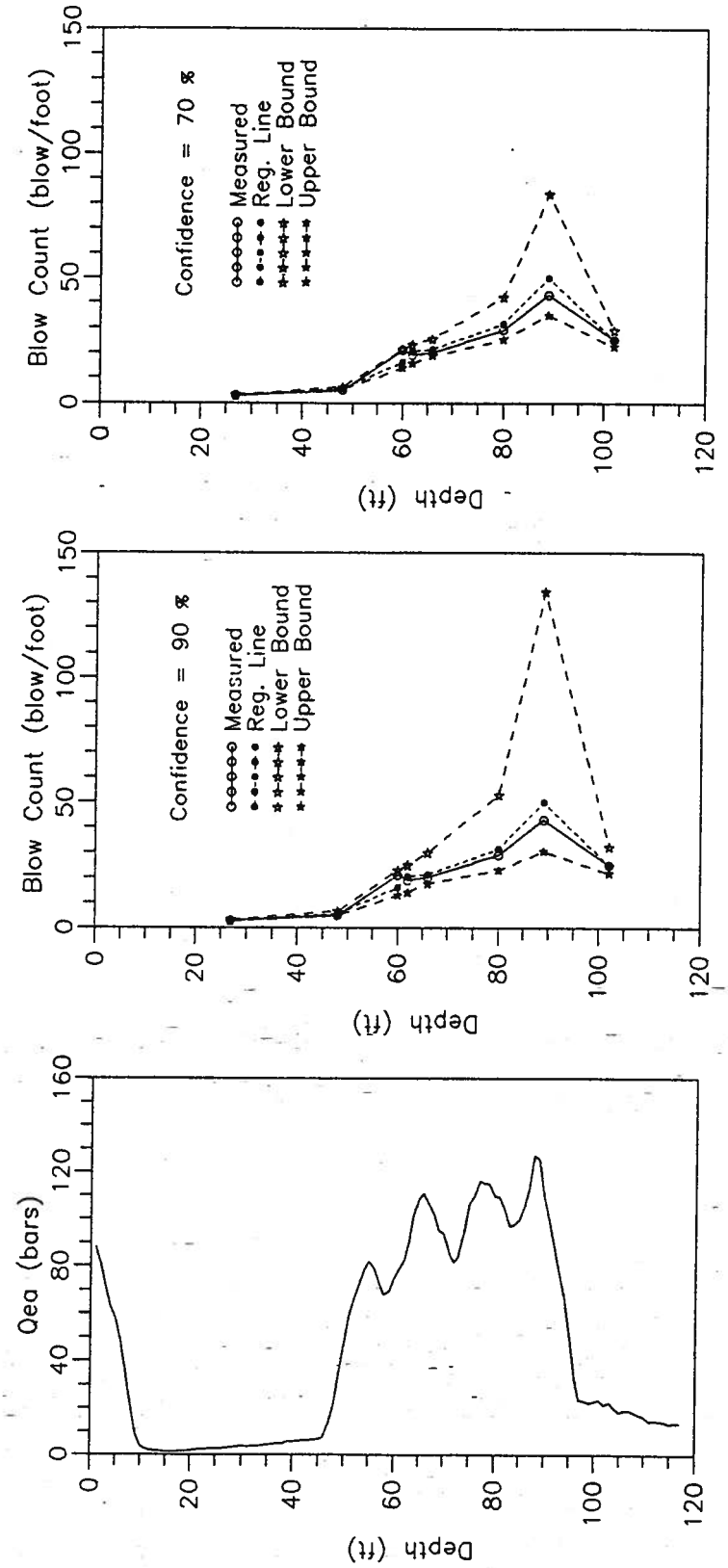

Figure 7.7: Blow Counts Predicted from Regression Line, Lower and Upper bounds with Different Confident Interval for UBC Pile 5

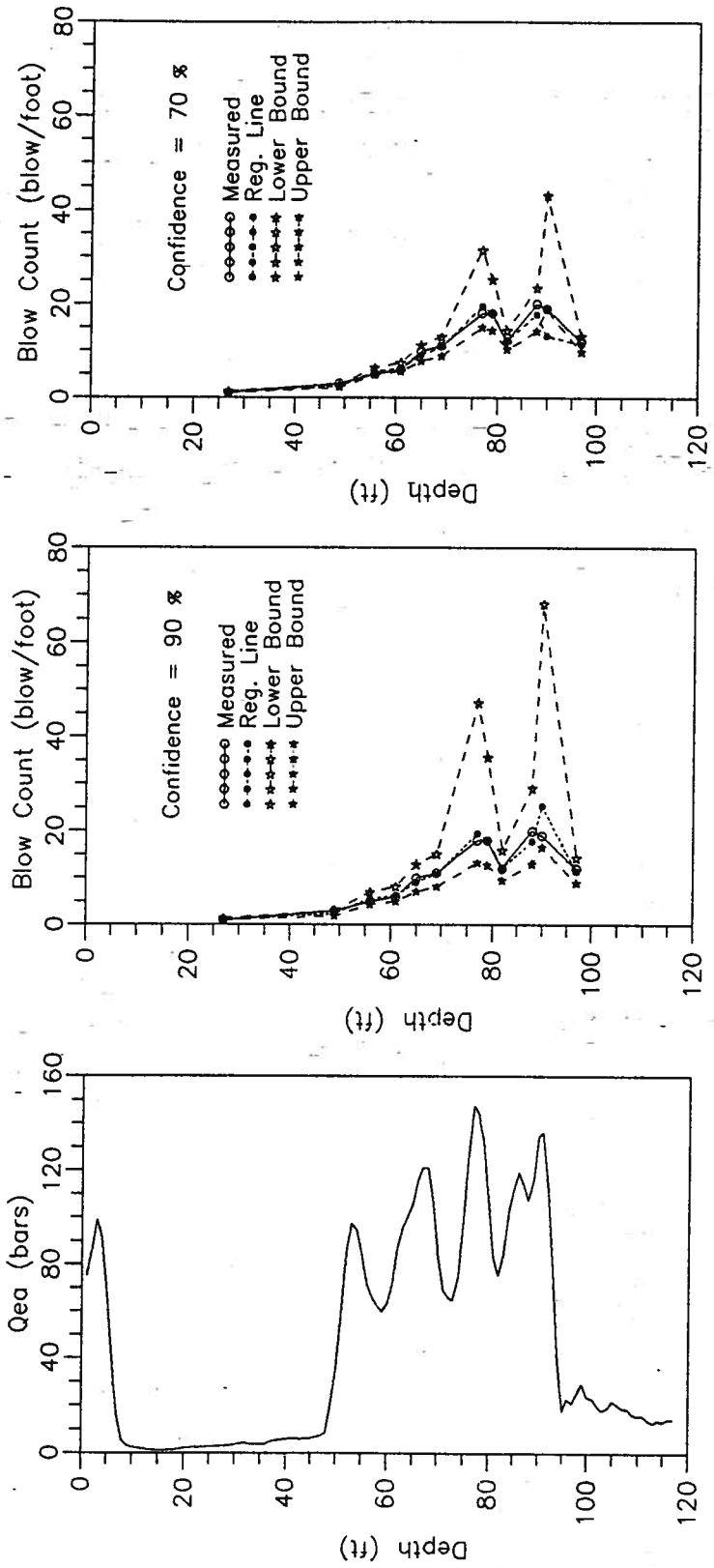

Figure 7.8: Blow Counts Predicted from Regression Line, Lower and Upper bounds with Different Confident Interval for UBC Pile 6

The values of q_{ea} and measured blow counts are shown as well. The following tends are observed based on these figures.

When the value of q_{ea} is smaller than 30 *bars*, the value of R_{sr}/R_{ut} is larger than 70 percent. The pile behaves as a friction pile and the blow count calculated from R_{ut} on the linear regression line agrees well with the measured blow count. Up to 30 percent error can be expected based on lower and upper bound corresponding to the 90 percent confidence, for predicted blow counts. 30 percent error is acceptable at relatively lower levels of blow count. For example, for the results from 102 *feet* depth of pile 6, the predicted blow counts based on lower and upper bound are 32.4 and 21.7, respectively, while the measured blow count is 25. If a lower confidence is used, a more reliable range of blow counts can be predicted. In comparing the results for the pile tip embedded in soft soils at different depths, it was shown that the errors of predicted blow count are not influenced by increasing depth, and the blow count only increases with increasing shaft resistance for friction pile condition.

When the values of q_{ea} are from 30 to 100 *bars*, the values of R_{sr}/R_{ut} change from about 80 to 60 percent, as shown in Figures 7.6 and 7.7. This happens when pile tip is embedded in depths of 60 and 62 *foot* for UBC pile 5, and in depths of 56, 61, and 82 *feet* for UBC pile 6. In this range, the calculated blow count based on linear regression line agrees well with measured blow count. The errors of predicted blow counts based on lower and upper bound are small, except that predicted lower blow counts of 60 *foot* depth of UBC pile 6 has an error of 28 percent. It seems that a better way to predict the blow counts is based on the range between regression line and lower bound. When the values of q_{ea} are between 100 and 120 *bars*, the values of R_{sr}/R_{ut} are about 54 percent and the pile behaves as an end bearing pile. The calculated blow counts based on the linear regression line agrees well with the measured blow counts. Since the values of R_{ut} are higher, a small change in R_{ut} will result in a large change in blow count. Even

though the percentage of error may be the same as for lower values of q_{ea}, there are some difference between predicted blow count and measured blow count, depending on if the prediction is based on lower or upper bound. A very large error can be made when predicting blow count using lower bound, especially for deep piles. For example, the error of blow count predicted with 90 percent confidence for UBC pile 6 at 80 *feet* is 83 percent with predicted blow count of 53 comparing to measured blow count of 29. However, the error of blow count calculated from the upper bound is smaller. The above phenomenon can be explained by the depth and pile size influence which result in increasing shaft resistance with increasing depth. The increase of shaft resistance with depth causes the values of R_{sr}/R_{ut} to be higher and the values of R_{sr}/R_{ut} determined from lower bound to be lower. This can be seen by comparing pile 5 and pile 6. Since the size of pile 5 with a diameter of 12.75 *in.* is smaller than that of pile 6 with a diameter of 24 *in.*, the R_{sr} of pile 6 is about twice the R_{sr} of pile 5 at the same depth. For pile 5 at a depth of 88 *feet*, the blow count calculated from lower bound is 29.1 comparing to measured blow count of 20, and for pile 6 at a depth of 89 *feet*, the predicted blow count from lower bound is 134.5 comparing to measured blow count of 43, with a confidence of 90 percent. It is recommended that at higher values of q_{ea}, the lower bound is not reliable to predict blow count, especially for large size piles embedded in deep pile condition. The band between the upper bound and linear regression line with 70 percent confidence is suggested to predict blow counts.

When the values of q_{ea} are between 120 *bars* and 150 *bars*, the predicted blow counts appear to have bigger errors, with a maximum error of up to 213 percent, from lower bound with a 90 percent confidence. At the same time, the blow count predicted based on linear regression line is higher than the measured blow counts for deep piles like pile 5 at a depth of 90 *feet* and pile 6 at a depth of 89 *feet*. Obviously, shaft resistance increases with increasing depths. From the analysis results, it can be concluded that

upper bound gives more reliable R_{ut} values than lower bound even with a confidence of 50 percent in predicting blow counts. This shows that the assumption of linear regression is no longer applicable at higher levels of q_{ea}, especially for large size piles. However, a combination of upper bound of 80 percent confidence with linear regression line can be used to predict the blow count for the piles of small size. A combination of upper bound of 70 percent confidence with linear regression line can be used to predict blow counts for the piles of large size. In this range of q_{ea}, the linear regression line can be considered as lower bound and the values of R_{sr}/R_{ut} in the range between regression line and upper bound can be used to predict blow counts.

7.4.3 H Piles

Figure 7.8 shows the predicted blow counts for the Tilbury H pile. As shown in Figure 7.8 the linear regression line is the characteristic of a shaft resistance pile. The values of R_{sr}/R_{ut} are larger than 75 percent when the values of q_{ea} are up to 170 *bars*. From Figure 7.8, the predicted blow counts based on lower bound overestimated R_{ut} in all depths even though the values of q_{ea} are higher than 160 *bars*. The error increases with increasing depth. This results from increasing shaft resistance with lower end bearing at depths. The predicted blow count based on regression line with upper bound represents a reliable interval when compared to measured blow counts. When the values of q_{ea} are lower than 30 *bars*, a value of 100 percent for R_{sr}/R_{ut} can used to estimate R_{ut}. A confidence interval of one σ, or about 70 percent, can be used to predicted R_{ut} within the band of the regression line and upper bound.

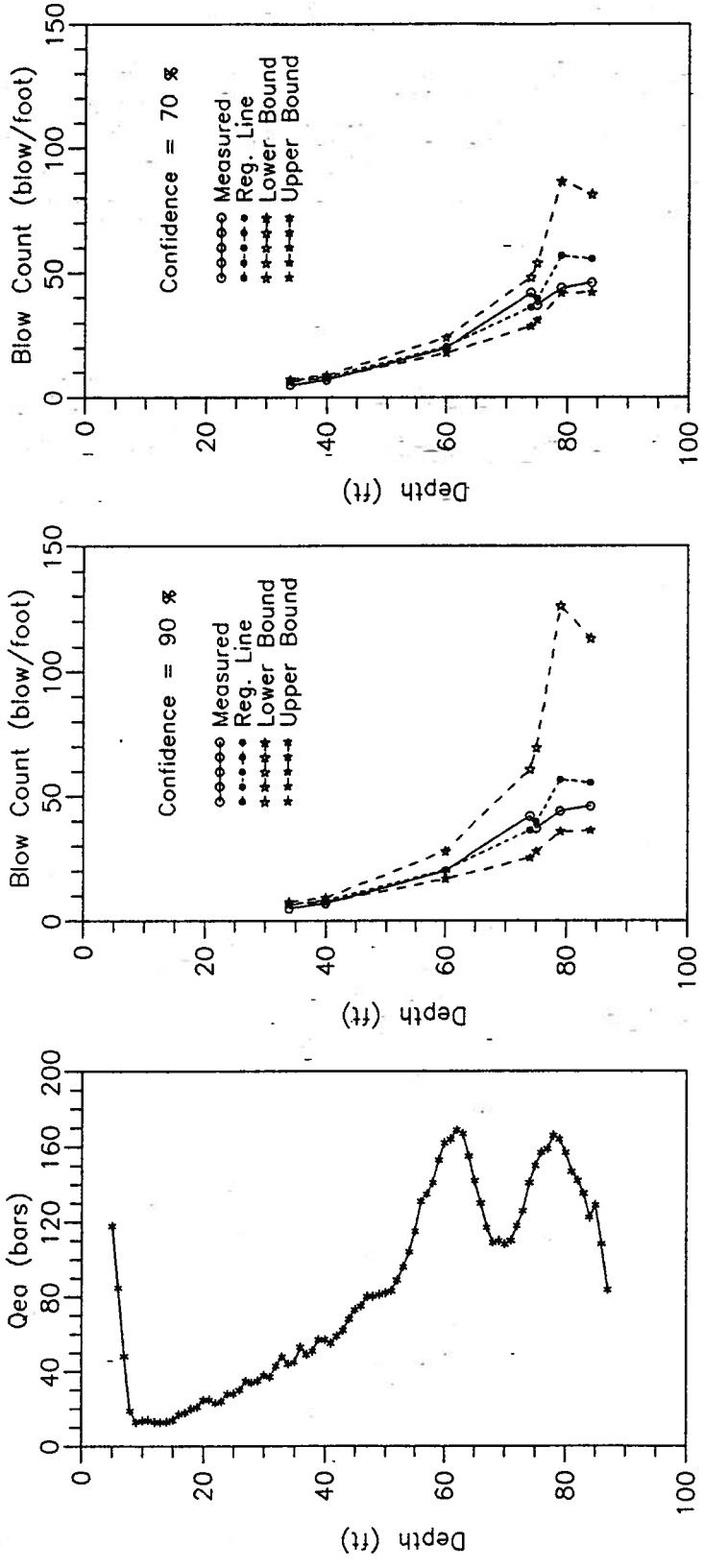

Figure 7.9: Blow Counts Predicted from Regression Line, Lower and Upper bounds with Different Confident Interval for Tilbury II Pile

7.5 Conclusion

The above analysis is only based on limited data. More analysis is recommended to do for piles at different sites. Some conclusions based on statistical analysis are summarized as follows.

For steel pipe piles:

(1) In predicting blow count of friction pile, which values of R_{sr}/R_{ut} are larger than 75 percent, a confident interval of 90 percent can present reliable R_{ut} value.

(2) When q_{ea} is smaller than 30 *bars* the linear regression line can only be used to predict blow count.

(3) When q_{ea} is between 30 and 80 *bars* the lower bound can be used to determine R_{ut} especially in the case of pile is embedded in loose sand.

(4) When q_{ea} is between 80 *bars* and 150 *bars*, the lower bound should not be used to predict blow count if the pile tip is embedded in a depth more than 80 *feet*, due to the fact that increasing depth causes increasing shaft resistance, especially for large size piles.

(5) When q_{ea} is between 100 to 150 *bars*, the upper bound with 70 percent confidence can be used with linear regression line to predict blow count.

(6) When q_{ea} is larger than 150 *bars*, the upper bound along with the linear regression line can be used to predict blow counts for small size piles. When a large size pile is embedded in depth over 100 *feet*, the upper bound with a correction of depth can be used to predict blow count, but in this case the linear regression line is no longer suitable.

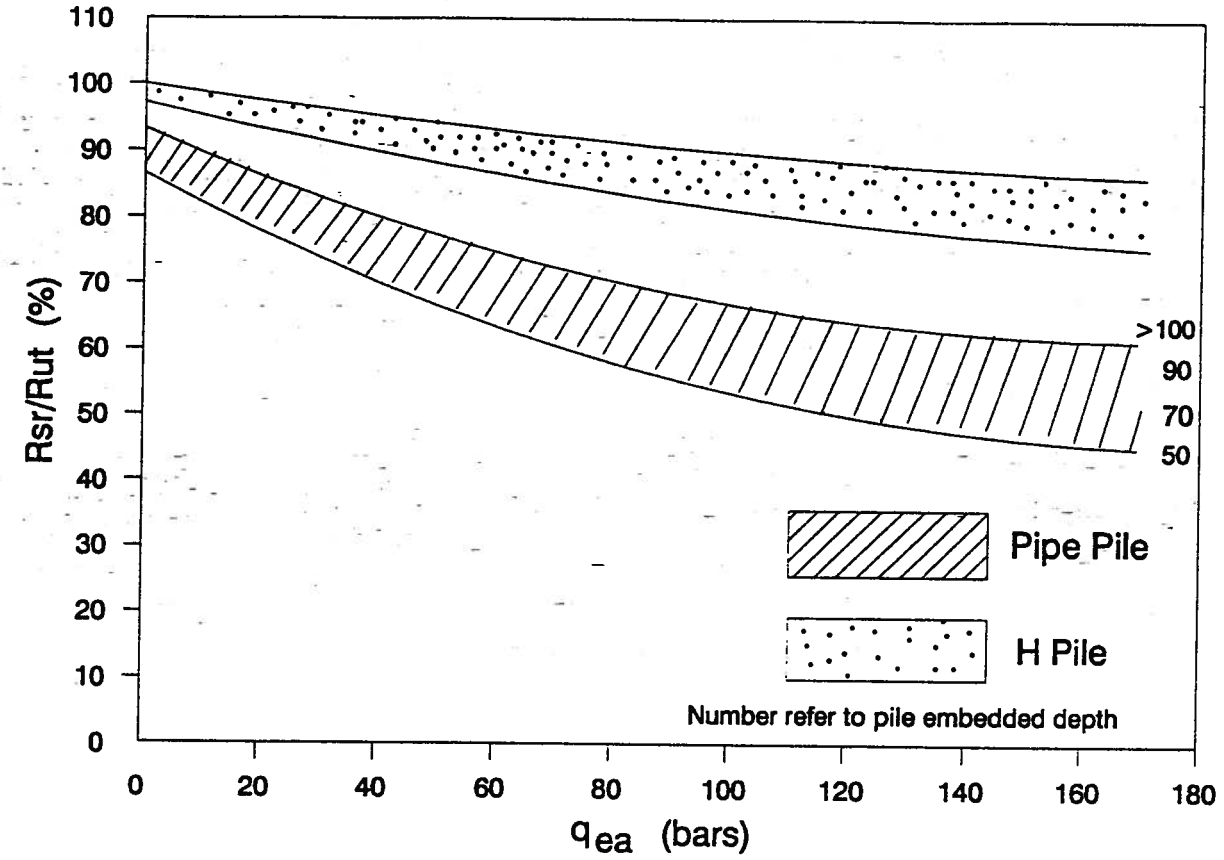

(1) When q_{ea} is lower than 40 *bars* a value of 90 to 100 percent R_{sr}/R_{ut} can be used to estimate R_{ut}.

(2) When q_{ea} is higher than 40 *bars* the linear regression line with upper bound can be used to determine R_{ut} in predicting the blow counts.

In Figure 7.9, each different band with correction depth was suggested to determine R_{ut} for different types of piles.

Chapter 8

Application

8.1 Outline

In this chapter, a case history of using the method proposed in previous chapters to predict blow count of driven pile is presented to show the applicability of this method in practice. This method is based on CPT q_c and shaft resistance determined from LCPC CPT method. Figure 7.10 derived based on statistical analysis in Chapter 7 is used to determine R_{ut} with 70 percent confidence. The prediction was performed based on Tilbury pile 3 which is a closed ended steel pipe pile. The details of the soil conditions have been presented in previous chapters. Comparison between predicted and measured blow count were made to show the accuracy of the predicted results. A sample of input and output data is presented in Appendix D.

8.2 Predicting Steps

The predicting steps are as follows:

(1) Calculate average q_c for each one foot depth from data file of q_c measured every *inch* by using CPTINT program and calculated q_{ca};

(2) Predict pile capacity, shaft resistance by using LCPC CPT method;

(3) Determine shaft resistance during pile driving, R_{sr}, by introducing reduction factors, 0.7 for sand and 0.5 for clay, into shaft resistance part of pile capacity;

(4) Calculate R_{sr}/R_{ut} based on Figure 7.10 recommended in Chapter 7;

(5) Determine R_{ut} with known q_{ea} and R_{sr};

(6) Input R_{ut} with soil, hammer and pile parameters into GRLWEAP program to calculate blow counts for each one foot depth until final pile penetration.

8.3 Results

The results based on above prediction steps are shown in Figure 8.1 with q_{ea}, R_{sr}, R_{sr}/R_{ut}, R_{ut} and predicted blow counts. For each depth the R_{ut} is used in prediction. Parameters, such as soil quake and damping, and hammer efficiency, were taken from the GRLWEAP menu as recommended for the D30-13 diesel hammer, type of pile and soil conditions of Tilbury Site.

According to the record given in Appendix A, the hammer fuel value was adjusted to minimum to give lowest combustion chamber pressure. Therefore, the hammer fuel setting option, $IFUEL$ was set to 4 corresponding to the minimum pressure value of 914 psi. The hammer stroke option $IOSTR$ was set to 0 or 1 to make the calculated hammer blow rate at a given depth the same as that recorded during pile driving. Since the recorded hammer blow rates are not available for every depths, an average hammer blow rate between two recorded hammer blow rates is used at the depth where no hammer blow rate was recorded.

The predicted blow counts are presented in Figure 8.2 with measured blow counts during pile driving.

8.4 Comparison between Predicted and Measured Blow Counts

The predicted blow counts agree well with the measured blow counts when the pile tip was embedded in depths above 21 $feet$. Soils above 21 $feet$ change from clayey silt to sand and silt. Lower blow counts were measured during pile driving because pile was

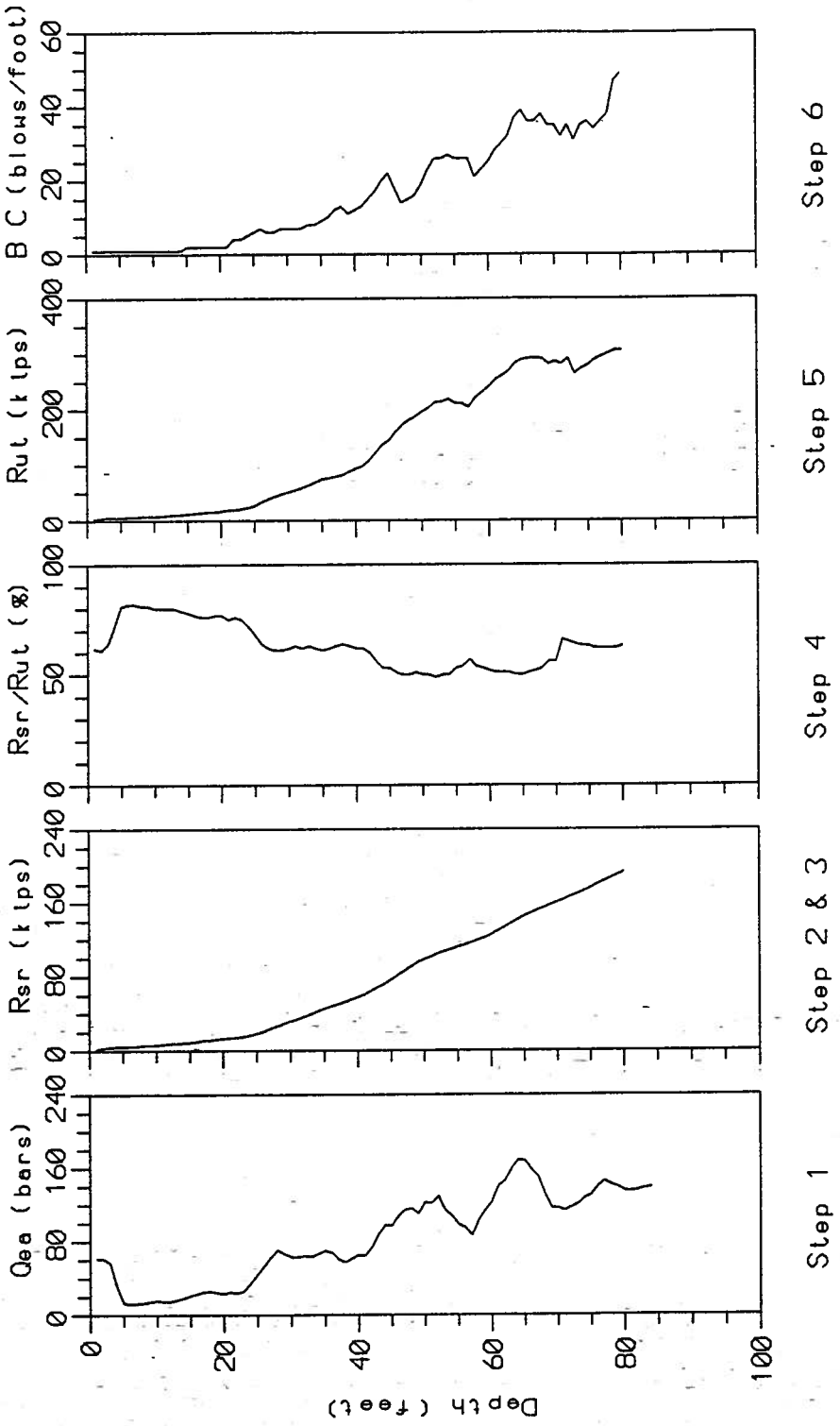

Figure 8.1: Procedure for Blow Count Prediction

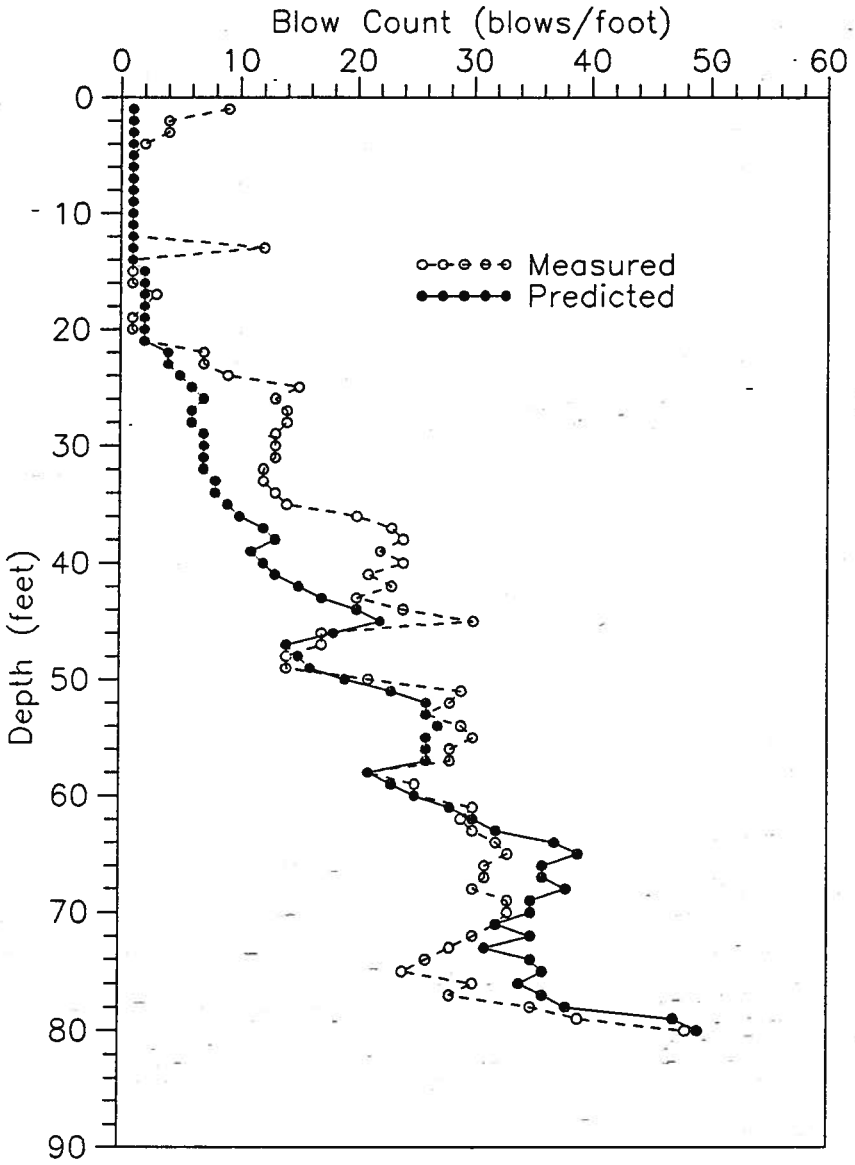

Figure 8.2: Predicted and Measured Blow Counts for Tilbury Pile 3

Table 8.1: Predicted and Measured Blow Counts at the Same Hammer Blow Rate

Depth	Blow Counts ($blows/foot$)		Hammer Blow Rate	ENTHRU
($feet$)	Predicted	Measured	($blows/min$)	($kip-ft$)
52	26	28	54	17.8
59	23	25	51	22.3
66	36	31	51	22.4
72	35	30	50	22.2
78	40	35	50	21.3
ENTHRU stands for transferred energy				

embedded in soft soil where q_c values are low. The same lower blow counts are predicted in terms of lower R_{ut} values determined from lower q_c values.

From depth of 22 to 42 $feet$, the soil is sand with density increasing from medium loose to dense with depth. The predicted blow counts are much lower compared to the measured blow counts, even though larger R_{ut} values were determined from the lower bound in Figure 7.10. This means that the values of R_{ut} were under-estimated. Q_c values are affected by soil density with q_c increasing with increasing density. In loose sand, q_c values are lower because of low density however this density will increase during pile driving because the soil is compacted by displacement and vibration. Therefore, lower R_{ut} values are determined by using the values of q_{ea}. However, the prediction can be used as a reference, even though the error is high, because the expected blow counts is limited to a lower level that will not cause refusal in pile driving. The highest error was made when the recorded blow counts had values smaller than 30 $blows/foot$.

Over depths of 42 $feet$, the sand is dense. The predicted blow counts agree well with measured blow counts except slight over-predicting at depths from 65 to 68 $feet$. The R_{ut} determined by using q_{ea} is more reliable in dense sand than in loose sand. Table 8.1 gives comparison between predicted and measured blow counts at the same hammer blow

rate. From this table it is clear that for a fixed hammer blow rate at depth greater than 50 $feet$, accurate prediction can be made.

8.5 Conclusion

The above results show that reasonable predictions can be made using the method described, especially in cases where high blow counts may be expected. The prediction is affected by the soil density. A useful evaluation of the drivability prediction can be made using this method before pile driving.

Chapter 9

Summary and Conclusion

The main purpose of this study was to examine methods of using CPT in conjunction with the one-dimensional wave equation program to predict blow counts of driven pile.

Three sites were included in this study: UBC Pile Research Site, Tilbury Island Site and Evanston Campus of Northwestern University (ECNU) Site. The pile types include steel pipe piles, both closed and open ended, and H piles.

An empirical correlation was established to estimate the driving toe resistance directly from the CPT q_c. The shaft resistances during driving were estimated from static long term pile resistances evaluated from the LCPC CPT method and multiplied by a set of reduction factors. Reduction factors, 0.5 for clay and 0.7 for sand, were used. The driving resistances were input into a commonly used program, GRLWEAP, to calculated blow counts for a given hammer-pile-soil system.

The proposed correlation of CPT to pile toe resistance during driving depends on soil density as characterized by CPT q_c values, pile embedded length and pile size. A statistical analysis was conducted to evaluate the confidence limits of the proposed correlation.

A case history was presented to show the application of the proposed method. The results show reasonable prediction of blow counts,

The results of wave equation analysis are sensitive to the input hammer efficiency and soil quake and damping. Average values of observed hammer efficiency , and typical values of soil quake and damping based on predominant soil type are compiled by the GRLWEAP menu used in this study.

It is recommended that further correlation studies include dynamic measurement of pile driving to directly determine the transmitted energy into the pile and to allow back calculation of the soil parameters.

Bibliography

[1] Alm, T., Bye, A. and Kvalstad, T. J. (1989), "A New Interpretation of Soil Resistance for Pile Drivability Analysis", Proceedings of the 12th International Conference on Soil Mechanics and Foundation Engineering, Rio de Janeiro, 1989, Vol. 2, pp. 1085-1088.

[2] Aurora, R. P. (1980), "Case Studies of Pile Set-Up in the Gulf of Mexico", Proceedings of 12th Offshore Technology Conference, Houston, Texas, USA, (1980), Vol.3, pp. 281-290.

[3] Begnemann, H. K. (1963), "The Use of the Static Soil Penetrometer in Holland", New Zealand Engineering Fev.

[4] Blunden, R. H. (1975), "Urban Geology of Richmond, British Columbia", Adventures in Earth Sciences Series No. 15, B. C. Govt. Publications.

[5] Burland, J. B. (1973), "Shaft Friction of Piles in Clay - A Simple Fundamental Approach", Ground Engineering, Vol.6, No.3, pp. 30-42.

[6] Bustamante, M. and Gianeselli, L. (1982), "Pile Bearing Capacity Prediction by Means of Static Penetrometer CPT" Penetrating Testing, ESOPT II, Amsterdam, Vol.2, pp.493-500.

[7] Campanella, R. G. and Sy, A., Davies, M. P. and Robertson, P. K., Davies, M. P., (1989), "Class a Prediction of Driven Piles Behaviour", Soil Mechanics Series, No. 135, Department of Civil Engineering, The University of British Columbia, Vancouver, Canada.

[8] Chow, Y. K., Wong, K. Y., Karunaratne, G. P. and Lee, S. L. (1988), "Wave Equation Analysis of Piles - A Rational Theoretical Approach", Third International Conference on Application of Stress-Wave Theory to Piles, Ottawa, Canada, 1988, pp. 208-218.

[9] Davies, M. P. (1987), "Prediction Axially and Laterally Loaded Pile Behaviour Using In-situ Testing Method", M.A.Sc. Thesis, Department of Civil Engineering, The University of British Columbia, Vancouver, Canada.

[10] Davisson, M. T. (1973), "High Capacity Piles", Proceedings, Lecture Series, Innovations in Foundation Construction, ASCE, Illinois Section, Chicago, USA.

[11] de Beer, E. E. (1963), "The Scale Effect in Transportation of the Results if Deep Sounding Tests on the Ultimate Bearing Capacity of Piles and Caisson Foundations", Geotechnique, Vol.8, p.39.

[12] de Mello, V. F. B. (1969), "Foundation of Buildings on Clay", State of the Art Report: 49 - 136 Proc. 7th Int. Conf. S.M. & F.E., Mexico City.

[13] de Ruiter, J. and Beringen, F. L. (1979), "Pile Foundations for large North Sea Structures", Marine Geotechnology, Vol.3, No.4, pp. 267-314.

[14] Dennis, N. D. and Olson, R. E. (1983a), "Axial Capacity of Steel Pipe Pile in Clay", Amer. Soc. of Civil Engineers, Geotechnical Practice in Offshore Engineering, Austin, pp. 370-387.

[15] Dennis, N. D. and Olson, R. E. (1983b), "Axial Capacity of Steel Pipe Pile in Sand", Amer. Soc. of Civil Engineers, Geotechnical Practice in Offshore Engineering, Austin, pp. 389-402.

[16] Dinesh Mohan and Virendra Kumar (1963), "Load Bearing Capacity of Piles", Geotechnique Inter. J. Soil Mechanics Vol.13, 1 Mars. pp. 76-86.

[17] Fenske, C. W. and Hirsch, T. J. (1986), "Pile Drivability Analysis", Planning and Design of Fixed Offshore Platforms, Van Nostrand Reinhold Company, New York, 1986.

[18] Finno, R. J. (1989), "Subsurface Conditions and Pile Installation Data: 1989 Foundation Engineering Congress Test Section", Geotechnical Special Publication No. 23, ASCE, New York, NY, USA.

[19] Flaate, K. and Selnes, P. (1977), "Side Friction of Piles in Clay", Proceedings of Ninth International Conference on Soil Mechanics and Foundation Engineering, Tokyo, Japan, Vol.1, pp. 517-522.

[20] Fellenius, B. H., Riker, R. E., O'Brien, A. J. and Tracy, G. R. (1989), "Dynamic and Static Testing in Soil Exhibiting Set-up", Journal of Geotechnical Engineering, ASCE, Vol.115, No.7, July 1989.

[21] Goble, G. G. and Rausche, F. (1976), "Wave Equation Analysis of Pile Driving - WEAP Program", Vol.1 through 4, FHWA # IP-76-14.1 through # IP-76-14.4, July 1976.

[22] Goble, G. G. and Rausche, F. (1981), "Wave Equation Analysis of Pile Driving - WEAP Program", Vol.1 through 4, FHWA # IP-76-14.1 through # IP-76-14.4, Updated March 1981.

[23] Goble, G. G., Rausche, F. and Hery, P. (1983), "Colorado University Modified Wave Equation Analysis of Pile Driving - CUWEAP Program", Vol.2, Department of Civil, Environmental and Architectural Engineering, University of Colorado, June 1983.

[24] Goble, G. G., Rausche, F. and Likins, G. E. Jr. (1980), "The Analysis of Pile driving - A State-of-the-Art", Proc. Int. Seminer on Appl. of Stress-Wave Theory on Piles, Stockholm, pp. 131-150.

[25] Heerema, E. P. and de Jong, A. (1980), "An Advanced Wave Equation Computer Program which Simulates Dynamic pile Plugging through a Coupled Mass-spring System", Proc. Int. Conf. on Numerical Methods in offshore Piling, London, ICE, pp. 37-42.

[26] Heerema, E. P. (1980), "Predicting Pile Driveability: Heather as An Illustration of the 'Friction Fatigue' Theory", Ground Engineering, April 1980, Vol.13, No.3.

[27] Isaacs, D. V. (1931), "Reinforce Concrete Pile Formula", Inst. Aust. Engineering Journal, Vol.12.

[28] Janbu, N. (1976), "Static Bearing Capacity of Friction Piles", Proceedings of the European Conference on Soil Mechanics and Foundation Engineering", Vol.1.2, pp. 479-488.

[29] Meyerhof, G. G. (1951), "The Ultimate Bearing Capacity of Foundations", Geotechnique, Vol.2, No.4, p.301.

[30] Meyerhof, G. G. (1959), "Penetration Tests and Bearing Capacity of Cohesionless Soils", J.S.M.F.D. ASCE, Vol.82, SM1, pp. 1-19.

[31] Meyerhof, G. G. (1976), "Bearing Capacity and Settlement of Pile Foundations", ASCE Journal of Geotechnique Engineering Division, Vol.102, No.GT3, pp. 197-228.

[32] Meyerhof, G. G. (1982), "Scale Effects of Ultimate Pile Capacity", Journal of Geotechnical Engineering, ASCE, Vol.109, No.6, June 1982.

[33] Middendorp, P. and Zandwijk, C. Van (1985), "Accuracy and Reliability of Dynamic Pile Testing Techniques", Behaviour of Offshore Structures, Delft, 1985.

[34] Nottingham, L. C. (1975), "Use of Quasi-Static Friction Cone Penetrometer Data to Predict Load Capacity of Displacement Piles", Ph.D. Dissertation, Department of Civil Engineering, University of Florida, USA.

[35] Robertson, P. K. and Campanella, R. G. (1986), "Guidelines for Use, Interpretation and Application of the CPT and CPTU", Soil Mechanics Series, No. 105, Department of Civil Engineering, The University of British Columbia, Vancouver, Canada.

[36] Robertson, P. K., Davies, M. P. Campanella, R. G. and Sy, A. (1987), "Capacity of Driven Piles in Deltaic Soils Using CPT", Soil Mechanics Series, No. 113, Department of Civil Engineering, The University of British Columbia, Vancouver, Canada.

[37] Robinsky, E. I. and Morrison, C. E. (1959), "Sand Displacement and Compaction Around Model Friction Piles", Canada Geotechnical Journal, Vol.1 No.2, pp. 81.

[38] Schmertmann, J. H. (1978), "Guidelines for Cone Penetration Test, Performance and Design", Federal Highway Administration, Report FHWA-TS-78-209, Washington, July, pp. 145.

[39] Smith, E. A. L. (1950), "Pile Driving Impact", Proc. Industrial Computation Seminar, Sept., International Business Mechanics Corp., New York, USA.

[40] Smith, E. A. L. (1960), "Pile Driving Analysis by the Wave Equation", Journal of the Soil Mechanics and Foundation Division, ASCE, Vol.86, No.EM4.

[41] Soderberg, L. (1962a), "Consolation Theory Applied to Foundation Pile Time Effects", Geotechnique, Vol.12.

[42] Tang Nian-Ci, Yuan Ji-Hong, Wang Yong and Lu Tong-Shen (1988), "Drivability Analysis of Long Steel Pipe Piles - Case History Studies", Third International Conference on Application of Stress-Wave Theory to Piles, Ottawa, Canada, 1988, pp. 499-512.

[43] Vijayvergiya, V. A. and Focht, J. A. (1972), "A New Way to Predict Capacity of Piles in Clays", Proc. Fourth Offshore Technology Conference, Houston, Vol.2, pp. 865-874.

[44] Zhe Jang University (1979), "Probability and Mathematical Statistics", Higher Education Publishing House, Beijing, China, 1979 (in Chinese).

[45] Zhou, J., Xie, Y., Zuo, Z. S., Luo, U. Y. and Tang, X. J. (1982), "Prediction of Limit Load of Driven Pile by CPT", Penetration Testing, Proc. 2nd, European Symp. Penetration Testing, ESOPT II, Amsterdam, Vol.2, pp.957-961.

Appendix A

Pile Driving Records

PILE PENETRATION DIAGRAM

DATE 19 AUG 85 TECHNICIAN AS PILE NO. 1

DEPTH (ft)	NO. BLOWS	DEPTH	NO. BLOWS	DEPTH	NO. BLOWS	DEPTH	NO. BLOWS
0-1		21	1	41	3	61	
1-2		22	1	42	2	62	
3		23	1	43	3	63	
4		24	1	44	3	64	
5		25	1	45	2	65	
6		26	1	46	3	66	
7	2/4"	27	1	47	2	67	
8	2	28	1	48		68	
9	2	29	1	49		69	
10	2	30	1	50		70	
11	1	31	1	51		71	
12	2	32	1	52		72	
13	1	33	2	53		73	
14	1	34	1	54		74	
15	1	35	1	55		75	
16	1	36	2	56		76	
17	1	37	2	57		77	
18	1	38	1	58		78	
19	1	39	1	59		79	
20	1	40	2	60		80	

PENETRATION RESISTANCE – BLOWS/FT.

DEPTH – FEET

PILE DATA

ELEVATION GROUND ≈ 1.84 m
TYPE HAMMER Drop
WT. HAMMER 4+coil
HT. DROP 4 ft
TYPE PILE Closed ended pipe
DIMENSIONS PILE 12 3/4" OD × 3/8" walls
REMARKS Approx. 18" above G.L.

I.D. Elev. 2.344

THE UNIVERSITY OF BRITISH COLUMBIA — UBC In-Situ Testing

JOB No. TECH. AS
PROJECT UBC Pile Research
LOCATION Queensborough, Lulu I.
HOLE No. Pile 1
DATE 19 Aug 85 PLATE

F-12

PILE PENETRATION DIAGRAM

DATE 16 AUG 85 TECHNICIAN AS PILE NO. 2 (237)

DEPTH	NO. BLOWS	DEPTH	NO. BLOWS	DEPTH	NO. BLOWS	DEPTH	NO. BLOWS
0-1	2	21	1	41	2	61	
1-2	2	22	1	42	2	62	
3	2	23	1	43	3	63	
4	3	24		44	2	64	
5	3	25		45	2	65	
6	3	26	1	46	End of pile	66	
7	2	27	2	47	2 blows 1/4 in	67	
8	1	28	1	48		68	
9	1	29	1	49		69	
10	1	30	1	50		70	
11	1	31	1	51		71	
12	2	32	1	52		72	
13	1	33	2	53		73	
14	1	34	1	54		74	
15	1	35	2	55		75	
16	1	36	2	56		76	
17	1	37	1	57		77	
18	1	38	2	58		78	
19	2	39	2	59		79	
20	1	40	2	60		80	

PENETRATION RESISTANCE – BLOWS/FT.

DEPTH – FEET

PILE DATA

ELEVATION GROUND ≈ 1.83 m
TYPE HAMMER Drop
WT. HAMMER 6200 lb
HT. DROP 3
TYPE PILE Close ended pipe pile
DIMENSIONS PILE 12 3/4" OD × 3/8" wall
REMARKS 3 × 3/4" plywood cushion (old)

THE UNIVERSITY OF BRITISH COLUMBIA — UBC In-Situ Testing

JOB No. TECH. AS
PROJECT UBC Pile Research
LOCATION Queensborough, Lulu I.
HOLE No. Pile 2
DATE 16 Aug 85 PLATE

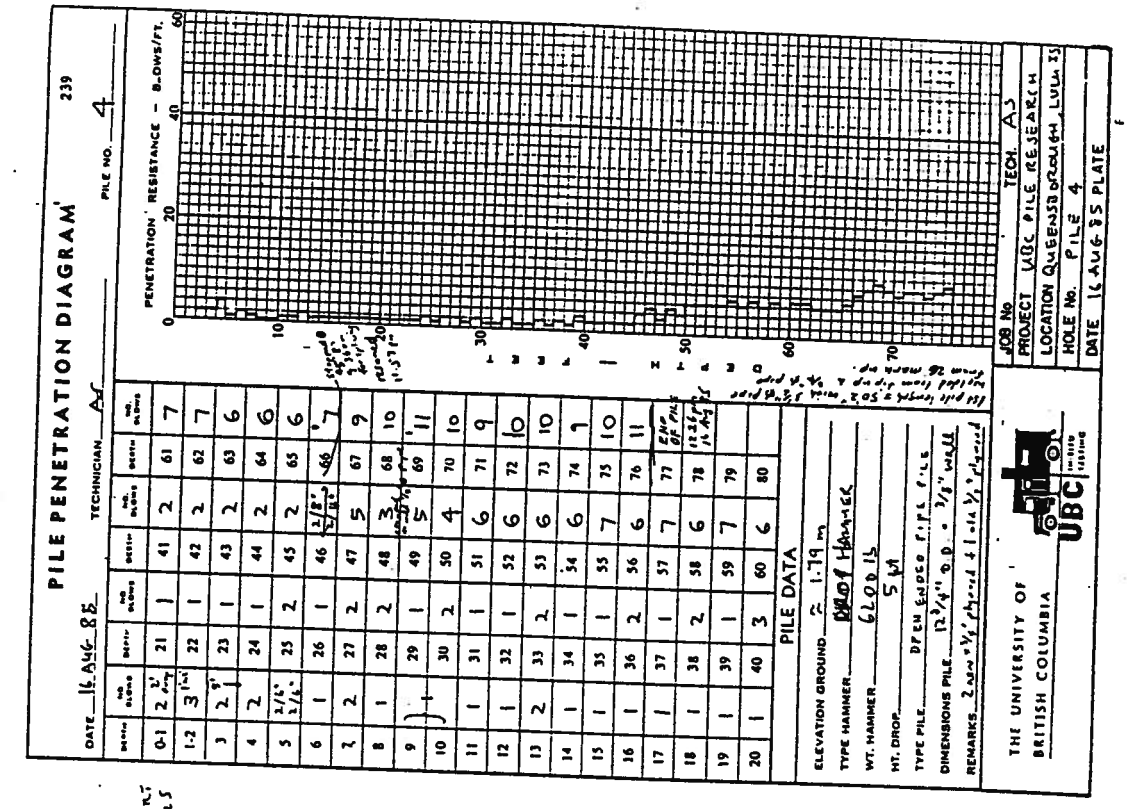
PILE PENETRATION DIAGRAM
239
DATE 16 AUG 85
TECHNICIAN AS
PILE NO. 4
PENETRATION RESISTANCE - BLOWS/FT.
PILE DATA
ELEVATION GROUND ≈ 1.79 m
TYPE HAMMER DROP HAMMER
WT. HAMMER 6100 lb
HT. DROP 5 M
TYPE PILE OPEN ENDED PIPE PILE
DIMENSIONS PILE 12 3/4" O.D. - 3/8" WALL
REMARKS 2 new 1/2" plates 41 in 1/2" plates
THE UNIVERSITY OF BRITISH COLUMBIA
UBC
JOB No
TECH. AS
PROJECT UBC PILE RESEARCH
LOCATION QUEENSBOROUGH, LULU I.
HOLE No. PILE 4
DATE 16 AUG 85 PLATE

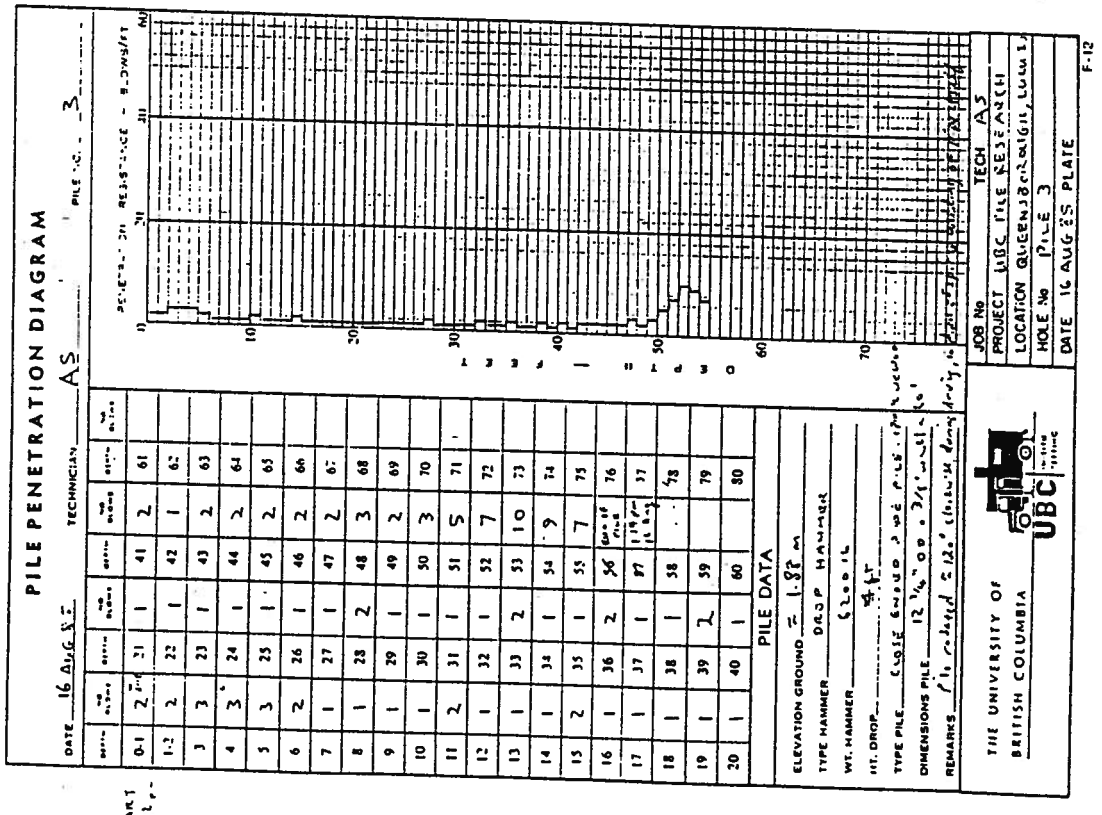
PILE PENETRATION DIAGRAM
DATE 16 AUG 85
TECHNICIAN AS
PILE NO. 3
PILE DATA
ELEVATION GROUND ≈ 1.82 m
TYPE HAMMER DROP HAMMER
WT. HAMMER 6100 lb
HT. DROP 5 M
TYPE PILE CLOSE ENDED PIPE PILE
DIMENSIONS PILE 12 3/4" O.D. - 3/8" WALL
REMARKS Pile reduced to 12" O.D. - 3/8" WALL
THE UNIVERSITY OF BRITISH COLUMBIA
UBC
JOB No
TECH AS
PROJECT UBC PILE RESEARCH
LOCATION QUEENSBOROUGH, LULU I.
HOLE No PILE 3
DATE 16 AUG 85 PLATE
F-12

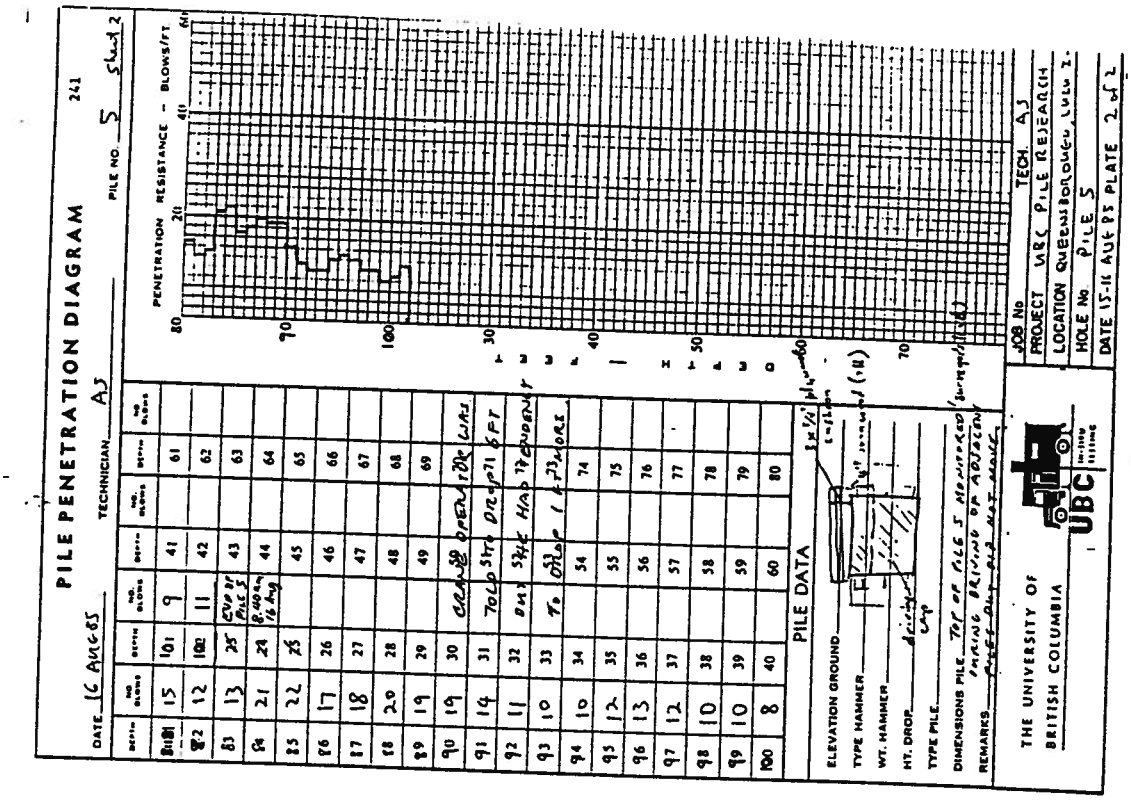
PILE PENETRATION DIAGRAM
DATE 16 AUGUST
TECHNICIAN AJ
PILE NO. S sheet 2
PENETRATION RESISTANCE - BLOWS/FT
PILE DATA
THE UNIVERSITY OF BRITISH COLUMBIA
UBC
JOB No
TECH. AJ
PROJECT UBC PILE RESEARCH
LOCATION QUEENSBOROUGH, LULU I.
HOLE No PILE S
DATE 15-16 AUG 85 PLATE 2 of 2

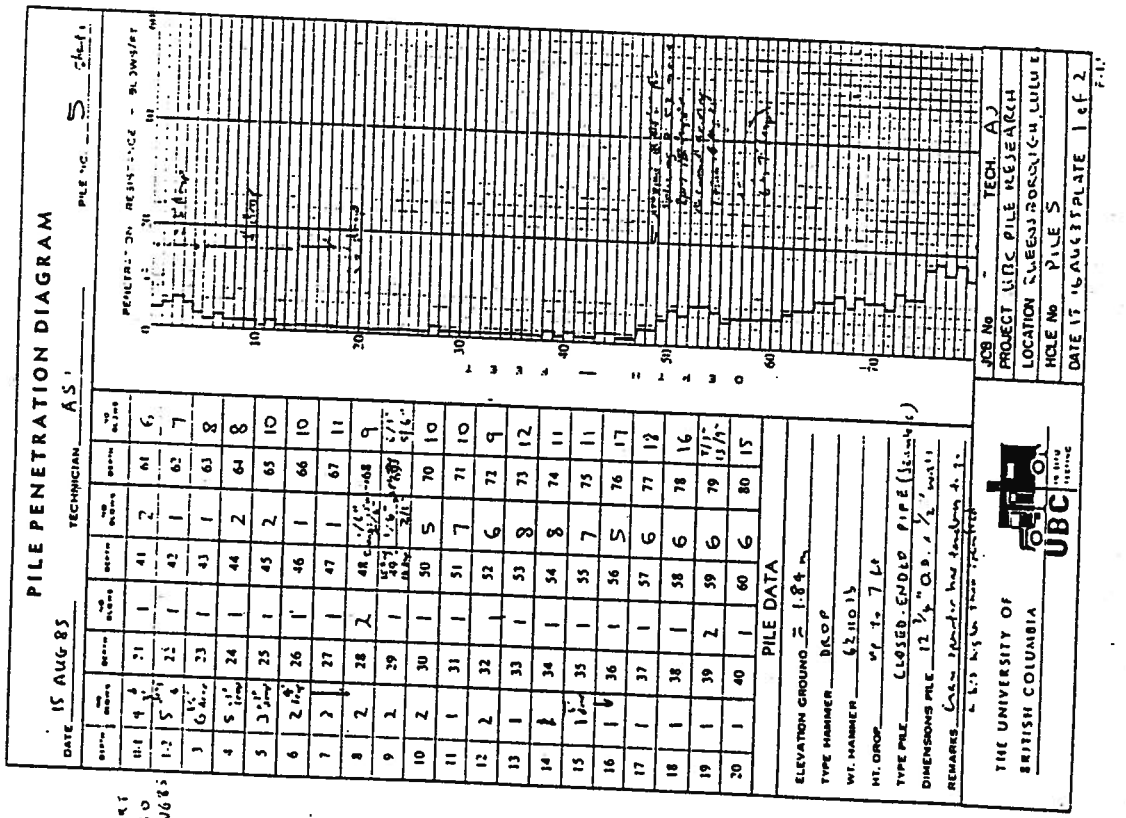
PILE PENETRATION DIAGRAM
DATE 15 AUG 85
TECHNICIAN AS
PILE NO. S sheet 1
PENETRATION RESISTANCE - BLOWS/FT
PILE DATA
THE UNIVERSITY OF BRITISH COLUMBIA
UBC
JOB No
TECH. AJ
PROJECT UBC PILE RESEARCH
LOCATION QUEENSBOROUGH, LULU I.
HOLE No PILE S
DATE 15-16 AUG 85 PLATE 1 of 2

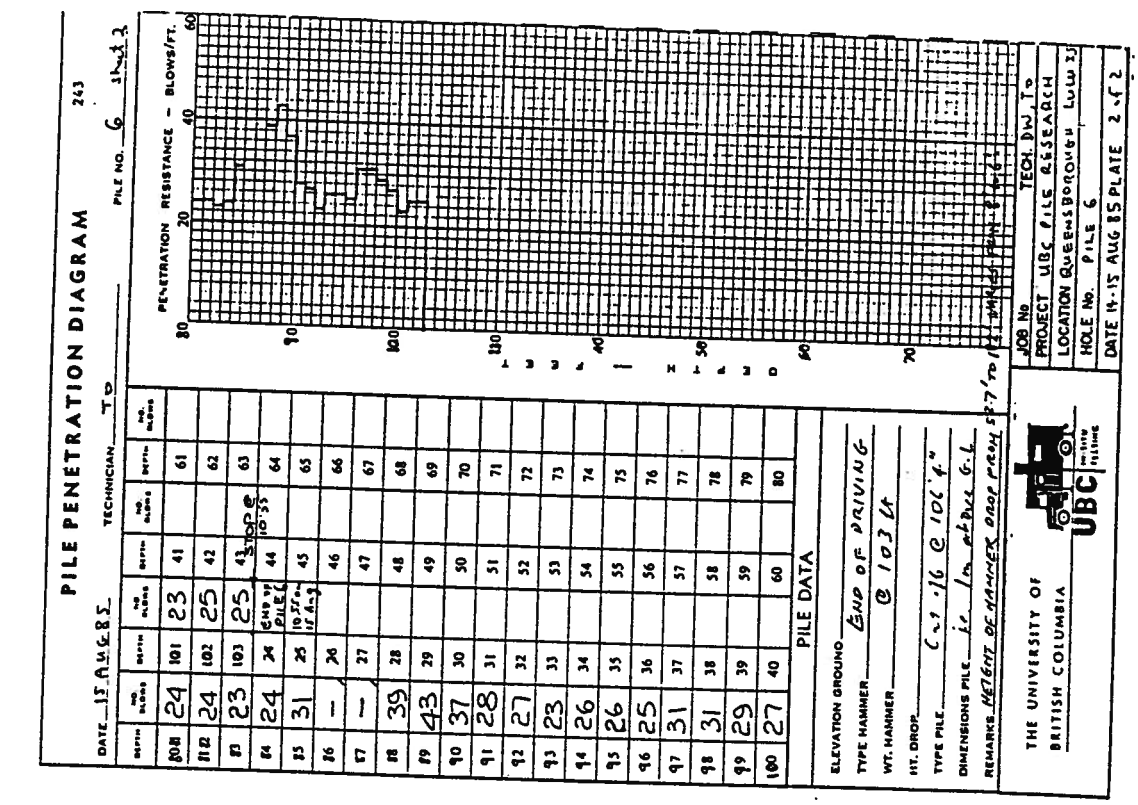
PILE PENETRATION DIAGRAM
PENETRATION RESISTANCE - BLOWS/FT.
PILE DATA
THE UNIVERSITY OF BRITISH COLUMBIA
UBC
JOB No.
TECH. DWJ TO
PROJECT UBC PILE RESEARCH
LOCATION QUEENSBOROUGH LUGS 3
HOLE No. PILE 6
DATE 14-15 AUG 85 PLATE 2 of 2

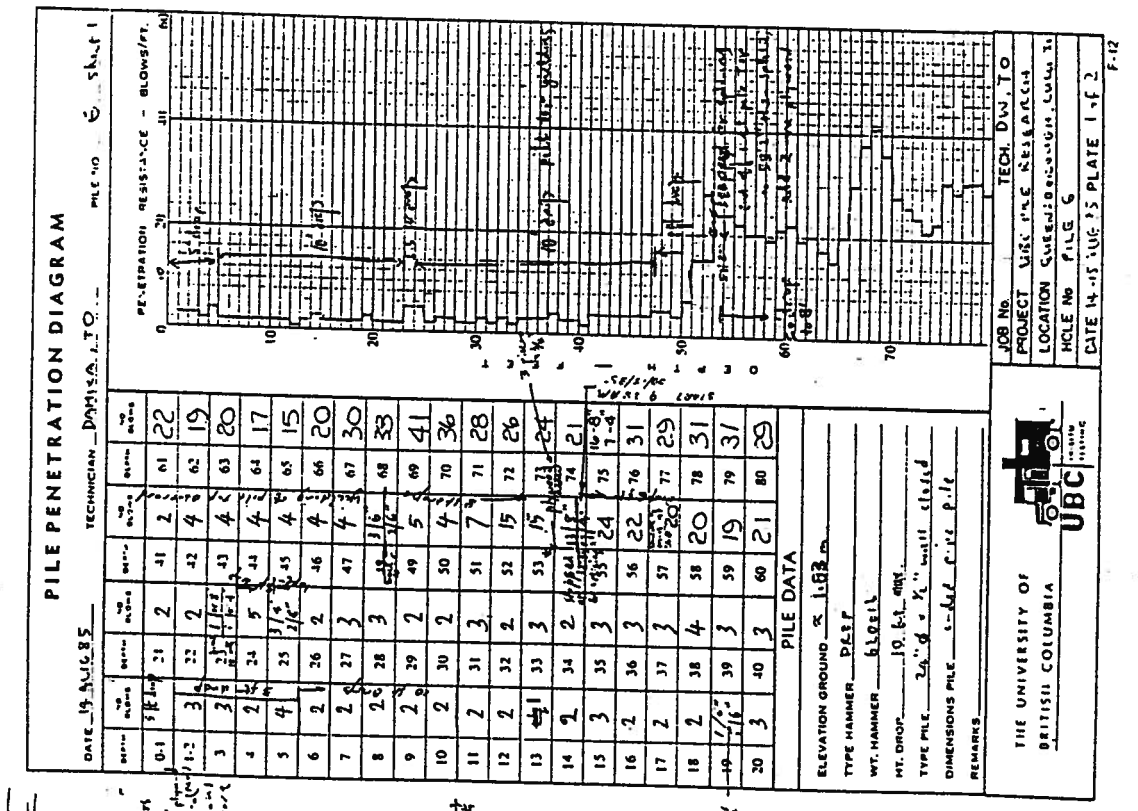
PILE PENETRATION DIAGRAM
PENETRATION RESISTANCE - BLOWS/FT.
PILE DATA
THE UNIVERSITY OF BRITISH COLUMBIA
UBC
JOB No.
TECH. DWJ TO
PROJECT UBC PILE RESEARCH
LOCATION QUEENSBOROUGH LUGS 3
HOLE No. PILE 6
DATE 14-15 AUG 85 PLATE 1 of 2

PILE PENETRATION DIAGRAM

DATE March 9/10, 1991 TECHNICIAN D.S. PILE NO. TP 1

Depth (ft)	No. blows	Depth (ft)	No. blows	Depth (ft)	No. blows	Depth (ft)	No. blows
0-1	2	21	5	41	21	61	49
1-2	6	22	6	42	20	62	52
3	6	23	6	43	21	63	49
4	3	24	4	44	21	64	49
5	2	25	2	45	24	65	50
6	2	26	8	46	23	66	48
7	3	27	6	47	22	67	45
8	3	28	8	48	22	68	51
9	3	29	20	49	28	69	49
10	3	30	12	50	26	70	45
11	3	31	10/9	31	16/6"	71	47
12	3	32	14	52	42	72	42
13	3	33	13	53	40	73	45
14	2	34	16	54	40	74	43
15	3	35	16	55	49	75	42
16	1/8"	36	16	56	38	76	46
17	5	37	18	57	39	77	49
18	6	38	17	58	40	78	48
19	6	39	19	59	40	79	63
20	6	40	19	60	45	80	57

PILE DATA Finish at 3:06 PM

ELEVATION GROUND +2.26m (Geodetic)
TYPE HAMMER Single-acting diesel (D30-13)
WT HAMMER 6,600 lb
HT. DROP Max. Rated Energy = 66,000 ft-lb
TYPE PILE Steel pipe pile
DIMENSIONS PILE 20 in O.D. x 0.5 in wall
REMARKS End plate = 20 3/4" ϕ x 1 3/8" thick

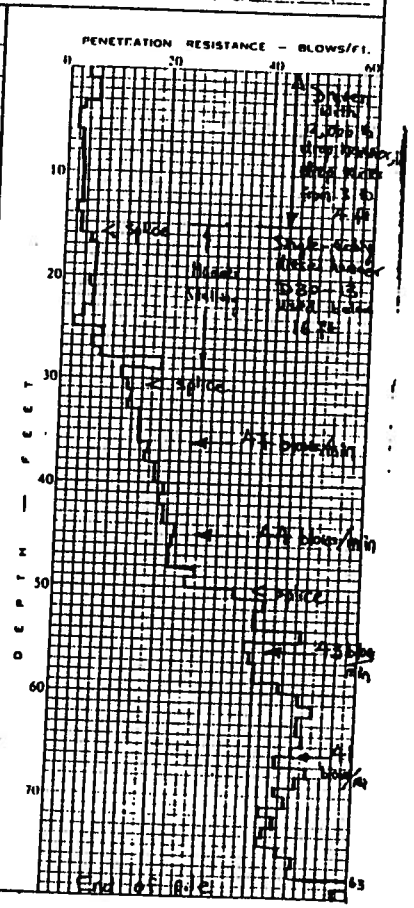

PILE PENETRATION DIAGRAM

DATE March 9/10, 1991 TECHNICIAN D.S PILE NO. TP 2

Depth (ft)	No. blows	Depth (ft)	No. blows	Depth (ft)	No. blows	Depth (ft)	No. blows
0-1	1	21	2	41	12	61	
1-2	2	22	2	42	13	62	
3	3	23	2	43	11/6"	63	
4	3	24	2	44	16	64	
5	3	25	1/6"	45	18	65	
6	3	26	9	46	15/1"	66	
7	3	27	7	47	24	67	
8	3	28	6	48	26	68	
9	3	29	6	49	26	69	
10	3	30	10	50	35	70	
11	2	31	9	51	27	71	
12	2	32	9	52	33	72	
13	2	33	10	53	34	73	
14	2	34	10	54	36	74	
15	2	35	11	55	34	75	
16	1	36	12	56	33	76	
17	1	37	12	57	34	77	
18	1	38	12	58	39	78	
19	1	39	14	59	35	79	
20	1	40	14	60	39	80	

PILE DATA Finish at 9:00 AM

ELEVATION GROUND +2.26 m (Geodetic)
TYPE HAMMER Single-Acting Diesel Hammer (D30-13)
WT HAMMER 6,600 lb
HT. DROP Max Rated Energy = 66,000 ft-lb
TYPE PILE Steel Pipe Pile
DIMENSIONS PILE 20" O.D. x 0.375" wall
REMARKS End-plate = 20 3/4" ϕ x 1 3/8" thick

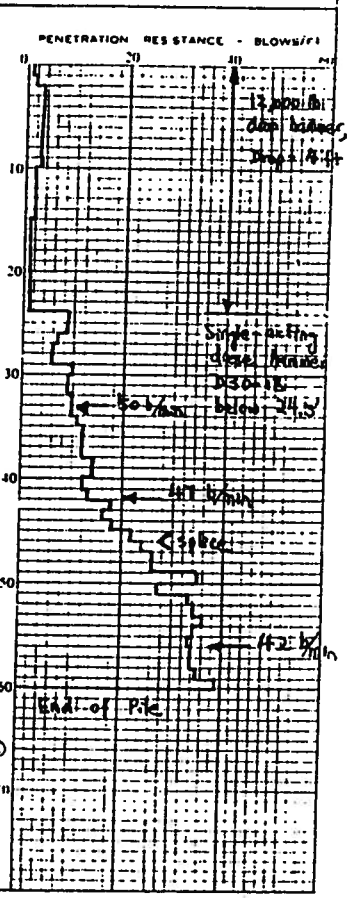

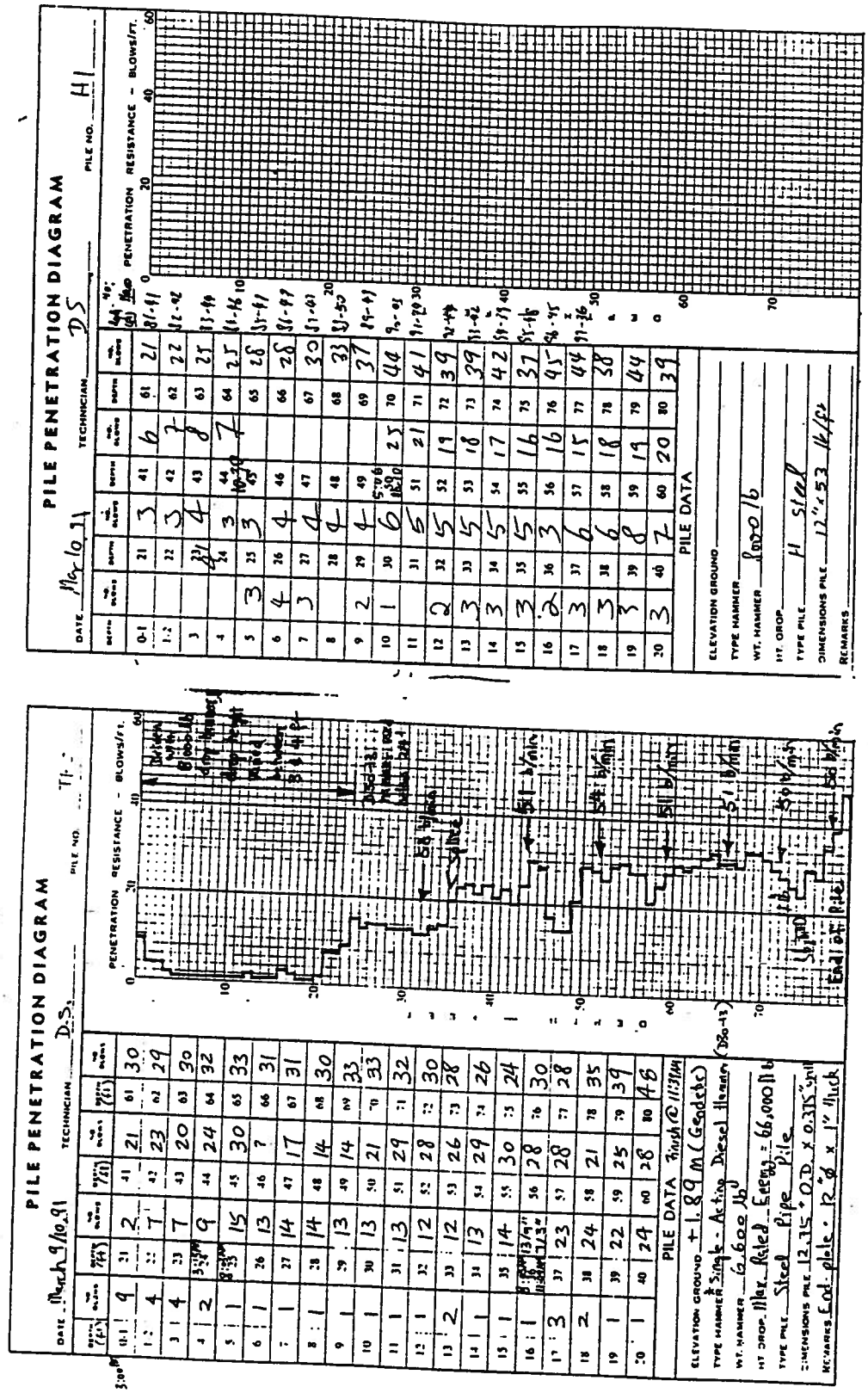

PILE PENETRATION DIAGRAM

DATE: March 9/10, 91 TECHNICIAN: D.S. PILE NO.: T1

PENETRATION RESISTANCE - BLOWS/FT.

PILE DATA

Rush @ 11:51AM

ELEVATION GROUND: +1.89 m (Geodetic)

TYPE HAMMER: Single - Acting Diesel Hammer (D30-13)

WT. HAMMER: 6,600 lb

HT. DROP: Max. Rated Energy = 66,000 ft lb

TYPE PILE: Steel Pipe Pile

DIMENSIONS PILE: 12.75" O.D. x 0.375" Shell

REMARKS: End plate - 12" x 1" thick

PILE PENETRATION DIAGRAM

DATE: March 11 TECHNICIAN: D.S. PILE NO.: H1

PENETRATION RESISTANCE - BLOWS/FT.

PILE DATA

ELEVATION GROUND:

TYPE HAMMER:

WT. HAMMER: D30-16

HT. DROP:

TYPE PILE: H Steel

DIMENSIONS PILE: 12"x53 lb/ft

REMARKS:

PILE DRIVING RECORD

STS Consultants Ltd.

STS Project No. _____

Date: MAY 24, 1988 Project: PILE CAPACITY PREDICTION EVENT Pile Length: 53 ft

Weather: CLOUDY, ~55°F Location: NORTHWESTERN UNIVERSITY Waste: _____

Permit: _____ Owner: _____ Pay Length: _____

Sheet: _____ Contractor: CASE INTERNATIONAL Cut-Off Elev.: _____

Column No.: _____ Foreman: ERIC WEISSER Tip Elev.: -50.5 ft

Pile No.: TEST PILE Pile Capacity & Type: Closed-ended pipe Stroke: 36 ins.

Ground Elev.: 0 ft Hammer: VULCAN 06 Energy: 19,500 ft-lb

DEVIATION — N | E | S | W | Signature (Inspector): D. McCARTHY

DEPTH	BLOWS	REMARKS	DEPTH	BLOWS	REMARKS	DEPTH	BLOWS	REMARKS
1	–	WEIGHT OF HAMMER	36	8	hammer speed = 55 bpm	71		NOTE: PRENGER 12-in.-diam. pile to 23 ft
2	–		37	7		72		
3	–		38	8		73		
4	–		39	8		74		
5	–		40	9		75		
6	6		41	9		76		
7	5		42	8		77		
8	6		43	8		78		
9	5		44	8		79		
10	7		45	9		80		
11	7		46	8		81		
12	9		47	9		82		
13	12		48	9		83		
14	14		49	8		84		
15	16		50	10		85		
16	19		51	5/6"		86		
17	22		52			87		
18	22		53			88		
19	24		54			89		
20	29		55			90		
21	32		56			91		
22	20		57			92		
23	15		58			93		
24	9		59			94		
25	8		60			95		
26	8		61			96		
27	9		62			97		
28	9		63			98		
29	8		64			99		
30	9		65			100		
31	9		66			101		
32	8		67			102		
33	8		68			103		
34	8		69			104		
35	8		70			105		

PILE DRIVING RECORD

STS Consultants Ltd.

STS Project No. _____

Date: MAY 24, 1988 Project: PILE CAPACITY PREDICTION EVENT Pile Length: 52 ft

Weather: CLOUDY, ~55°F Location: NORTHWESTERN UNIVERSITY Waste: _____

Permit: _____ Owner: _____ Pay Length: _____

Sheet: _____ Contractor: CASE INTERNATIONAL Cut-Off Elev.: _____

Column No.: _____ Foreman: ERIC WEISSER Tip Elev.: -50 ft

Pile No.: TEST PILE Pile Capacity & Type: HPNX73 Stroke: 36 ins.

Ground Elev.: 0 ft Hammer: VULCAN 06 Energy: 19,500 ft-lb

DEVIATION — N | E | S | W | Signature (Inspector): D. McCARTHY

DEPTH	BLOWS	REMARKS	DEPTH	BLOWS	REMARKS	DEPTH	BLOWS	REMARKS
1	–	WEIGHT OF HAMMER	36	13	hammer speed = 54 bpm	71		
2	–		37	14		72		
3	–		38	13		73		
4	7		39	13		74		
5	7		40	14		75		
6	7		41	13		76		
7	5		42	14		77		
8	5		43	13		78		
9	5		44	14		79		
10	7		45	12		80		
11	8		46	12		81		
12	10		47	13		82		
13	9		48	12		83		
14	10		49	11		84		
15	13		50	12		85		
16	15		51			86		
17	17		52			87		
18	18		53			88		
19	21		54			89		
20	22		55			90		
21	24		56			91		
22	24		57			92		
23	17	HAMMER SPEED = 55 bpm	58			93		
24	14		59			94		
25	14		60			95		
26	14		61			96		
27	13		62			97		
28	13		63			98		
29	12		64			99		
30	12		65			100		
31	12		66			101		
32	13		67			102		
33	13		68			103		
34	14		69			104		
35	13		70			105		

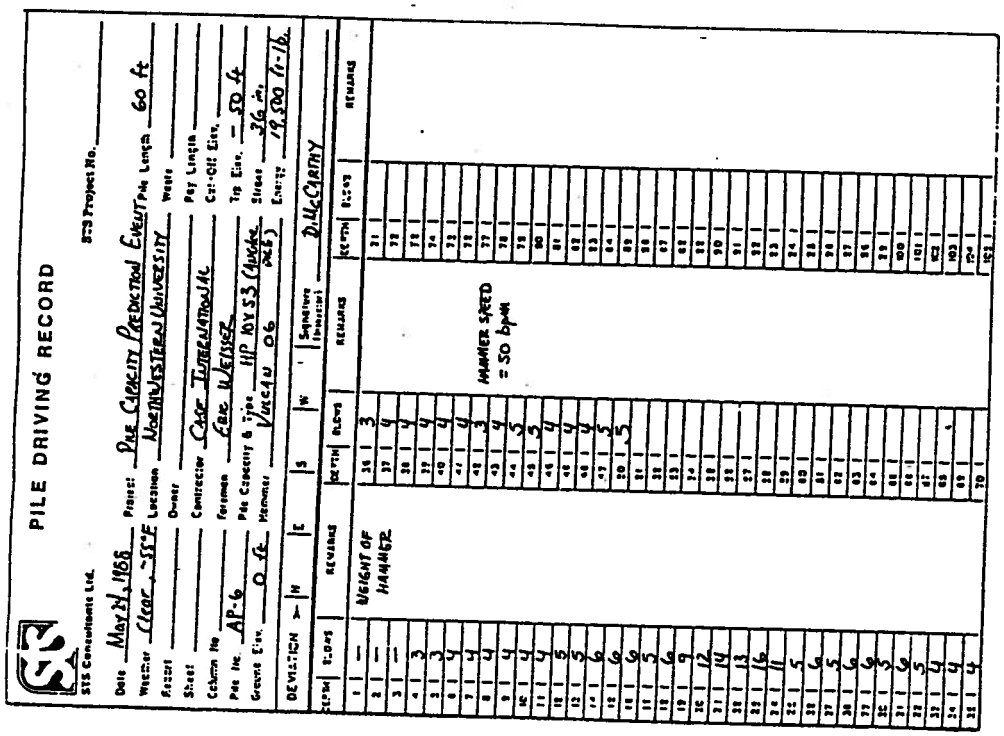

PILE DRIVING RECORD

STS Consultants Ltd. STS Project No.

Date May 31, 1966 Project Pile Capacity Prediction Evaluation Pile Length 60 ft

Weather Clear, ~55°F Location Northwestern University Water

Record Owner Pay Length

Sheet Contractor Case Foundation Co. Cut-Off Elev.

Column No. Foreman Lee Weiser Tip Elev. −50 ft

Pile No. AP-6 Pile Capacity & Type HP 10×53 Chucks Stroke 36 in.

Ground Elev. 0 ft. Hammer Vulcan 06 (MEP) Energy 19,500 ft-lb.

DEVIATION N | W | E | S | W | Signature Inspector D. McCarthy

BLOWS	REMARKS	DEPTH	BLOWS	REMARKS	DEPTH	BLOWS	REMARKS
1 | —	WEIGHT OF HAMMER	26 | 3			51 |		
2 | —		27 | 4			52 |		
3 | —		28 | 4			53 |		
4 | 3		29 | 4			54 |		
5 | 3		30 | 4			55 |		
6 | 4		31 | 4			56 |		
7 | 4		32 | 3	HAMMER SPEED = 50 bpm		57 |		
8 | 4		33 | 4			58 |		
9 | 4		34 | 5			59 |		
10 | 4		35 | 5			60 |		
11 | 4		36 | 4			61 |		
12 | 5		37 | 4			62 |		
13 | 5		38 | 4			63 |		
14 | 6		39 | 5			64 |		
15 | 6		40 | 5			65 |		
16 | 6		41 |			66 |		
17 | 5		42 |			67 |		
18 | 6		43 |			68 |		
19 | 9		44 |			69 |		
20 | 12		45 |			70 |		
21 | 14		46 |			71 |		
22 | 13		47 |			72 |		
23 | 16		48 |			73 |		
24 | 11		49 |			74 |		
25 | 5		50 |			75 |		
26 | 6		51 |			76 |		
27 | 5		52 |			77 |		
28 | 6		53 |			78 |		
29 | 6		54 |			79 |		
30 | 3		55 |			80 |		
31 | 3		56 |			81 |		
32 | 5		57 |			82 |		
33 | 4		58 |			83 |		
34 | 4		59 |			84 |		
35 | 4		60 |			85 |		
						86 |		
						87 |		
						88 |		
						89 |		
						90 |		
						91 |		
						92 |		
						93 |		
						94 |		
						95 |		
						96 |		
						97 |		
						98 |		
						99 |		
						100 |		
						101 |		
						102 |		
						103 |		
						104 |		
						105 |		

Appendix B

Definition of Confident Interval

In regression, y is assumed normally distribution for each fixed x_i. Supposedly, it is needed to know a 100(1-γ) percent confident interval for the expected value of y for $x = x_0$.

$$y_0 = a + bx_0 + \varepsilon_0 \ , \varepsilon_0 \sim N(0, \sigma^2) \tag{B.1}$$

Consider random variable

$$u = y_0 - \tilde{y}_0 \tag{B.2}$$

The $\tilde{y}_0$ is defined as following Equation:

$$\tilde{y}_0 = \bar{y} + \hat{b}(x_0 - \bar{x}) \ \sim \ N(a + bx_0, [\frac{1}{n} + \frac{(x_0 - \bar{x})^2}{\sum_{i=1}^{n}(x_0 - \bar{x})^2}]) \tag{B.3}$$

where

n is the number of samples

$\bar{x}$ is the average value of samples x_i

$\bar{y}$ is the average value of samples y_i

$\hat{b}$ is the linear regression factor of which was calculated from Least Square method

Then:

$$E(u) = E(Y_0) - E(\tilde{y}_0) = 0 \tag{B.4}$$

y_0 and $\tilde{y}_0$ are normally distribution variables and independent to each other, since

$$\begin{aligned} D(u) = D(y_0 - \tilde{y}_0) &= D(y_0) + D(\tilde{y}_0) \\ D(y_0) &= \sigma^2 \\ D(\tilde{y}_0) &= [1 + \tfrac{1}{n} + \tfrac{(x_0 - \bar{x}_0)^2}{\sum_{i=1} n^n (x_i - \bar{x})^2}]\sigma^2 \end{aligned} \tag{B.5}$$

we get

$$\sigma_u{}^2 = [1 + \frac{1}{n} + \frac{(x_0 - \bar{x}_0)^2}{\sum_{i=1} n^n (x_i - \bar{x})^2}]\sigma^2 \tag{B.6}$$

Equation B.6 can be expressed as:

$$\frac{u}{\sigma_u} \sim N(0,1) \tag{B.7}$$

The unbiased estimator, $\hat{\sigma}^2$, of square deviation from Least Square has the freedom of $n-2$.

$$\hat{\sigma}^2 = \frac{1}{n-2}\sum_{i=1}^{n}(y_i - \tilde{y}_i)^2 \tag{B.8}$$

Then, the following Equation is derived.

$$\frac{(n-2)\hat{\sigma}^2}{\sigma^2} \sim \chi^2(n-2) \tag{B.9}$$

Since u/σ_u is independent of $(n-2)\hat{\sigma}^2/\sigma^2$, the following Equation can be derived.

$$\frac{\frac{u}{\sigma_u}}{\sqrt{\frac{\hat{\sigma}^2}{\sigma^2}}} \sim t(n-2) \tag{B.10}$$

Equation B.10 is written as following form:

$$\frac{y_0 - \tilde{y}_0}{\hat{\sigma}}\sqrt{1 + \frac{1}{n} + \frac{(x_0 - \bar{x})^2}{\sum_{i=1}^{n}(x_i - \bar{x})^2}} \sim t(n-2) \tag{B.11}$$

A 100(1-γ) percent confident interval about the regression line for each value x_0 is defined by Equation B.12.

$$(\tilde{y}_0 \pm t_{\frac{\alpha}{2}}(n-2)\hat{\sigma}\sqrt{1 + \frac{1}{n} + \frac{(x_0 - \bar{x})^2}{\sum_{i=1}^{n}(x_i - \bar{x})^2}}) \tag{B.12}$$

let

$$\delta(x_0) = t_{\frac{\alpha}{2}}(n-2)\hat{\sigma}\sqrt{1 + \frac{1}{n} + \frac{(x_0 - \bar{x})^2}{\sum_{i=1}^{n}(x_i - \bar{x})^2}} \tag{B.13}$$

For the given values of x, a confident interval can be determined in which the regression line is located. The band of confident interval is defined by Equation B.14.

$$\begin{cases} y_1(x) = \tilde{y} - \delta(x_0) \\ y_2(x) = \tilde{y} + \delta(x_0) \end{cases} \tag{B.14}$$

Appendix C

Predicted Blow Count with Different Confidence

Table C.2: Predicted Blow Counts Based on Confident Interval for UBC Pile 5

Depth	q_{ea}	R_{sr}	R_{ut} $(kips)$			Blow Counts $(blows/foot)$			Measured
$(feet)$	$(bars)$	$(kips)$	Lower	Reg. Line	Upper	Lower	Reg. Line	Upper	Blow Count
Confident = 90%									
27	2.98	13.35	17.3	14.7	13.4	1.4	1.1	0.9	1
49	20.65	23.98	34.3	28.2	24.2	3.0	2.4	1.9	3
56	72.10	37.40	72.0	56.7	46.2	7.0	5.5	4.3	5
61	71.64	45.26	87.0	68.6	55.9	8.2	6.3	5.0	6
65	106.04	53.63	137.6	99.4	78.9	12.9	9.1	7.1	10
69	106.27	64.39	165.1	119.2	94.7	15.1	10.8	8.1	11
77	147.68	81.81	340.9	209.8	151.5	47.3	19.5	13.2	18
79	132.70	87.71	302.4	199.3	148.7	35.7	18.0	12.7	18
82	75.28	94.01	184.3	144.7	119.0	16.0	12.1	9.4	12
88	107.14	108.46	278.1	204.6	159.5	29.1	17.8	13.0	20
90	134.62	113.92	392.8	258.9	194.6	68.2	25.3	16.6	19
97	21.21	121.11	173.0	143.5	122.3	14.3	11.4	9.0	12
Confident = 80%									
27	2.98	13.35	16.7	14.7	13.4	1.4	1.1	1.0	1
49	20.65	23.98	32.4	28.2	25.0	2.8	2.4	2.0	3
56	72.10	37.40	68.0	56.7	48.6	6.6	5.5	4.6	5
61	71.64	45.26	82.3	68.6	58.0	7.7	6.3	5.3	6
65	106.04	53.63	124.8	99.4	82.5	11.7	9.1	7.4	10
69	106.27	64.39	153.3	119.2	99.1	14.0	10.8	8.6	11
77	147.68	81.81	303.0	209.8	163.6	36.2	19.5	14.3	18
79	132.70	87.71	365.8	199.3	156.6	27.9	18.0	13.5	18
82	75.28	94.01	174.1	144.7	123.7	15.0	12.1	9.9	12
88	107.14	108.46	258.2	204.6	166.9	25.4	17.8	13.7	20
90	134.62	113.92	356.0	258.9	207.1	50.6	25.3	17.8	19
97	21.21	121.11	165.9	143.5	126.2	13.6	11.4	9.5	12
Confident = 70%									
27	2.98	13.35	16.3	14.7	13.4	1.3	1.1	0.9	1
49	20.65	23.98	31.7	28.2	25.5	2.7	2.4	2.1	3
56	72.10	37.40	65.6	56.7	49.9	6.3	5.5	4.8	5
61	71.64	45.26	79.4	68.6	60.4	7.5	6.3	5.5	6
65	106.04	53.63	119.2	99.4	85.2	11.2	9.1	7.7	10

Table C.2: Predicted Blow Counts Based on Confident Interval for UBC Pile 5 Continuous

Depth	q_{ea}	R_{sr}	R_{ut} (*kips*)			Blow Counts (*blows/foot*)			Measured
(*feet*)	(*bars*)	(*kips*)	Lower	Reg. Line	Upper	Lower	Reg. Line	Upper	Blow Count
Confident = 70%									
69	106.27	64.39	143.0	119.2	102.2	13.0	10.8	8.9	11
77	147.68	81.81	282.1	209.8	170.4	31.4	19.5	15.0	18
79	132.70	87.71	250.6	199.3	165.5	25.2	18.0	14.3	18
82	75.28	94.01	167.9	144.7	127.0	14.3	12.1	10.3	12
88	107.14	108.46	246.5	204.6	172.2	23.5	17.8	14.2	20
90	134.62	113.92	335.1	258.9	214.9	43.2	13.2	18.8	19
97	21.21	121.11	161.5	143.5	128.8	13.2	11.4	9.8	12
Confident = 60%									
27	2.98	13.35	15.9	14.7	13.4	1.2	1.1	0.8	1
49	20.65	23.98	31.1	28.2	26.1	2.7	2.4	2.1	3
56	72.10	37.40	63.4	56.7	50.5	6.1	5.5	4.8	5
61	71.64	45.26	76.7	68.6	61.2	7.2	6.3	5.6	6
65	106.04	53.63	116.6	99.4	88.0	11.0	9.1	7.9	10
69	106.27	64.39	140.0	119.2	105.6	12.7	10.8	9.3	11
77	147.68	81.81	263.9	209.8	177.9	27.8	19.5	15.8	18
79	132.70	87.71	237.1	199.3	168.7	23.1	18.0	14.6	18
82	75.28	94.01	162.1	144.7	130.6	13.8	12.1	10.7	12
88	107.14	108.46	235.8	204.6	177.8	21.9	17.8	14.8	20
90	134.62	113.92	316.4	258.9	223.4	37.7	25.3	19.9	19
97	21.21	121.11	157.3	143.5	131.6	12.8	11.4	10.2	12
Confident = 50%									
27	2.98	13.35	15.7	14.7	13.7	1.1	1.1	0.7	1
49	20.65	23.98	30.4	28.2	26.4	2.5	2.4	2.1	3
56	72.10	37.40	62.3	56.7	51.9	6.0	5.5	5.0	5
61	71.64	45.26	75.4	68.6	62.9	7.1	6.3	5.8	6
65	106.04	53.63	111.8	99.4	89.4	10.5	9.1	8.1	10
69	106.27	64.39	134.1	119.2	107.3	12.2	10.8	9.5	11
77	147.68	81.81	247.9	209.8	181.8	25.0	19.5	16.2	18
79	132.70	87.71	230.8	199.3	175.4	22.1	18.0	15.3	18
82	75.28	94.01	159.3	144.7	132.4	13.5	12.1	10.9	12
88	107.14	108.46	230.8	204.6	183.8	21.2	17.8	15.4	20
90	134.62	113.92	307.9	258.9	227.8	35.5	25.3	20.5	19
97	21.21	121.11	153.3	143.5	133.1	12.4	11.4	10.3	12

Table C.3: Predicted Blow Counts Based on Confident Interval for UBC Pile 6

Depth	q_{ea}	R_{sr}	R_{ut} (*kips*)			Blow Counts (*blows/foot*)			Measured
(*feet*)	(*bars*)	(*kips*)	Lower	Reg. Line	Upper	Lower	Reg. Line	Upper	Blow Count
Confident = 90%									
27	2.95	38.60	47.3	40.2	38.6	3.3	2.7	2.6	3
48	20.97	57.40	76.5	64.5	57.4	6.8	5.7	5.0	5
60	74.83	95.57	180.3	140.5	116.6	23.0	16.1	12.9	21
62	82.02	103.09	202.1	158.6	128.9	25.0	20.5	14.1	19
66	110.82	121.56	311.7	225.1	178.8	30.0	21.3	17.6	20
80	109.50	190.75	476.9	353.2	276.5	53.0	31.4	22.9	29
89	125.03	231.36	680.5	482.0	367.2	134.5	49.9	30.5	43
102	21.41	273.06	369.0	306.8	273.1	32.4	25.0	21.7	25
Confident = 80%									
27	2.95	38.60	45.0	40.2	38.6	3.1	2.7	2.6	3
48	20.97	57.40	73.6	64.5	57.4	6.5	5.7	5.0	5
60	74.83	95.57	167.7	140.5	121.0	21.8	16.1	13.4	21
62	82.02	103.09	190.9	158.6	135.7	23.8	20.5	15.0	19
66	110.82	121.56	289.4	225.1	187.0	27.5	21.3	18.2	20
80	109.50	190.75	443.6	353.2	289.0	45.9	31.4	24.1	29
89	125.03	231.36	625.3	482.0	385.6	98.9	49.9	33.0	43
102	21.41	273.06	350.1	306.8	273.1	30.0	25.0	21.7	25
Confident = 70%									
27	2.95	38.60	44.4	40.2	38.6	3.1	2.7	2.6	3
48	20.97	57.40	71.8	64.5	57.4	6.3	5.7	5.3	5
60	74.83	95.57	162.0	140.5	124.0	21.2	16.1	13.8	21
62	82.02	103.09	185.5	158.6	139.3	23.1	20.5	15.5	19
66	110.82	121.56	270.1	225.1	193.0	25.4	21.3	18.7	20
80	109.50	190.75	423.9	353.2	298.1	42.2	31.4	25.0	29
89	125.03	231.36	593.3	482.0	398.9	83.9	49.9	34.9	43
102	21.41	273.06	341.3	306.8	278.6	28.9	25.0	22.2	25
Confident = 60%									
27	2.95	38.60	43.3	40.2	38.6	3.0	2.7	2.6	3
48	20.97	57.40	70.0	64.5	57.4	6.2	5.7	5.3	5
60	74.83	95.57	156.7	140.5	127.4	20.7	16.1	14.3	21
62	82.02	103.09	177.7	158.6	141.2	22.4	20.5	18.7	19
66	110.82	121.56	264.3	225.1	199.3	24.9	21.3	19.2	20
80	109.50	190.75	405.9	353.2	307.7	39.1	31.4	26.0	29
89	125.03	231.36	564.3	482.0	413.1	72.8	49.9	37.0	43
102	21.41	273.06	337.1	306.8	284.4	28.4	25.0	22.8	25

Table C.3: Predicted Blow Counts Based on Confident Interval for UBC Pile 6 Continuous

Depth	q_{ea}	R_{sr}	R_{ut} $(kips)$			Blow Counts $(blows/foot)$			Measured
$(feet)$	$(bars)$	$(kips)$	Lower	Reg. Line	Upper	Lower	Reg. Line	Upper	Blow Count
Confident = 50%									
27	2.95	38.60	42.9	40.2	38.6	3.0	2.7	2.6	3
48	20.97	57.40	69.2	64.5	60.4	6.1	5.7	5.3	5
60	74.83	95.57	154.1	140.5	129.2	20.5	16.1	14.5	21
62	82.02	103.09	174.7	158.6	145.2	22.1	20.5	18.7	19
66	110.82	121.56	253.3	225.1	202.6	23.8	21.3	19.4	20
80	109.50	190.75	397.4	353.2	317.9	37.7	31.4	27.1	29
89	125.03	231.36	550.9	482.0	428.4	68.3	49.9	39.5	43
102	21.41	273.06	329.0	306.8	287.4	27.4	25.0	23.1	25

Table C.4: Predicted Blow Counts Based on Confident Interval for Tilbury H Pile

Depth	q_{ea}	R_{sr}	R_{ut} $(kips)$			Blow Counts $(blows/foot)$			Measured
$(feet)$	$(bars)$	$(kips)$	Lower	Reg. Line	Upper	Lower	Reg. Line	Upper	Blow Count
Confident = 90%									
34	44.49	65.53	77.1	69.0	65.5	7.7	6.8	6.4	5
40	57.07	81.18	97.8	87.3	81.1	9.4	8.2	7.6	7
60	162.35	159.68	238.3	207.4	185.7	27.9	20.5	16.8	20
74	141.70	224.54	320.8	280.7	249.5	60.9	36.2	25.3	42
75	150.74	228.36	331.0	289.1	259.5	69.6	39.7	27.8	37
79	164.17	247.76	369.8	321.8	288.1	126.2	56.7	35.8	44
84	122.43	270.43	370.5	325.8	294.0	113.2	55.5	36.2	46
Confident = 70%									
34	44.49	65.53	73.6	69.0	65.5	7.3	6.8	6.4	5
40	57.07	81.18	93.3	87.3	82.0	8.9	8.2	7.7	7
60	162.35	159.68	224.9	207.4	192.4	24.2	20.5	17.8	20
74	141.70	224.54	303.4	280.7	261.1	48.2	36.2	28.7	42
75	150.74	228.36	312.8	289.1	268.7	53.9	39.7	31.0	37
79	164.17	247.76	349.0	321.8	298.5	86.5	56.7	41.8	44
84	122.43	270.43	351.2	325.8	303.9	81.3	55.5	42.1	46

Appendix D

Input and Output Data Sample of Application

GRLWEAP: WAVE EQUATION ANALYSIS OF PILE FOUNDATIONS

1987 VERSION 1.00
English Units

TILBURY PILE3 BLOW COUNT PREDICTION

HAMMER MODEL OF: D 30-13 MADE BY: DELMAG

ELEMENT	WEIGHT (kips)	STIFFNESS (k/in)	COEFF. OF RESTITUTION	D-NL. ft	CAP DAMPG (k/ft/s)
1	2.200				
2	2.200	157707.9	1.000	.0100	
3	2.200	157707.9	1.000	.0100	
IMP. BLK	1.200	96454.2	.900	.0100	
CAP/RAM	2.020	33390.0	.800	.0100	11.3

HAMMER OPTIONS:

HAMMER NO.	FUEL SETTG.	STROKE OPT.	HAMMER TYPE	DAMPNG-HAMR
13	4	1	1	2

HAMMER PERFORMANCE DATA

RAM WEIGHT (kips)	RAM LENGTH (in)	MAX STROKE (ft)	STROKE (ft)	EFFICIENCY
6.60	118.10	10.00	5.70	.720

MAX PRESS. (psi)	ACT PRESS. (psi)	TIME DELAY (s)	COMP/EXPN	V START (in3)	INJ.
1254.0	914.0	.00050	1.350/1.250	.0	

THE HAMMER DATA INCLUDES ESTIMATED (NON-MEASURED) QUANTITIES

HAMMER CUSHION	AREA (in2)	E-MODULUS (ksi)	THICKNESS (in)	STIFFNESS (kips/in)
	238.50	280.0	2.000	33390.0

INSITU RESEARCH 05/02/92 GRLWEAP TILBURY PILE3 BLOW COUNT PREDICTION

PILE PROFILE:

L b Top (ft)	Area (in2)	E-Mod (ksi)	Spec Wt (lb/ft3)	Wave Spd (ft/s)	EA/c (k/ft/s)
.00	14.6	30000.	492.000	16806.8	26.0
86.00	14.6	30000.	492.000	16806.8	26.0

Wave Travel Time - 2L/c - = 10.234 ms

Pile and Soil Model for Rut = 261.0 kips

No.	Weight (kips)	Stiffn (k/in)	C-Slk (ft)	T-Slk (ft)	CoR	Soil-S (kips)	Soil-D (s/ft)	Quake (in)	L b Top (ft)	Area (in2)
1	.252	7205.	.010	.000	.850	.0	.000	.100	5.06	14.6
2	.252	7205.	.000	.000	1.000	.0	.000	.100	10.12	14.6
5	.252	7205.	.000	.000	1.000	.1	.000	.100	25.29	14.6
6	.252	7205.	.000	.000	1.000	1.3	.050	.100	30.35	14.6
7	.252	7205.	.000	.000	1.000	3.1	.100	.100	35.41	14.6
8	.252	7205.	.000	.000	1.000	4.9	.100	.100	40.47	14.6
9	.252	7205.	.000	.000	1.000	6.7	.100	.100	45.53	14.6
10	.252	7205.	.000	.000	1.000	8.4	.100	.100	50.59	14.6
11	.252	7205.	.000	.000	1.000	10.2	.050	.100	55.65	14.6
12	.252	7205.	.000	.000	1.000	12.0	.050	.100	60.71	14.6
13	.252	7205.	.000	.000	1.000	13.7	.050	.100	65.76	14.6
14	.252	7205.	.000	.000	1.000	15.5	.050	.100	70.82	14.6
15	.252	7205.	.000	.000	1.000	17.3	.050	.100	75.88	14.6
16	.252	7205.	.000	.000	1.000	19.1	.050	.100	80.94	14.6
17	.252	7205.	.000	.000	1.000	20.8	.050	.100	86.00	14.6
Toe						127.9	.150	.106		

PILE OPTIONS:

N/UNIFORM	AUTO S.G.	SPLICES	DAMPNG-P	D-P VALUE (k/ft/s)
0	0	0	1	.521

SOIL OPTIONS:

% SKIN FR	% END BG	DIS. NO.	S DAMPING
51	49	-1	SMITH-1

ANALYSIS/OUTPUT OPTIONS:

ITERATNS	DTCR/DT(%)	RES STRESS	IOUT	AUTO SGMNT OUTPT INCR	MAX T(ms)
0	160	0	10	0	2	0

Rut= 261.0, Rtoe= 127.9 kips, Time Inc.= .119 ms

No.	min F, t (kips)	max F, t (kips)	min Str, t (ksi)	max Str, t (ksi)	max V, t (ft/s)	max D, t (in)
1	.0, 0	405.2, 5	.00, 0	27.79, 5	13.69, 5	1.008, 16
2	.0, 0	407.0, 5	.00, 0	27.91, 5	13.71, 5	.973, 16
3	.0, 0	408.5, 5	.00, 0	28.02, 5	13.68, 5	.937, 15
4	.0, 0	410.2, 5	.00, 0	28.13, 5	13.61, 6	.903, 17
5	.0, 0	411.6, 6	.00, 0	28.23, 6	13.57, 6	.868, 17
6	.0, 0	413.5, 6	.00, 0	28.36, 6	13.42, 6	.832, 17
7	.0, 0	414.7, 7	.00, 0	28.44, 7	13.14, 7	.797, 17
8	.0, 0	415.1, 7	.00, 0	28.47, 7	12.83, 7	.763, 18
9	.0, 0	412.7, 7	.00, 0	28.31, 7	12.44, 7	.729, 18
10	.0, 0	406.3, 7	.00, 0	27.86, 7	12.01, 8	.696, 18
11	.0, 0	395.8, 8	.00, 0	27.15, 8	11.67, 8	.664, 18
12	.0, 0	388.6, 8	.00, 0	26.65, 8	11.30, 8	.634, 19
13	.0, 0	378.6, 8	.00, 0	25.96, 8	10.88, 9	.605, 19
14	.0, 0	367.0, 9	.00, 0	25.17, 9	10.53, 9	.578, 19
15	.0, 0	350.3, 9	.00, 0	24.02, 9	10.35, 9	.553, 19
16	.0, 0	324.4, 9	.00, 0	22.25, 9	10.00, 9	.531, 19
17	.0, 0	334.0, 10	.00, 0	22.91, 10	8.66, 10	.510, 19

Rut kips	Bl Ct bpf	Stroke (ft) down	Stroke (ft) up	min Str ksi	i,t	max Str ksi	i,t	ENTHRU kip-ft	Bl Rt b/min
261.0	29.5	5.7	4.8	.00(	1, 0)	28.47(	8, 7)	21.5	50.9

ECHO PRINT OF INPUT DATA